A Screen for Axon Guidance Genes in Parallel to Heparan Sulfate Proteoglycans in *C. elegans*

Dissertation
zur

Erlangung der naturwissenschaftlichen Doktorwürde
(Dr. sc. nat)

vorgelegt der
Mathematisch-naturwissenschaftlichen Fakultät

der

Universität Zürich

von

Stephan Gysi

aus

Winterthur ZH/Aarau AG

Promotionskomitee
Prof. Michael O. Hengartner (Vorsitz, Leiter der Dissertation)
Prof. Dieter Zimmermann
Prof. Alex Hajnal
Prof. Mario De Bono

Zürich 2011

Table of Contents

Summary

During animal development the establishment of a functional nervous system is an absolutely crucial step. Neurons send axons, sometimes over long distances to reach a certain target with very high accuracy. If errors occur during this process a wide range of neuronal defects can appear ranging from simple motor dysfunction to severe psychological diseases in humans. While increasing anatomical complexity is usually accompanied by increasing complexity in the nervous system the developmental cues that orchestrate the establishment of nervous systems are amazingly conserved from animals as simple as *Caenorhabditis elegans* all the way to humans. Therefore studies in model organisms have revealed a fair number of conserved major axon guidance cues. However it seems unlikely that these major cues are the only ones responsible for building the nervous system. In order to achieve the complexity of an adult nervous system there must be other mechanisms that fine-tune the major cues. We have identified Syndecan and Glypican, two Heparan Sulfate Proteoglycan (HSPG) core proteins, plus a number of Heparan Sulfate (HS) modifying enzymes as minor modulators of axon guidance. Typically mutations in genes coding for these proteins do not lead to severe defects in axon guidance. However, since there are multiple HS related pathways acting in parallel mutations in more than one branch of these pathways lead to clear defects. Since little is known about downstream factor of HS signalling we designed screens to find such components, e.g. axon guidance cues that could interact with HS or other components of established axon guidance pathways. We were able to find a large number of candidates with a possible link to axon guidance (Chapter III) and still did not saturate the genome with the mutagenesis. We also found a mutation in the gene called *zfp-1* for which there has not been any indication so far that it would play a role in axon guidance. Furthermore a mutation in the *C. elegans* homologue of the Retinoblastoma protein *lin-35* results in comparable defects. Both genes play roles in vulval development and the RNAi pathway. We decided to focus on these two genes (Chapter IV) because they were the most unexpected ones and a possible involvement of the RNAi pathway in nervous system development certainly seemed to be an interesting topic to explore. In order to visualize the neurons that we were focusing our study on (D-type motor neurons) we used the

transgene *oxIs12* labelling these neurons with *green fluorescent protein* (*gfp*). Initially we assumed that this transgene is not interfering with the phenotype we screened for and for the average candidate this also seems to be true. However for mutations in *zfp-1* and *lin-35* we found that they only exhibited axon guidance defects if combined with *oxIs12* and not with other transgenes labelling the same neurons. Our efforts to shed light onto this surprising effect led to the conclusion that the integration site of *oxIs12* is playing a role. We also gained considerable insight to the nature of *oxIs12* being a large multi copy transgene spanning roughly 3.6Mb enlarging the X chromosome by about 20%. Nevertheless, mechanistically the transgene dependent effect of *zfp-1* and *lin-35* mutations remains a mystery.

Zusammenfassung

Während der Embyonalentwicklung von Tieren bildet der Aufbau eines funktionierenden Nervensystems einen grundlegend wichtigen Schritt. Neurone senden Axone zum Teil über weite Distanzen um mit sehr hoher Genauigkeit ein bestimmtes Ziel zu erreichen. Falls während diesem Prozess Fehler auftreten kann dies zu einer breiten Palette von Defekten führen, die von eher simplen Bewegungsproblemen bis zu gravierenden psychischen Erkrankungen reichen. Im Tierreich wird normalerweise eine grössere anatomische Komplexität auch in einem komplexeren Nervensystem widergespiegelt. Trotzdem sind die Entwicklungssignale, welche diese Prozesse steuern stark konserviert von simplen Tieren wie *Caenorhabditis elegans* bis zum Menschen. Deshalb haben genetische Studien an Modelorganismen zur Entdeckung einiger konservierter sogenannter Axon Guidance Cues geführt. Allerdings wurde auch klar, dass die doch eher kleine Anzahl dieser Cues wohl kaum alleine für den Aufbau eines Systems von der Komplexität eines adulten Nervensystems zuständig sein kann. Es wird deshalb angenommen, dass es weitere Komponenten gibt, welche die Feinregulierung der bekannten Guidance Cues übernehmen. Wir haben Syndecan und Glypican, zwei Heparan Sulfat Proteoglykane (HSPGs) und verschieden Enzyme welche Heparan Sulfate (HS) modifizieren als solche Feinregulatoren charakterisiert. Mutationen in diesen Genen führen typischerweise zu keinen gravierenden Defekten im Nervensystem. Da es aber verschiedene Signalwege gibt, die auf HS basieren und parallel zu einander agieren, entstehen starke Defekte wenn zwei Gene von unterschiedlichen Signalwegen mutiert sind. Wenig ist bekannt darüber wie die HSPGs genau das Wachstum von Nerven beeinflussen. Deshalb haben wir genetische Screens entworfen um solche Downstream-Komponenten zu finden, zum Beispiel ein Axon Guidance Cue welches an HS bindet oder andere Komponenten von etablierten Axon Guidance Systemen. Wir fanden verschiedene Kandidaten mit einer möglichen Verbindung zu Axon Guidance (Kapitel III), allerdings hat die Mutagenese nicht zu einer Sättigung des Genoms geführt und wir könnten wahrscheinlich noch mehr Kandidaten finden. Einer der Kandidaten hatte eine Mutation im Gene *zfp-1*, für welches bis jetzt keine Funktion in der Entwicklung des Nervensystems bekannt ist. Zusätzlich wussten wir, dass eine Mutation im Gene *lin-35*,

dem *C. elegans* Homolog des Retinoblastoma Proteins, zu vergleichbaren Defekten wie die *zfp-1* Mutation führt. Beide Gene spielen eine Rolle in der Entwicklung der Vulva von *C. elegans* und im RNAi Signalweg. Wir entschieden uns, unsere Studie auf diese zwei Gene zu fokussieren (Kapitel IV), da es sich um die beiden überraschendsten Kandidaten handelte und weil wir es als sehr interessant beurteilten, eine Verbindung zwischen dem RNAi Signalweg und der Entwicklung des Nervensystems herstellen zu können. Um in *C. elegans* die Nervenzellen zu sehen, auf welche wir unsere Studie fokussierten (die D-type Motor Neurone) verwendeten wir das Transgen *oxIs12*, welches diese Neurone mit einem grün fluoreszierenden Protein (*gfp*) anfärbt. Wir nahmen anfänglich an, dass dieses Transgen keinen Einfluss auf unseren Phänotypen hat, was für die Mehrheit der Kandidaten auch stimmt. Mutationen in *zfp-1* und *lin-35* allerdings resultieren nur in Defekten in Kombination mit *oxIs12*. Zusammen mit anderen Transgenen, welche dieselben Neuronen anfärben zeigen diese Mutanten keine Defekte. Die Suche nach dem Grund für diese doch eher überraschende Entdeckung führte zur Schlussfolgerung, dass die Integrationsstelle von *oxIs12* eine Rolle spielt. Während unseren Untersuchungen gelang es uns auch mehr über die Beschaffenheit von *oxIs12* herauszufinden. *oxIs12* ist ein etwa 3.6Mb grosses multi-copy Transgen und vergrössert somit das X Chromosom um etwa 20%. Trotz aller Anstrengungen gelang es uns nicht den genauen Mechanismus der Transgenabhängigkeit von *zfp-1* und *lin-35* Mutanten zu ergründen.

Acknowledgment

This project could not have happened without the help and support from a number of people. I would like to thank my supervisor Prof. Michael Hengartner for allowing me to do this project in his lab and giving me absolute freedom to push the project in the direction I wanted. The Syndecan and HSPG project in our lab was started by a former PhD student Christa Rhiner. During my time as a Diploma student she introduced me to working with *C. elegans* and to the world of science. I am very thankful for this experience. I would also like to mention all other Hengartner lab members for a great atmosphere and interesting discussions about science and other things.

During the time of my PhD I had the pleasure to supervise two students. Ronny Egli did his master thesis and Lucia Reh a semester project with me. I would like to thank both of them for their enthusiasm and help.

From the Institute of Molecular Life Sciences I would like to thank Mathias Bodmer and Martin Moser for FLP mapping and qPCR, Michael Daube for bombardment and Eliane Escher for sequencing. Dr. Valeria Gagliardini from the Institute of Plant Biology of the University of Zurich gave me advice on qRT PCR. I am also thankful to Stephane Flibotte from Don Moerman's lab in Vancouver for array CGH for mutation detection and the group of Christian Beisel at the D-BSSE in Basel for whole genome sequencing.

I am very grateful to the members of my PhD committee Prof. Mario De Bono, Prof. Dieter Zimmermann and Prof. Alex Hajnal for fruitful discussions and guidance. I also would like to thank the members of the Grishok Lab at Columbia University in New York, in particular Lisa Kennedy and Dr. Germano Cecere for interactions and advice. I am thankful to Dr. Elia Di Schiavi for interactions at conferences and support during the darker times of my PhD.

Last but not least a great thank you goes to all my friends and my family for support and never giving up on me.

CHAPTER I

Introduction

Preface

The nervous system is a delicate network of axons and synapses, innervating organs or making connections with other axons. In order to get a fully functioning nervous system, its development relies on axon guidance cues making neuronal cells migrate, guiding axons along one specific tract, preventing them from growing past certain body structures and eventually reaching their proper target. In the past, a number of these axon guidance cues have been identified. However it seems unlikely that these few guidance cues manage to build up such a complicated system. Rather, there is increasing evidence that there must be other systems that fine-tune the already known, major axon guidance cue families. Heparan Sulfate Proteoglycans (HSPGs), proteins that carry long unbranched and differentially modified sugar side chains, have been shown to encode specific information for nervous system development. The nematode *C. elegans* is a good model system for studying the function of HSPGs, as all the core proteins that are known from vertebrates and *Drosophila* are also present in the worm. Additionally genes involved in the biosynthesis of the sugar chains are known and mutants are available. Furthermore working with *C. elegans* offers a number of other advantages. It is very well suited for genetics with a lot of new techniques such as whole genome sequencing for mutation detection facilitating work with this animal. Due to its transparent body structure cellular processes can be followed in the life animal, which is particularly helpful for axon guidance studies, since neurons labelled with *green fluorescent protein* (*gfp*) can be followed easily through the whole body of the worm.

Heparan Sulfate Proteoglycan (HSPG) Core Proteins and Modifications

HSPG core proteins

Heparan Sulfate Proteoglycans (HSPGs) are cell-surface or secreted proteins with specifically modified covalently attached carbohydrate polymers, the glycosaminoglycan (GAG) heparan sulfate (HS). The core can be grouped in two classes (i) membrane associated core proteins and (ii) core proteins of the extra cellular matrix (ECM). The transmembrane Syndecans and the glycosylphosphoinositol (GPI) anchored Glypicans belong to the group of membrane associated core proteins. The Syndecans are a gene family with four members in mammals (Syndecan 1-4), one in *Drosophila* (*sdc*) and one in *C. elegans* (*sdn-1*). They have a rather short cytoplasmic tail with a PDZ-binding motive at its end and an extra cellular domain of varying size with conserved Serine residues to which the HS chains are attached. The Glypican family contains six mammalian genes, *dally* and *dally-like protein* in *Drosophila* and two homologues in *C. elegans* (*gpn-1* and *lon-2*) (for a review see Bernfield et al., 1999).

Perlecan and Agrin are HSPGs of the basement membrane in the ECM, and unlike membrane associated HSPGs, they are only present in single copies in all species studied so far. Perlecan has been reported in mammals, *Drosophila* (*trol*) and *C. elegans* (*unc-52*). Agrin has been described in mammals and *C. elegans* (Princivalle et al., 2002; Perrimon et al., 2000).

HS biosynthesis

Although the core proteins for HS chains are responsible for some diversity of HSPGs in different cell types, the largest source of diversity comes from variable modifications of heparan sulfate disaccharides, including epimerization of the fifth carbon atom in hexuronic acid and sulfation at several sites. The large negative charge of HS chains is a result of sulfation and is one reason why many molecules bind HS. The modifications are complex and incomplete, giving an enormous number of possible modification patterns. The biochemical pathways that are involved in synthesis and modification of HS chains are well known and can be divided into five different steps (Fig. 1). The first step, the synthesis of monosaccharides, takes place in the cytoplasm. They are then transported

into the Golgi where step number two, the synthesis of the initial tetrasaccharide, takes place. This tetrasaccharide is common to all GAG chains and is composed of xylose (Xyl) - galactose (Gal) - Gal - glucuronic acid (GlcA). In the third step an N-acelylglucosamin (GlcNAc) residue is added to initiate the HS chain. Subsequently GlcA - GlcNAc disaccharides are added repeatedly in step four to elongate the HS chain. Step five includes all modifications of sugar residues such as deacetylation, epimerization and sulfation. Similar to core proteins genes coding for enzymes catalysing these modifications are well conserved in *C. elegans*. Deacetylation is performed by *hst-1*, which is an essential gene in the worm, probably due to the fact that deacetylation precedes and paves the way for all sulfations. HS chains in *hst-1* mutants are most likely entirely unsulfated and therefore lack any specificity. 2-O-, 3-O-, and 6-O sulfations are catalyzed by *hst-2*, *hst-3.1* and *hst-3.2*, and *hst-6* respectively, the gene for C5 epimerisation is *hse-5.* Finally HS chains are about 100 or more sugar units long and have numerous structural heterogeneities. All modification reactions are incomplete and mostly occurring in blocks producing highly modified regions, spaced apart by relatively unmodified regions (Lin, 2004; Lee and Chien, 2004; Holt, 2005).

HSPGs in nervous system development

Studies in different organisms such as worm, fly and mammals have shown that HSPGs play diverse roles in nervous system development. Mammalian members of the Syndecan and Glypican families act in axon guidance. Syndecans and Agrin have been shown to be important for synapse development. Furthermore Glypican-1 and possibly other HSPG core proteins have been assigned a role in axon regeneration after neuronal injury (reviewed in Van Vactor et al., 2006). However, studying HSPGs in mammals is difficult because most members are present in multiple copies, most probably acting redundantly. Most knowledge about HSPG function in nervous system development comes from *Drosophila*. In particular the *Drosophila* Syndecan (Sdc) has been shown to play a role in axon guidance at the midline. Steigemann and co-workers found that mutations in *sdc* display similar axon guidance defects as mutations in *robo* and *robo2* and they could

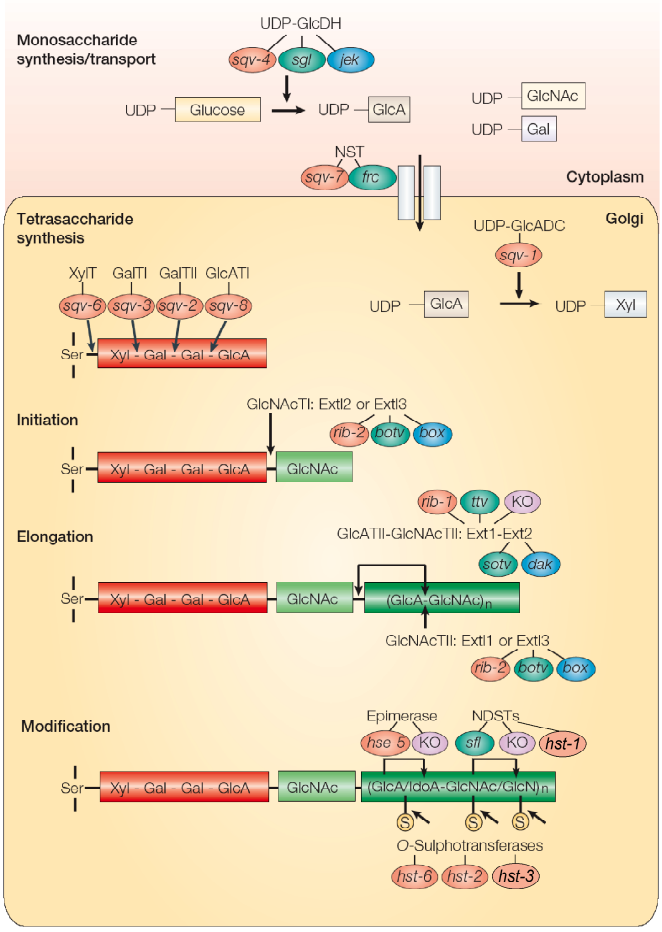

Figure 1: The five steps of HS biosynthesis.

(1) Synthesis of monosaccharides in the cytoplasm and transport of them into the Golgi.

(2) The initial tetrasaccharide xylose (Xyl) - galactose (Gal) - Gal - glucuronic acid (GlcA), which is common to all GAG chains, is synthesised and attached to a Serin residue in the core protein. This process is catalyzed by four enzymes (xylosyltransferase (XylT), galactosyltransferase I+II (GalTI+II) and glucuronyltransferase I (GalTI)), which add individual sugar residues.

(3) Initiation of the HS chain by adding an N-acetylglucosamin (GlcNAc). This step is catalyzed by GlcNAc tranferase I (GlcNAcTI).

(4) Elongation of the HS chain by adding GlcA - GlcNAc disaccharides, which is catalyzed by the Exostosin (EXT) family proteins glucuronyltransferase II (GlcATII) and GlcNAc transferase II (GlcNAcTII).

(5) Modification of the HS chain including GlcNAc N-deacetylation and N-sulfation by N-deacetylase/N-sulfotransferase (NDST), C5 epimerization of GlcA to iduronic acid (IdoA), and variable O-sulfation at C2 of IdoA and GlcA, at C6 of GlcNAc and N-sulfo-glucosamin (GlcNS) units, and, occasionally, at C3 of glucosamin (GlcN) residues by O-sulfotransferases.

Shown in ovals are the corresponding genes from different model organisms:

Orange for *C. elegans* mutants: *sqv*, squashed vulva; *rib*, related to mammalian RIB-affecting EXT gene family; *hse*, heparan sulfate epimerase; *hst*, heparan sulfo transferase

Green for *D. melanogaster* mutants: *sgl*, sugarless; *frc*, fringe connection; *botv*, brother of tout velu; *ttv*, tout velu; *sotv*, sister of tout velu; *sfl*, sulfateless.

Blue for zebrafish mutants: *jek*, jekyll; *box*, boxer; *dak*, dackel.

Purple for mouse knockouts (KO).

(modified from Lee and Chien, 2004; Lin, 2004)

show that Sdc is expressed in all tissue types that are affected by mutations in *slit* and that express *robo*. Sdc did not regulate Slit or Robo expression or localization, but reduced the efficiency of Slit signalling (Steigemann et al., 2004). Furthermore it has been shown that Sdc interacts genetically and physically with Slit and its receptor Robo (Johnson et al., 2004). Taken together both studies have clearly shown that Sdc is important for correct Slit signalling through Robo. Interestingly, neuronal expression of another HSPG, *dally-like protein* (*dlp*), one of the two *Drosophila* Glypican homologues, partially rescued the defects caused by *sdc* mutations (Johnson et al., 2004). In a recent mammalian study Bespalov and co-authors found that Syndecan-3 is a novel receptor for glial cell line-derived neurotrophic factor (GDNF) family ligands (GFLs) (Bespalov et al., 2011). The interaction of Syndecan-3 and GFLs influences neurite outgrowth and, on a more general level, it is thought to play an important role in cortical development. While GFLs are known to bind and signal through GPI anchored GDNF family receptors this study shows that some of the GFLs bind with high affinity to the HS chains of Syndecan-3 and this binding is depending on 2-O and 6-O sulfations. In our past effort to characterize the *C. elegans* Syndecan homologue *sdn-1* we made a similar observation in that different cell migration and axon guidance events rely on different modification patterns (Rhiner et al., 2005).

In addition to HSPGs, other proteoglycans (PG) have been assigned a role in nervous system development too, namely chondroitin sulfate PG (CSPG), dermatan sulfate PG (DSPG) and keratan sulfate PG (KSPG), grouped according to the type of their sugar side chains. CSPGs are widely expresses in mammalian brains, often coinciding with tracts of growing axons and seem to modulate axon outgrowth. DSPGs and KSPGs are less abundant in the nervous system but their presence has also been reported (for a review on PG see Bovolenta et al., 2000).

The mode of action of HSPGs is still under debate and probably depends on the context. There are three models for how HSPGs interact with ligand/receptor complexes:

1. HSPGs bind ligands directly to HS chains and regulate the concentration as well as transportation of the molecule by passing the ligand form one HS chain to another. Lateral HSPG movement at the cell membrane may also facilitate ligand movement.
2. HSPGs facilitate dimerization or oligomerization of ligands with their receptors to initiate signalling acting as some sort of a coreceptor.
3. Rather than being required for the formation of an active ligand-receptor complex, HSPGs may bind ligands to stabilize or protect them from degradation, thereby accumulating ligand and facilitating ligand/receptor interaction.

(Lin, 2004)

Motor Neurons in *C. elegans*

The GABAergic nervous system

GABA is the most abundant inhibitory neurotransmitter in vertebrates and invertebrates. Antibody staining in *C. elegans* revealed that 26 of the 302 neurons express GABA (McIntire et al., 1993). Among these 26 GABA positive neurons are the D-type motor neurons (6 DD neurons and 13 VD neurons). Furthermore 4 RME neurons, an RIS neuron, an AVL neuron and a DVB neuron were GABA positive (Fig. 2).

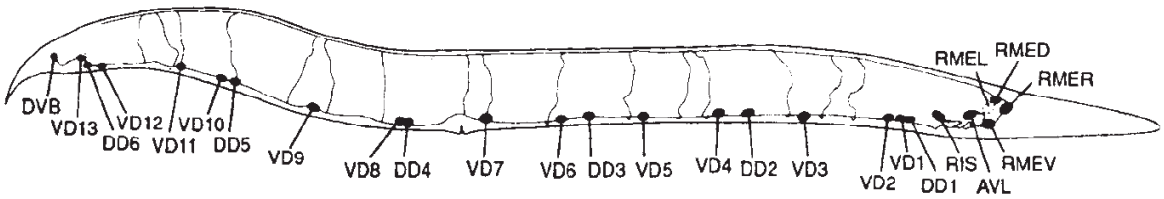

Figure 2: The GABAergic nervous system in *C. elegans*. The 26 GABA positive cells are the 19 D-type motor neurons, 4 RME neurons, an RIS neuron, an AVL neuron and a DVB neuron; anterior is to the right, dorsal is up (from McIntire et al., 1993)

DD and VD motor neurons innervate dorsal and ventral body muscles, respectively. Their cell bodies are located in the ventral nerve cord (VNC). VD motor neurons extend their

axons in the VNC, DD motor neurons, however, have commissural axons that grow circumferentially around the body to the dorsal side, where they bifurcate and build up the dorsal nerve cord (DNC). These 19 D-type motor neurons inhibit contraction of ventral and dorsal body wall muscles during locomotion. A bend in the body is made by contracting muscles on one side of the body while relaxing muscles via GABA innervation on the opposite side (Fig. 3). Therefore animals that lack functional D-type motor neurons or are defective in GABA-mediated relaxation of body wall muscles show uncoordinated locomotion (McInitre et al., 1993; reviewed by Schuske et al., 2004).

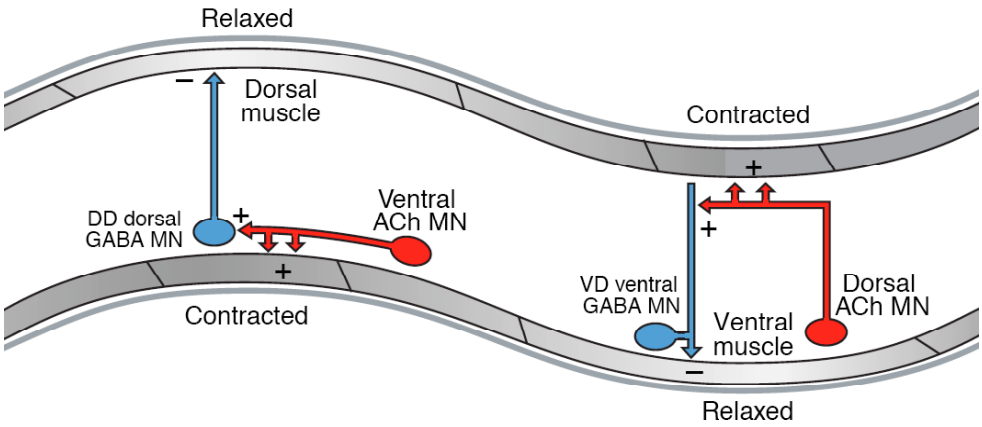

Figure 3: Schematic drawing of motor axon connectivity. Cholinergic motor neurons (DA, DB, VA, VB and AS) synaps onto body wall muscles to induce contraction. Additionally they stimulate GABAergic motor neurons (DD and VD) to release GABA on the contra lateral side and cause relaxation of body wall muscles (from Schuske et al., 2004).

The cholinergic nervous system

Acetylcholine (ACh) is the neurotransmitter of excitatory motor neurons and therefore the counterpart of GABA. The cholinergic motor neurons VA and VB cause contraction of ventral body wall muscles, the DA, DB and AS neurons cause contraction of dorsal body wall muscles. Cholinergic motor neurons also activate GABAergic VD or DD neurons to cause relaxation of body wall muscles (Fig. 3) (McIntire et al., 1993).

Netrin is the Major Axon guidance cue for commissural axons in *C. elegans*

Netrins are a small family of conserved secreted guidance molecules with one known member in *C. elegans* (UNC-6, Hedgecock et al., 1990) and two in *Drosophila* (netrin-A and -B). In mammals there are three netrins termed netrin 1-3 (reviewed in Chisholm et al., 1999). In all species there are populations of axons projecting to or away from the midline of the nervous system. This attraction and repulsion is mediated, in part, by members of the netrin family, which act bifunctionally. Also the receptor mechanisms for netrin are highly conserved throughout the animal kingdom. Growth cone attraction is triggered by binding of UNC-6/Netrin to homodimers of deleted in colorectal cancer (DCC) receptor family proteins. DCC receptors are transmembrane proteins that have multiple immunoglobulin (Ig) repeats and fibronectin type III (FNIII) repeats. *C. elegans* and *Drosophila* each have one DCC homologue, called UNC-40 (Hedgecock et al., 1990) and Frazzled respectively, whereas vertebrates have two DCC family proteins, DCC and neogenin. Growth cone repulsion is mediated by UNC-5 family receptor proteins, in some cases together with UNC-40. UNC-5 proteins are also transmembrane proteins that belong to the Ig super-family, however they are structurally quite different from UNC-40/DCC. So far no UNC-5 receptor has been found in *Drosophila* however in mammals there are three UNC-5 family proteins (UNC5H1, UNC5H2 and UNC5H3) (Chisholm et al., 1999; reviewed by Huber et al., 2003)

In worms UNC-5, UNC-6 and UNC-40 represent the major system for circumferential guidance of migrating cells and axons to and away from the ventral nerve cord (VNC). If the system is disturbed dorsal migration in the major classes of motor neurons, linker cell, and the distal tip cell is affected. Ventral migration is affected in several sensory and motor axons, the linker cell and the anchor cell (Hedgecock et al., 1990).

Motor axon guidance

The outgrowth of commissural axons of motor neurons has to be precisely regulated. DA and DB motor neurons send out two commissures, one growing anteriorly along the VNC the other growing circumferentially to the DNC. There commissures of DAs turn and grow anteriorly, whereas commissures of DBs grow posteriorly. AS motor neurons have only one commissure that grows to the DNC and then turns anterior. DD and VD motor

neurons have only one commissure too. DD motor neurons first send commissures out in the VNC until they reach the next anterior cell body of a DB motor neuron. There they turn and grow circumferentially to the DNC where they bifurcate and grow anterior and posterior. Commissures of VD motor neurons fasciculate with the VNC before they turn and grow to the DNC. In all cases commissures grow out very consistently either along the right or the left body wall of the worm depending on the commissure (Lim et al., 1999; Durbin 1987).

UNC-6/Netrin signalling has been shown to play the major role in commissural outgrowth (Hedgecock et al., 1990). UNC-6 is expressed ventrally to form a gradient. UNC-5 and UNC-40 are expressed in dorsally migrating axons to mediate a repulsive response to UNC-6, whereas UNC-40 is expressed in ventrally migrating axons to mediate an attractive response to UNC-6 (Fig. 4) (Lim et al, 1999).

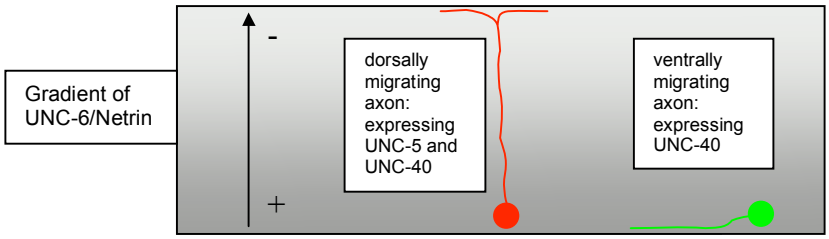

Figure 4: Schematic drawing of motor axon guidance; dorsal is up. UNC-6 is expressed ventrally and forms a gradient with high concentrations in ventral regions and low concentrations in dorsal regions. Dorsally migrating axons (red) express UNC-5 and UNC-40 and are repelled by UNC-6. Ventrally migrating axons (green), on the other hand, are attracted by UNC-6 and express the UNC-40 receptor only.

In addition to UNC-6/Netrin the SAX-3/Robo and VAB-1/Ephrin systems have been shown to have minor effects on commissure outgrowth. If *sax-3* or *vab-1* are mutated there are more commissures growing out on the inappropriate side of the worm (Hobert O. and Bülow H., 2003). Also INA-1/Integrin plays a minor role (Poinat et al, 2002). Taken together this gives a tightly regulated system with multiple guidance systems acting redundantly.

Most if not all, signalling pathways finally act on RhoGTPases to transmit their signal and evoke a change in the cytoskeleton of axons. Therefore it is not surprising that genes involved in this downstream part of the signalling interrupt correct motor axon outgrowth

too if mutated. The *C. elegans* genome contains three Rac genes, called *ced-10, rac-2* and *mig-2*. Each of them alone causes very mild defects in axon guidance, including D-type motor neurons. However, double mutants of *ced-10; mig-2* display strong defects, loss of function of all three Rac genes leads to early larval lethality (Lundquist et al., 2001). Furthermore also mutations in *unc-73*, which is the guanine nucleotide exchange factor (GEF) of CED-10 and MIG-2, show similarly severe phenotypes (Wu et al., 2002; Merz DC. and Culotti JG., 2000). This finding is consistent with the expression pattern of *unc-73* in the nervous system from early embryogenesis on (Steven et al., 1998). The protein is most concentrated in the two major structures in the *C. elegans* nervous system, the nerve ring and the VNC. It affects actin polymerization, axon guidance and cell migration.

Aim of the PhD Project

Screen for axon guidance genes depending on HSPGs

During studies of double mutants of *sdn-1* and each one of the modifying enzymes we observed a striking increase in axon guidance defects of D-type motor neurons in *hse-5(tm472); sdn-1(zh20)* double mutants. These animals exhibited strong uncoordinated locomotion and the commissures of D-type motor neurons, if present at all, almost never reached the DNC, whereas *sdn-1(zh20)* or *hse-5(tm472)* single mutants had only mild defects in D-type motor neurons and showed almost wild type locomotion. This additive defect led to the hypothesis that *sdn-1* and *hse-5* act in two parallel pathways that contribute to correct axon guidance.

In an attempt to find new genes involved in *sdn-1* - or *hse-5* - dependent signalling we performed EMS screens. We aimed to enhance defects in D-type motor neuron guidance seen in the two single mutants *hse-5(tm472)* or *sdn-1(zh20)*. Mutagenizing animals carrying one of the two mutations in the background and screening for candidates with defective D-type motor axon guidance, as observed in *hse-5(tm472); sdn-1(zh20)* double mutants, should allow us to isolate new genes involved in *hse-5* or *sdn-1* dependent signalling.

References

Bernfield M, Gotte M, Park PW, Reizes O, Fitzgerald ML, Lincecum J, Zako M. (1999). Functions of cell surface heparan sulfate proteoglycans. *Annu. Rev. Biochem*. **68**: 729-77.

Bespalov MM, Sidorova YA, Tumova S, Ahonen-Bishopp A, Magalhães AC, Kulesskiy E, Paveliev M, Rivera C, Rauvala H, Saarma M. (2011). Heparan sulfate proteoglycan syndecan-3 is a novel receptor for GDNF, neurturin, and artemin. *J Cell Biol.* **192**(1): 153-69.

Bovolenta P, Fernaud-Espinosa I. (2000). Nervous system proteoglycans as modulators of neurite outgrowth. *Prog. Neurobiol*. **61**(2):113-32.

Chisholm A, Tessier-Lavigne M. (1999). Conservation and divergence of axon guidance mechanisms. *Curr Opin Neurobiol*. **9**(5): 603-15.

Durbin (1987) PhD thesis

Hedgecock EM, Culotti JG, Hall DH. (1990). The unc-5, unc-6, and unc-40 genes guide circumferential migrations of pioneer axons and mesodermal cells on the epidermis in *C. elegans. Neuron* **4**(1): 61-85.

Hobert O, Bulow H. (2003). Development and maintenance of neuronal architecture at the ventral midline of *C. elegans. Curr. Opin. Neurobiol*. **13**(1): 70-8.

Holt CE, Dickson BJ. (2005). Sugar codes for axons? *Neuron*. **46**(2): 169-72.

Huber AB, Kolodkin AL, Ginty DD, Cloutier JF. (2003) .Signaling at the growth cone: ligand-receptor complexes and the control of axon growth and guidance. *Annu. Rev. Neurosci*. **26**: 509-63.

Johnson KG, Ghose A, Epstein E, Lincecum J, O'Connor MB, Van Vactor D. (2004). Axonal heparan sulfate proteoglycans regulate the distribution and efficiency of the repellent slit during midline axon guidance. *Curr Biol.* **14**(6): 499-504.

Lee JS, Chien CB. (2004). When sugars guide axons: insights from heparan sulphate proteoglycan mutants. *Nat Rev Genet*. **5**(12): 923-35.

Lin X. (2004). Functions of heparan sulfate proteoglycans in cell signaling during development. *Development* **131**(24): 6009-21.

Lim YS, Mallapur S, Kao G, Ren XC, Wadsworth WG. (1999). Netrin UNC-6 and the regulation of branching and extension of motoneuron axons from the ventral nerve cord of *Caenorhabditis elegans. J. Neurosci*. **19**(16): 7048-56.

Lundquist EA, Reddien PW, Hartwieg E, Horvitz HR, Bargmann CI. (2001). Three *C. elegans* Rac proteins and several alternative Rac regulators control axon guidance, cell migration and apoptotic cell phagocytosis. *Development*. **128**(22): 4475-88.

McIntire SL, Jorgensen E, Kaplan J, Horvitz HR. (1993). The GABAergic nervous system of *Caenorhabditis elegans. Nature* **364**(6435): 337-41.

Merz DC, Culotti JG. (2000). Genetic analysis of growth cone migrations in *Caenorhabditis elegans. J. Neurobiol*. **44**(2):281-8.

Perrimon N, Bernfield M. (2000). Specificities of heparan sulphate proteoglycans in developmental processes. *Nature* **404**(6779): 725-8.

Poinat P, De Arcangelis A, Sookhareea S, Zhu X, Hedgecock EM, Labouesse M, Georges-Labouesse E. (2002). A conserved interaction between beta1 integrin/PAT-3 and Nck-interacting kinase/MIG-15 that mediates commissural axon navigation in *C. elegans. Curr. Biol.* **12**(8): 622-31.

Princivalle M, de Agostini A. (2002). Developmental roles of heparan sulfate proteoglycans: a comparative review in *Drosophila*, mouse and human. *Int. J. Dev. Biol.* **46**(3): 267-78.

Rhiner C, Gysi S, Fröhli E, Hengartner MO, Hajnal A. (2005). Syndecan regulates cell migration and axon guidance in *C. elegans. Development.* **132**(20): 4621-33.

Schuske K, Beg AA, Jorgensen EM. (2004). The GABA nervous system in *C. elegans*. *Trends Neurosci*. **27**(7): 407-14.

Steigemann P, Molitor A, Fellert S, Jäckle H, Vorbrüggen G. (2004). Heparan sulfate proteoglycan syndecan promotes axonal and myotube guidance by slit/robo signaling. *Curr Biol.* **14**(3): 225-30.

Steven R, Kubiseski TJ, Zheng H, Kulkarni S, Mancillas J, Ruiz Morales A, Hogue CW, Pawson T, Culotti J. (1998). UNC-73 activates the Rac GTPase and is required for cell and growth cone migrations in *C. elegans*. *Cell* **92**(6): 785-95.

Van Vactor D, Wall DP, Johnson KG. (2006). Heparan sulfate proteoglycans and the emergence of neuronal connectivity. *Curr Opin Neurobiol.* **16**(1): 40-51.

Wu YC, Cheng TW, Lee MC, Weng NY. (2002). Distinct rac activation pathways control *Caenorhabditis elegans* cell migration and axon outgrowth. *Dev Biol*. **250**(1): 145-55.

CHAPTER II

A Screen for Genes Acting in Parallel to HSPGs During Guidance of D-type Motor Neurons

Preface

During our efforts to shed light on the network of HSPG core proteins and HS modifying enzymes and how it influences guidance of D-type motor neurons we noted that there are at least two parallel pathways. For each of the two pathways we know one characteristic gene, one side is depending on *sdn-1*, the other one on *hse-5*. With the aim to find new components and to gain mechanistic insight we designed two forward genetic screens that revealed a total of 14 candidates. Furthermore, through candidate gene approaches we identified additional genes leading to the screening phenotype when mutated. This chapter summarizes the screen and gives an overview of the candidates.

Results

HSPGs and HS modifying enzymes in D-type motor axon guidance.

Others and we have previously characterized the role played by HSPGs and their modifying enzymes during various developmental processes in *C. elegans* (Rhiner et al., 2005, Kinnunen et al., 2005, Gumienny et al., 2007). In a double mutant analysis focussing on axon guidance defects of D-type motor neurons we could show that SDN-1 and HSE-5 act in parallel. Mutations in both genes result in severe axon guidance defects, despite the fact that the single mutants have almost no defects (Fig. 1A, B). At the same time we found that LON-2/Glypican acts in parallel to SDN-1 too and in the same pathway as HSE-5, however *sdn-1(zh20) lon-2(e678)* double mutants show less severe defects than *sdn-1(zh20); hse-5(tm472)* double mutant animals. HST-2 seems to act in parallel to SDN-1 and in the same pathway as HSE-5 too (Fig. 1C).

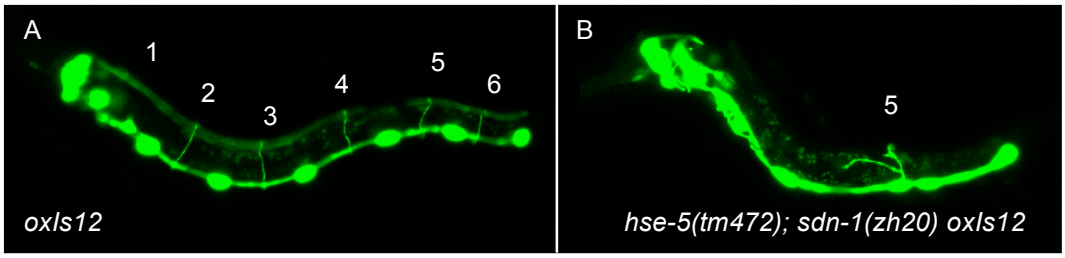

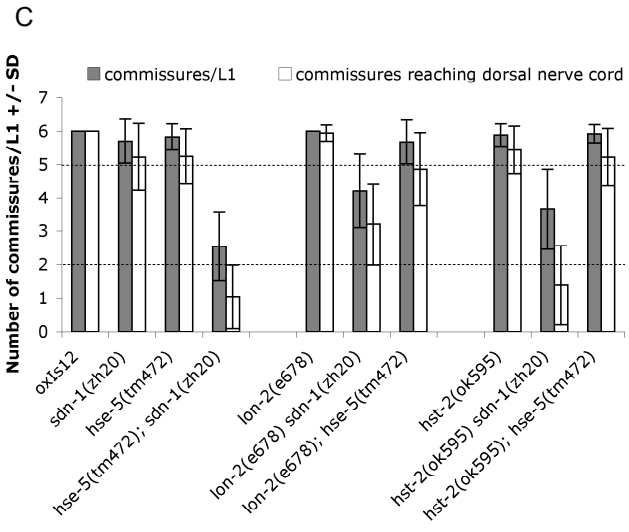

Figure 1: SDN-1 acts in parallel to LON-2, HST-2, and HSE-5 in D-type motor axon guidance. A: A wild type L1 animal with nicely organized D-type motor neurons (Nr. 1 is out of focus). B: The *hse-5 sdn-1* double mutant has very severe defects. C: While each of the single mutants alone has no dramatic effect on D-type axon guidance double mutants of *sdn-1(zh20)* and either *lon-2(e678), hst-2(ok595),* or *hse-5(tm472)* show increased defects, indicating that they are all acting in parallel to *sdn-1*. LON-2, HST-2 and HSE-5 seem to be in the same pathway since mutations in two of them do not lead to enhanced axon guidance defects.

Forward genetic screens identified a wide variety of genes acting in D-type motor axon guidance.

To identify genes interacting with HSPGs during guidance of D-type motor axons in *C. elegans* we performed two screens. The logic of these approaches is based on the fact that SDN-1, an HSPG core protein, and HSE-5, an enzyme modifying heparan sulfate (HS) chains attached to a core protein, act in parallel. Loss-of-function alleles of either of the two genes lead to minor defects in axon guidance. In contrast, animals with mutations in both genes show a dramatic increase in axon guidance defects and exhibit the characteristic uncoordinated (unc) phenotype. In our screens we EMS mutagenized animals carrying either the *sdn-1(zh20)* or *hse-5(tm472)* null allele as genetic background and searched for candidate animals phenocopying the defects observed in *hse-5(tm472); sdn-1(zh20)* double mutants. For both approaches we screened roughly 11'000 genomes and recovered a total of 14 candidates, resulting in a mutation frequency of about one mutation in 1'600 genomes.

Table 1: Summary of all mutants recovered from the screen and the corresponding type of mutation plus the gene affected

Allele	Gene	Mutation type	5' flanking sequence	3' flanking sequence
op459	*unc-130*	point, ms	caatggatcgtttctgcgca	aaggaagaggtaaggggagc
op460	*unc-5*	point, ms	ttgttgcgtgattggctcgg	attgaagacgcaatggctta
op462	*zag-1*	point, ns	agggtctcttctcgtgcgat	aatgtgacaaggtgttcggc
op464	*unc-73*	point, intron	catttcagtcaaataaaaaa	ttacgaagtaacttcaaata
op468	*unc-5*	337bp deletion	atacagctaaatgaactctt	cgattgctgaaatattgatt
op469	*unc-5*	point, ms	cttctcccttacagtactct	cgtcgttcaatggagctgga
op472	nd	-	-	-
op474	nd	-	-	-
op476	nd	-	-	-
op477	*unc-5*	point, ms	tctcgtcatttcttcttctc	cttacagtactctccgtcgt
op479	*unc-53*	point, ns	ggcaccgtgcatgaacattc	gattgtagttgaggaagtaa
op480	nd	-	-	-
op481	*zfp-1*	point, ns	acagctgttggaacgacaat	ggatcaaggatcaagtcttc
op482	*max-1*	point, ns	tctgtcagtgccaaatggcc	caataatgtctcattcgaag

ms: mis-sense; ns: non-sense (premature stop codon); 5' and 3' flanking sequences are corresponding to chromosomal orientation

Mapping these mutations using the FLP mapping strategy described by Zipperlen et al., (2005) revealed that most of them map to separate intervals distributed over the whole *C. elegans* genome. Therefore we conclude that our screening efforts did not result in a saturation of the genome and more candidate genes could possibly be found. Additionally, from candidate gene approaches, we were able to find genes resulting in the desired phenotype when mutated even if we have failed to recover mutations in these genes from the screen. In order to find the mutation responsible for the phenotype we either performed classical FLP mapping (Zipperlen et al., 2005) followed by RNAi of genes in the resulting interval, or we made use of two novel mapping approaches array CGH (Maydan et al., 2007, Flibotte et al., 2009) and whole genome sequencing (Sarin et al., 2008). For a description of the work program involved in these two techniques see Materials and Methods of this chapter. Table 1 is showing a summary of all genes identified in the screen that will be discussed in more detail.

sdn-1 and *hse-5* interact genetically with *ptp-3*/LAR

In a candidate gene approach for two candidates mapping to LGII the RNAi clone for *ptp-3*, a receptor protein tyrosine phosphatase (RPTP) of the LAR type gave a positive phenotype. Several studies in the past have shown that LAR type RPTPs bind HS chains of Syndecan and Glypican during synapse formation (Fox et al., 2005, Johnson et al., 2006), therefore making *ptp-3* a likely target of our screen. By testing different available alleles of *ptp-3* we were able to confirm that PTP-3 acts in parallel to SDN-1 and HSE-5 during guidance of D-type motor axons (Fig. 2).

Due to the fact that the *ok244* allele leads to an enhancement of axon guidance defects when combined with mutations in *sdn-1* or *hse-5* we conclude that the long isoform PTP-3A is involved in the process. In contrast, the *op147* allele affects all possible isoforms of PTP-3 and shows a strong temperature sensitive phenotype. Grown at 25°C *ptp-3(op147); sdn-1(zh20)* double mutants have stronger defects than at 20°C and the *ptp-3(op147); hse-5(tm472)* double mutants are fully sterile at 25°C. Taken together, this data is rather inconclusive, implicating multiple isoforms of PTP-3 in the axon guidance process. Since we do not know whether the *op147* allele, if grown at the non-permissive

temperature, results in a complete loss of PTP-3 function it is very difficult to estimate the importance of PTP-3 in the whole process

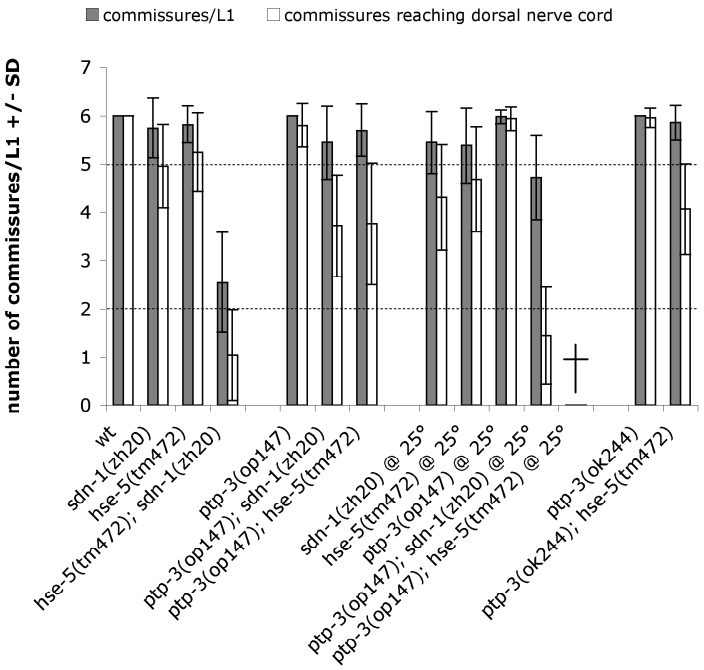

Figure 2: Mutations in *ptp-3* enhance *sdn-1(zh20)* and *hse-5(tm472)* alleles. Both tested alleles of *ptp-3* lead to an increase of axon guidance defects of *sdn-1(zh20)* and *hse-5(tm472)* mutants. *op147* additionally is temperature sensitive resulting in a further increase of defects of *sdn-1(zh20); ptp-3(op147)* animals and fully penetrant sterility of *hse-5(tm472); ptp-3(op147)* animals if grown at 25°C.

Components of LAR signalling interact genetically with HSPGs

To explore the relevance of LAR signalling in guidance of D-type motor axons in more detail we decided to study other components of the LAR signalling pathway. As mentioned earlier studies from flies to vertebrates have shown that the two HSPGs Syndecan and Glypican are extra cellular binding partners of LAR. Furthermore Nidogen binds to the extra cellular part of LAR as well. Most intracellular components of LAR signalling are recruited to the phosphatase domains via Liprin α. One such component is Unc-10/RIM. For a review of the function of LAR and Liprin α during synapse formation see Stryker and Johnson, (2007). We decided to combine mutations in *lon-2*/Glypican, *gpn-1*/Glypican, *nid-1*/Nidogen and *unc-10*/RIM with mutations in *hse-5*, *sdn-1* and *ptp-3* and tested the resulting double mutants for an increase of axon guidance defects of D-type motor neurons. Mutations in both non-HSPG binding partners of PTP-3, NID-1 and UNC-10, resulted in a slight increase of axon guidance defects in combination with *sdn-1(zh20)* or *hse-5(tm472)* (Fig. 3). However, no increase of defects was observed if

combined with *ptp-3(op147)*. A mutation in *gpn-1* only enhanced *sdn-1(zh20)* in a very mild way. No increase of defects was observed for *gpn-1(tm588)* together with *hse-5(tm472)* or *ptp-3(op147)*. The same can be stated for the *lon-2(e678)* allele, although, conversely to *gpn-1(tm588)* it leads to a stronger increase of defects in the double mutant with *sdn-1(zh20)*, but still not to levels observed in *hse-5(tm472); sdn-1(zh20)* double mutants. The fact that *gpn-1(tm588)* and *lon-2(e678)* reveal a similar pattern in our double mutant analysis raised the question whether GPN-1 and LON-2 act redundantly. To address this question we scored axon guidance defects in the *sdn-1(zh20) gpn-1(tm588) lon-2(e678)* triple mutant. These animals are indistinguishable of *sdn-1(zh20) lon-2(e678)* double mutants indicating that, on one hand GPN-1 is not playing a major role in D-type motor axon guidance and on the other hand there is another as yet unknown HSPG core protein acting in parallel to SDN-1 and LON-2.

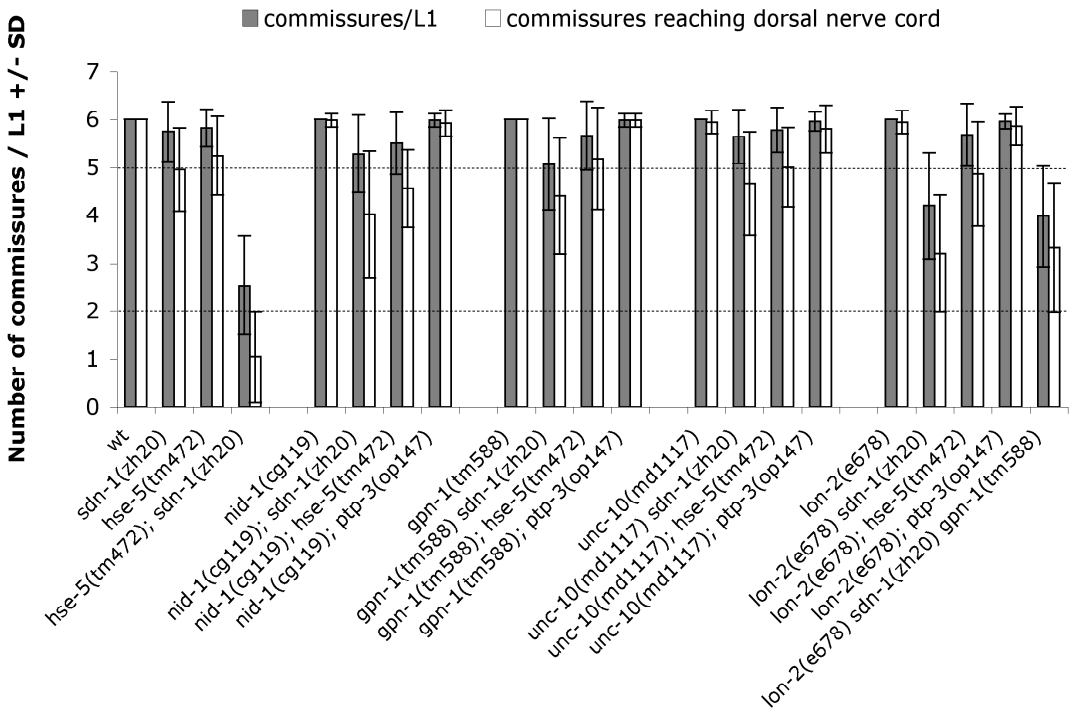

Figure 3: LAR signalling components play a minor role in guidance of D-type motor axons. Mutations in *nid-1, gpn-1,* and *unc-10* only mildly enhance *sdn-1* or *hse-5* mutations. A double mutant for *lon-2* and *sdn-1* shows clear but not dramatic defects that cannot be further enhance by adding a *gpn-1* mutation.

It is interesting to note that while *lon-2(e678)* and *ptp-3(op147)* both enhance the *sdn-1(zh20)* mutation they do not enhance each other. In summary this indicates that there is a minor involvement of LAR signalling in motor axon guidance requiring the help of HSPGs which in turn need HSE-5 to modify HS chains.

***unc-53* is involved in a wide range of axon guidance and cell migration events.**

unc-53 has primarily been involved in anterior posterior migration of neuron cell bodies and guidance of axons (Stringham et al., 2002). The fact that little is known about a function of *unc-53* in D-type motor axon guidance makes this gene an interesting candidate. The *unc-53(ok2736)* allele fails to complement *op479* and enhances axon guidance defects of *sdn-1(zh20)* and *hse-5(tm472)* (Fig. 4). Sequencing of *unc-53* in *op479* revealed that it contains a G to A transition at position 30057 from the ATG resulting in R1258Stop (numbers corresponding to the F45E10.1a isoform). UNC-53 is thought to be involved in cytoskeleton remodelling, linking an axon guidance signal to the cytoskeleton (Schmidt et al., 2009).

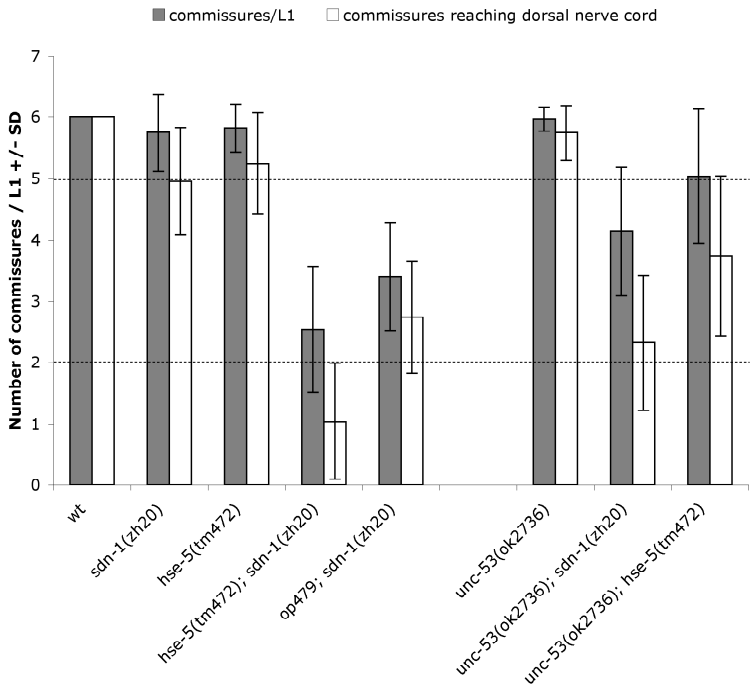

Figure 4: *unc-53(ok2736)* phenocopies the defects of the *op479* allele. While a mutation in *unc-53* alone has almost no influence on guidance of D-type motor axons it clearly enhances both *sdn-1(zh20)* and *hse-5(tm472)* mutations.

***unc-129* and *unc-130* have identical effects on D-type motor axon guidance.**

unc-130 is a transcription factor for the *unc-129* TGFβ growth factor signalling molecule that is known to act in parallel to *unc-6/*Netrin in guidance of commissural axons (Nash et al., 2000). Both, the *unc-129(ok1443)* deletion allele and the *unc-130(oy10)* point mutant result in an increase of axon guidance defects when combined with either the *sdn-1(zh20)* or *hse-5(tm472)* mutation (Fig. 5).

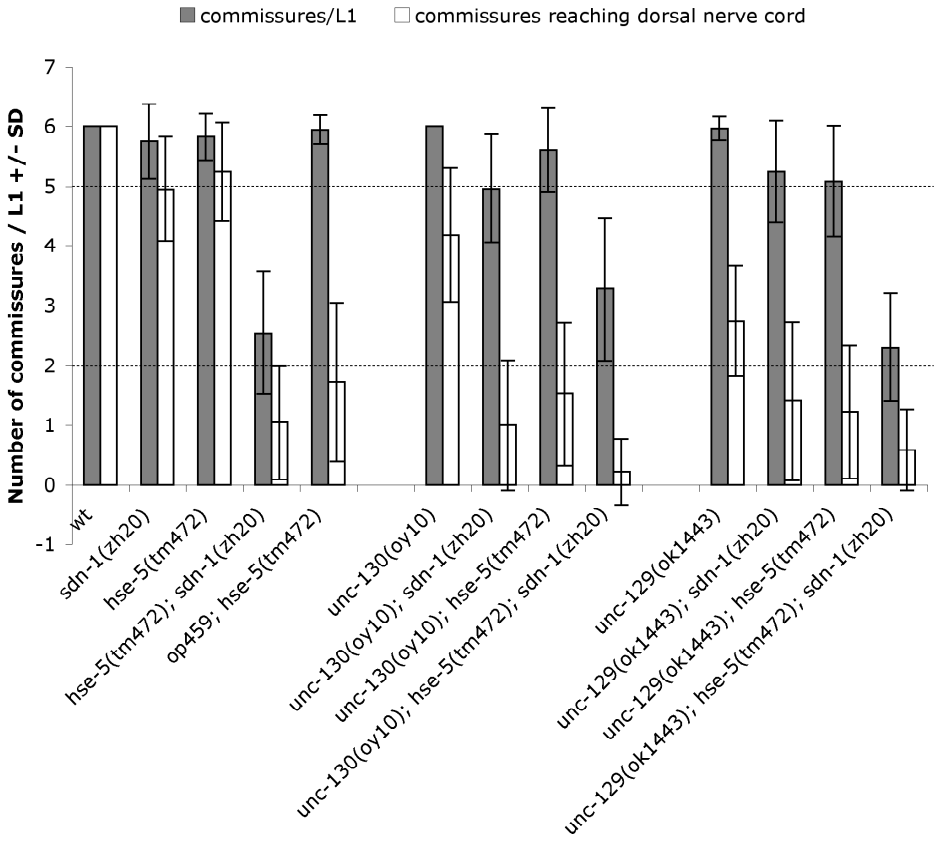

Figure 5: Mutations in *unc-129* and *unc-130* lead to considerable D-type axon guidance defects independent of HSPGs. *unc-130(oy10)* animals show less severe defects than *unc-129(ok1443)* indicating that UNC-130 is not the only protein influencing *unc-129* transcription. Nevertheless double mutants of *unc-129(ok1443)* or *unc-130(oy10)* with *sdn-1(zh20)* or *hse-5(tm472)* have comparable defects. The double mutants with *unc-129(ok1443)* show a more severe phenotype than *unc-129(ok1443)* alone but the increase is not dramatic. The triple mutants *unc-129(ok1443); hse-5(tm472); sdn-1(zh20)* and *unc-130(oy10); hse-5(tm472); sdn-1(zh20)* are indistinguishable of *hse-5(tm472); sdn-1(zh20)* pointing towards a possible function of all four genes in one pathway.

Additionally *oy10* fails to complement *op459.* The two mutations *oy10* and *op459* affect two neighbouring amino acids within the highly conserved area of the DNA binding site resulting in R218C in *oy10* (Nash et al., 2000) and R219K in *op459*. The triple mutants of *sdn-1(zh20), hse-5(tm472)* plus either *unc-129(ok1443)* or *unc-130(oy10)* have similar defects as the *sdn-1(zh20); hse-5(tm472)* double mutants, which indicates that UNC-129 and UNC-130 act in a way that may depend on HSPGs.

Netrin is the major axon guidance cue affecting guidance of D-type motor neurons

UNC-6/Netrin and its receptors UNC-5 and UNC-40/DCC have been described already in the 90s by Hedgecock et al., 1990 to be an important system required for circumferential guidance of commissural axons in *C. elegans.* Therefore we expected to hit these three genes in our screens. However, while neither mutations in *unc-6* nor *unc-40* were recovered from the screen, we found 4 different *unc-5* mutations, *op460, op468, op469* and *op477.*

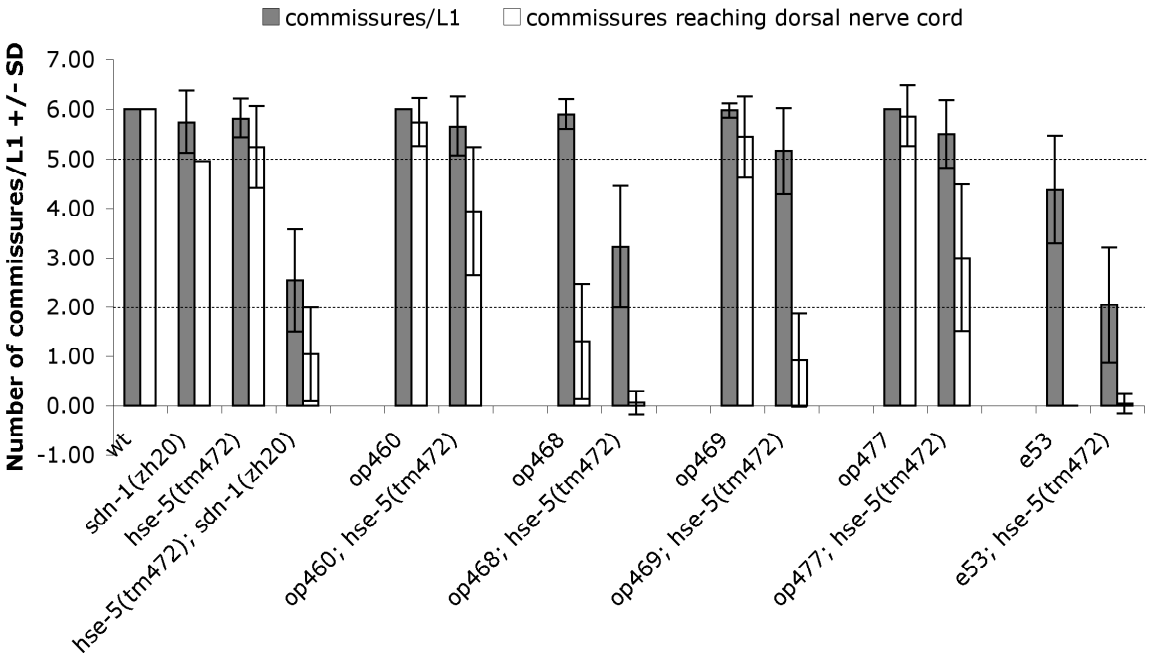

Figure 6: Effects of mutations in *unc-5.* The influence of *op460, op469* and *op477* alone is small but they lead to varying increases in defects in combination with *hse-5(tm472)*. *op468* has a clear single mutant phenotype as does *e53* the canonical null allele. Nevertheless both clearly enhance *hse-5(tm472).*

The mutations carried in these alleles are:

- *op460*: G to A transition at position 74 after the ATG resulting in C25Y.
- *op468*: 337bp deletion starting at position 1664 after the ATG making E555 be the last correct amino acid (aa), introducing 3 novel aa before creating a stop.
- *op469*: G to A transition at position 761 after the ATG resulting in G254E.
- *op477*: G to A transition at position 775 after the ATG resulting in G257R.

Of these *unc-5* mutants only *op468* has axon guidance defects in a single mutant state. The other three mutations show no phenotype in a single mutant situation but enhance *hse-5(tm472)* (Fig. 6). Based on reasoning we would expect that *unc-5, unc-6* and *unc-40* are equally sensitive for mutations in this screening setup. However our data clearly suggest that *unc-5* is very prone to being mutated, being the only gene we recovered multiple mutations for. The reason for this accumulation of mutations remains unclear.

Other candidates

Not surprisingly we also recovered mutations in a couple genes that have been described to act in guidance of D-type motor axons in the past. *op462* carries a mutation in *zag-1* (Wacker et al., 2003), *op464* has a mutation in an intron in *unc-73,* which may or may not be the relevant mutation (Merz and Culotti, 2000), and *op482* has a premature stop codon in *max-1* (Huang et al., 2002). Additionally for *op472, op474, op476* and *op480* the mutation causing the phenotype has so far not been found.

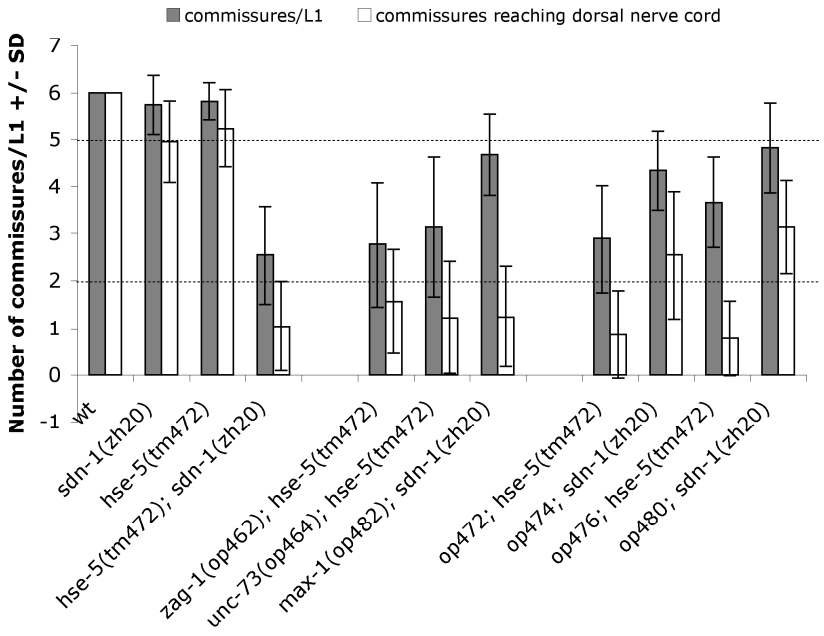

Figure 7: phenotypes of remaining candidates. For *op472, op474, op476,* and *op480* the mutations responsible for the phenotype were not found.

Discussion

Our screening efforts have lead to about one mutation in 1'600 mutagenized haploid genomes, which is a reasonable amount of mutations particularly because we screened in a sensitised background and would therefore expect to find genes that only result in minor perturbations of the system, apart from the major players *unc-5, unc-6,* and *unc-40*. However, despite the large number of genomes screened the mutagenesis has certainly not saturated the genome. Three different observations led to this interpretation. (i) From the candidate gene approaches we found genes that were not recovered in the mutagenesis. (ii) None of the mutated genes was found more than once with the notable exception of *unc-5*. (iii) We expected to isolate new *sdn-1* and/or *hse-5* alleles. These positive controls were never affected by a mutation. Therefore the screen could theoretically be continued and new candidates would possibly be found.

Our candidate gene approach for LAR signalling components revealed that *ptp-3* is acting in parallel to *sdn-1* and *hse-5* and probably in the same pathway as *lon-2*. The other tested LAR signalling components *nid-1* and *unc-10* seem not to play a role in axon guidance. Their definition as being a part of LAR signalling results from observations of synapse formation, which probably goes through different routes. It remains to be tested how PTP-3 acts in axon guidance, but it is tempting to speculate that there could be a link to UNC-6/Netrin signalling.

Not surprisingly most genes found are in some relation to the Netrin pathway, notably *max-1, zag-1, unc-129, unc-130* and the repulsive Netrin receptor *unc-5*. It is important to note that of the four *unc-5* mutations only the deletion allele *op468* has a phenotype on its own. The other three alleles *op460, op469,* and *op477* are very weak alleles that do not result in axon guidance defects in a single mutant situation. Only in combination with the *sdn-1(zh20)* or the *hse-5(tm472)* mutation clear defects appear. It has been postulated before that Netrin signalling relies on functional HSPGs. In mice commissural axons that respond to Netrin-1 fail to do so if they lack all HS, because EXT1, one of the genes responsible for initiation of HS chains is tissue specifically knocked out in those neurons (Matsumoto et al., 2007). Therefore it is interesting to speculate that a similar mechanism exists in *C. elegans* with HS chains attached to either SDN-1 or LON-2 or both being

necessary for efficient UNC-6/Netrin signalling. The fact that UNC-5 but not UNC-6 is very sensitive to even only subtle changes in its amino acid sequence points towards a direct interaction between HSPGs and UNC-5. Mutating a single amino acid in the region of UNC-5 that would normally be bound by HS may destroy the "epitope" and therefore reduce or abrogate this interaction all together.

Taking all the data from the screen together may allow for building a model, which however would need to be rigorously tested. The candidates seem to split in two groups: (1) the genes with a link to Netrin signalling (*unc-5, max-1, zag-1, unc-129, unc-130*) and (2) the genes without link to Netrin but rather PTP-3 (*lon-2, ptp-3*).

MAX-1 is known to be an intracellular component of Netrin signalling (Huang et al., 2002). Huang and co-workers hypothesise that MAX-1 could act to enrich UNC-5 at the cell membrane. ZAG-1 is a transcription factor with a fairly wide spread influence. Among other things it influences UNC-129 expression and also UNC-53 expression seems to be slightly altered (Wacker et al., 2003, Clark and Chiu, 2003). MacNeil and co-authors have shown that UNC-129 physically interacts with UNC-5 and by doing so probably increases the sensitivity of axonal growth cones to lower doses of UNC-6 (MacNeil et al., 2009). It is thought that this interaction switches the response to UNC-6/Netrin from going only through UNC-5 to the more sensitive UNC-5 + UNC-40 signalling. Since *unc-5* is very sensitive to mutations in our screen we hypothesis that there could be an interaction between UNC-5 and an HSPG, may be SDN-1. This interaction could in turn influence binding affinities of UNC-6 or UNC-129 to UNC-5.

From our double mutant analysis we conclude that PTP-3 and LON-2 act in the same pathway. Receptor protein tyrosine phosphatases (RPTPs) have been implicated in axon guidance in the past. CLR-1 for example has been shown to counteract Netrin mediated attraction of AVM neurons that send an axon ventrally towards the source of Netrin (Chang et al., 2004). Similarly PTP-3 could be responsible for dephosphorylation of components of Netrin signalling in D-type motor neurons or of a parallel pathway that also requires LON-2.

Further double mutant or biochemichal analysis would be required to test whether the UNC-6/Netrin part of the candidates in fact merges with the PTP-3 side. Additionally it is

unlikely that we have found all involved factors and in order to shed more light on the situation and gain deeper mechanistic insight the screen would need to be continued.

Materials and Methods

Strains, general handling and procedures

Standard methods were used for maintenance and handling of *C. elegans* as described by Brenner, 1974. Briefly, worms were grown on *op50* bacteria and the *C. elegans* variety Bristol N2 was used as wild type and kept at 20°C if not stated otherwise. For mapping of mutations the Hawaii variety (CB4856) was used.

The following mutations were used:

LGI: *lin-35(n745)* (Lu and Horvitz, 1998), *oxIs268*(P_{unc-47}*::gfp*) (Hammarlund et al., 2009), *lin-65(n3441)* (Ceol et al., 2006)

LGII: *ptp-3(op147* (Harrington et al., 2002)*, ok244), unc-53(ok2736), unc-130(oy10)* (Sarafi-Reinach and Sengupta, 2000), *lin-8(n2738)* (Riddle et al., 1997), *juIs76*(P_{unc-25}*::gfp; lin-15*$^{+}$) (Huang et al., 2002)

LGIII: *hse-5(tm472)* (Bülow and Hobert, 2004), *vab-7(e1562)* (Ahringer, 1996), *zfp-1(ok554* (Cui et al., 2006)*, tm3840), lin-9(n112)* (Horvitz and Sulston, 1980)

LGIV: *unc-129(ok1443), unc-5(e53)* (Brenner, 1974)

LGV: *nid-1(cg119)* (Ackley et al., 2003), *oyIs14* (Piali Sengupta), *VC5.2(ok1796, ok1797)*

LGX: *lon-2(e678)* (Brenner, 1974), *sdn-1(zh20)* (Rhiner et al., 2005), *hst-2(ok595)* (Bülow and Hobert, 2004), *gpn-1(tm588)* (Hudson et al., 2006), *unc-10(md1117)*, *oxIs12*(P_{unc-47}*::gfp; lin-15*$^{+}$) (Bülow and Hobert, 2004).

Ethyl Methanesulfonate (EMS) Enhancer screens

For mutagenesis staged *hse-5(tm472)* or *sdn-1(zh20)* mutant L4 animals carrying the *oxIs12* transgene were spun at 2000rpm and resuspended in 4ml M9 buffer. 20µl of ethyl methanesulfonate (EMS, Sigma-Aldrich, 9.7M stock solution) were added to a final concentration of about 50Mm EMS. The worms were incubated for 4h at room temperature on a rotating wheel. Following mutagenesis they were washed with M9 four times, placed on fresh, seeded plates, and allowed to recover over night at 15°C. The next morning 12 young adult hermaphrodites were chosen and distributed on 4 big, seeded

plates, 3 animals each. These P0 animals were kept at 15°C at all time for about 5 days until they stopped laying eggs. They were put on new plates twice a day in the morning and in the evening. F1 animals were grown at 20°C and removed from plates when the F2 generation reached the L1 stage. Before removal the number of F1 animals was counted to estimate the number of haploid genomes screened. When the F2s reached the adult stage they were screened for animals with severely defective D-type motor neurons. Candidates were singled out and rescreened a couple days later to confirm their adult phenotype. For screening worms were grown on NGM agarose plates to reduce background fluorescence. Commissural axon guidance phenotypes were examined with a Leica MZ16FA fluorescent dissecting microscope with a Planapo 2.0x lens. For both genetic backgrounds (*sdn-1(zh20)* and *hse-5(tm472)*) two full rounds of screening were done.

Fragment length polymorphism (FLP) mapping was performed as described by Zipperlen et al., 2005. Briefly candidates were raised in the Bristol N2 background and crossed to animals of the Hawaii (CB4856) background to map mutations based on recombination frequencies. After sampling about 200 – 300 recombinants interval sizes were narrowed to containing 100 – 300 genes that were subsequently treated with RNAi by feeding to find possible candidate genes.

Alternatively mutations were mapped to intervals of roughly 1Mb in size and then subjected to array CGH to find the mutation as described by Maydan et al., 2007 and Flibotte et al., 2009. The CGH approach was carried out in the lab of Don Moerman. Worms strains were sent and the whole procedure done by Stephane Flibotte.

As a third means to find mutations we made use of the whole genome sequencing strategy described by Sarin et al., 2008. FLP mapping was needed to map candidates to roughly 4Mb intervals. For each strain 10-15 big plates (90mm) of worms were grown up. Genomic DNA was prepared using the Gentra Puregene Tissue kit from Qiagen (cat. nr. 158622) according to manufacturers protocol. Sequencing was carried out on an Illumina sequencer by the group of Christian Beisel at the Department of Biosystems Science and Engineering (D-BSSE) of the ETH in Basel. For alignment of sequencing reads to the N2 reference and detection of mutations the MAQGene software was used (Bigelow et al., 2009).

Following identification of mutations by either means (RNAi, array CGH or whole genome sequencing) they were confirmed by standard Sanger sequencing.

Scoring of D-type axon guidance defects

D-type motor neurons were stained with the *oxIs12* (*P*$_{unc-47}$*::gfp; lin-15*$^{+}$) transgene. Two different decision points during axon outgrowth were scored in L1 animals: (i) the number of commissural axons that turn away from the VNC (commissures/L1) and (ii) the number of commissural axons that reach the DNC (commissures reaching dorsal nerve cord). In wild-type L1 animals very consistently six commissures grow out of the VNC and reach the DNC. For every genotype presented in this thesis n = 50 animals have been scored. Due to the high n statistical significance is observed for even only small phenotypic changes. In order to assign biological significance to a phenotype at least the values for "commissures reaching dorsal nerve cord" are required to be well below 5.

Equipment and software

Microscopes:	General handling: Leica MZ125
	Fluorescent dissecting scope: Leica MZ16FA
	Fluorescent microscope: Leica DMRA2
Cameras:	Fluorescent pictures: HAMAMATSU ORCA-ER
	Gel pictures: MultImage Light Cabinet of Alpha Innotech
PCR machine:	PTC-225 of MJ Research
Software:	Picture taking: Openlab 3.1.7
	Data analysis: Excel 11.1.1

References

Ackley BD, Kang SH, Crew JR, Suh C, Jin Y, Kramer JM. (2003). The basement membrane components nidogen and type XVIII collagen regulate organization of neuromuscular junctions in *Caenorhabditis elegans*. *J Neurosci.* **23**(9): 3577-87.

Ahringer J. (1996). Posterior patterning by the *Caenorhabditis elegans* even-skipped homolog *vab-7*. *Genes Dev.* **10**(9): 1120-30.

Bigelow H, Doitsidou M, Sarin S, Hobert O. (2009). MAQGene: software to facilitate *C. elegans* mutant genome sequence analysis. *Nat Methods.* 6(8): 549.

Brenner S. (1974). The genetics of *Caenorhabditis elegans*. *Genetics.* **77**(1): 71-94.

Bülow HE, Hobert O. (2004). Differential sulfations and epimerization define heparan sulfate specificity in nervous system development. *Neuron.* **41**(5): 723-36.

Ceol CJ, Stegmeier F, Harrison MM, Horvitz HR. (2006). Identification and classification of genes that act antagonistically to *let-60* Ras signaling in *Caenorhabditis elegans* vulval development. *Genetics.* **173**(2): 709-26.

Chang C, Yu TW, Bargmann CI, Tessier-Lavigne M. (2004). Inhibition of netrin-mediated axon attraction by a receptor protein tyrosine phosphatase. *Science*. **305**(5680): 103-6.

Clark SG, Chiu C. (2003). *C. elegans* ZAG-1, a Zn-finger-homeodomain protein, regulates axonal development and neuronal differentiation. *Development.* **130**(16): 3781-94.

Flibotte S, Edgley ML, Maydan J, Taylor J, Zapf R, Waterston R, Moerman DG. (2009) Rapid high resolution single nucleotide polymorphism-comparative genome hybridization mapping in *Caenorhabditis elegans*. *Genetics*. **181**(1): 33-7.

Fox AN, Zinn K. (2005). The heparan sulfate proteoglycan Syndecan is an in vivo ligand for the Drosophila LAR receptor tyrosine phosphatase. *Curr Biol.* **15**(19): 1701-11.

Gumienny TL, MacNeil LT, Wang H, de Bono M, Wrana JL, Padgett RW. (2007). Glypican LON-2 is a conserved negative regulator of BMP-like signaling in *Caenorhabditis elegans*. *Curr Biol*. **17**(2): 159-64.

Hammarlund M, Nix P, Hauth L, Jorgensen EM, Bastiani M. (2009). Axon regeneration requires a conserved MAP kinase pathway. *Science.* **323**(5915): 802-6.

Harrington RJ, Gutch MJ, Hengartner MO, Tonks NK, Chisholm AD. (2002). The *C. elegans* LAR-like receptor tyrosine phosphatase PTP-3 and the VAB-1 Eph receptor tyrosine kinase have partly redundant functions in morphogenesis. *Development.* **129**(9): 2141-53.

Hedgecock EM, Culotti JG, Hall DH. (1990). The *unc-5*, *unc-6*, and *unc-40* genes guide circumferential migrations of pioneer axons and mesodermal cells on the epidermis in *C. elegans. Neuron* **4**(1): 61-85.

Horvitz HR, Sulston JE. (1980). Isolation and genetic characterization of cell-lineage mutants of the nematode *Caenorhabditis elegans. Genetics*. **96**(2): 435-54.

Huang X, Cheng HJ, Tessier-Lavigne M, Jin Y. (2002). MAX-1, a novel PH/MyTH4/FERM domain cytoplasmic protein implicated in netrin-mediated axon repulsion. *Neuron*. **34**(4): 563-76.

Hudson ML, Kinnunen T, Cinar HN, Chisholm AD. (2006). *C. elegans* Kallmann syndrome protein KAL-1 interacts with Syndecan and Glypican to regulate neuronal cell migrations. *Dev Biol.* **294**(2): 352-65.

Johnson KG, Tenney AP, Ghose A, Duckworth AM, Higashi ME, Parfitt K, Marcu O, Heslip TR, Marsh JL, Schwarz TL, Flanagan JG, Van Vactor D. (2006). The HSPGs Syndecan and Dallylike bind the receptor phosphatase LAR and exert distinct effects on synaptic development. *Neuron.* **49**(4): 517-31.

Kinnunen T, Huang Z, Townsend J, Gatdula MM, Brown JR, Esko JD, Turnbull JE. (2005). Heparan 2-O-sulfotransferase, *hst-2*, is essential for normal cell migration in *Caenorhabditis elegans*. *Proc Natl Acad Sci U S A*. **102**(5): 1507-12.

Lu X, Horvitz HR. (1998). *lin-35* and *lin-53*, two genes that antagonize a *C. elegans* Ras pathway, encode proteins similar to Rb and its binding protein RbAp48. *Cell.* **95**(7): 981-91.

MacNeil LT, Hardy WR, Pawson T, Wrana JL, Culotti JG. (2009). UNC-129 regulates the balance between UNC-40 dependent and independent UNC-5 signaling pathways. *Nat Neurosci.* **12**(2): 150-5.

Maydan JS, Flibotte S, Edgley ML, Lau J, Selzer RR, Richmond TA, Pofahl NJ, Thomas JH, Moerman DG. (2007). Efficient high-resolution deletion discovery in *Caenorhabditis elegans* by array comparative genomic hybridization. *Genome Res*. **17**(3):337-47.

Matsumoto Y, Irie F, Inatani M, Tessier-Lavigne M, Yamaguchi Y. (2007). Netrin-1/DCC signaling in commissural axon guidance requires cell-autonomous expression of heparan sulfate. *J Neurosci*. **27**(16): 4342-50.

Merz DC, Culotti JG. (2000). Genetic analysis of growth cone migrations in *Caenorhabditis elegans. J. Neurobiol*. **44**(2):281-8.

Nash B, Colavita A, Zheng H, Roy PJ, Culotti JG. (2000). The forkhead transcription factor UNC-130 is required for the graded spatial expression of the UNC-129 TGF-beta guidance factor in *C. elegans*. *Genes Dev.* **14**(19): 2486-500.

Riddle DL, Blumenthal T, Meyer BJ, Priess JR. (1997). Introduction to *C. elegans* . *Cold Spring Harbor Laboratory Press*. *C. elegans* II. 2nd edition.Chapter 1.

Sarafi-Reinach TR, Sengupta P. (2000). The forkhead domain gene *unc-130* generates chemosensory neuron diversity in *C. elegans. Genes Dev.* **14**(19): 2472-85.

Sarin S, Prabhu S, O'Meara MM, Pe'er I, Hobert O. (2008). *Caenorhabditis elegans* mutant allele identification by whole-genome sequencing. *Nat Methods*. **5**(10): 865-7.

Schmidt KL, Marcus-Gueret N, Adeleye A, Webber J, Baillie D, Stringham EG. (2009). The cell migration molecule UNC-53/NAV2 is linked to the ARP2/3 complex by ABI-1. *Development.* **136**(4): 563-74.

Stringham E, Pujol N, Vandekerckhove J, Bogaert T. (2002). *unc-53* controls longitudinal migration in *C*. *elegans*. *Development* **129**(14): 3367-79.

Stryker E, Johnson KG. (2007). LAR, liprin alpha and the regulation of active zone morphogenesis. *J Cell Sci.* **120**(Pt 21): 3723-8.

Rhiner C, Gysi S, Fröhli E, Hengartner MO, Hajnal A. (2005). Syndecan regulates cell migration and axon guidance in *C. elegans. Development.* **132**(20): 4621-33.

Wacker I, Schwarz V, Hedgecock EM, Hutter H. (2003). *zag-1*, a Zn-finger homeodomain transcription factor controlling neuronal differentiation and axon outgrowth in *C. elegans*. *Development*. **130(**16): 3795-805.

Zipperlen P, Nairz K, Rimann I, Basler K, Hafen E, Hengartner M, Hajnal A. (2005). A universal method for automated gene mapping. *Genome Biol*. **6**(2): R19.

CHAPTER III

The Strange Case of *zfp-1* and *lin-35*

Preface

In the screen described in chapter II we identified a number of candidates. Among them were the two genes *zfp-1* and *lin-35* that seemed to be very interesting and unexpected candidates, which is why we decided to put our focus on them.

ZFP-1 and LIN-35 seem to have opposing function

LIN-35 has received a fair amount of attention in the past because it has been found to be the *C. elegans* homologue of the human Retinoblastoma Protein (RB). Originally the gene *lin-35* has been discovered due to its function in vulval development in a screen for synthetic multivulva genes (SynMuv genes) (Ferguson and Horvitz, 1989). SynMuv genes can be split in three classes SynMuvA/B/C genes. Any single mutant shows no aberrant vulval development, the same being true for double mutants of genes placed in the same class. However if two genes of different classes are mutated animals show the characteristic multivulva phenotype. ZFP-1 is a zinc finger protein that has been found to play a role in *C. elegans* vulva development by counteracting SynMuv genes such as *lin-35* (Cui et al., 2006). Cui et al. find that a mutation in or RNAi against *zfp-1* leads to a suppression of the multi vulva phenotype of SynMuvA/B double mutants. Additionally there is evidence that ZFP-1 acts in the RNAi pathway and does this again in an opposite manner to SynMuv genes (Lehner et al., 2006). Dudley and co-workers report that lethality resulting from injection of dsRNA against various lethal genes can be counteracted unspecifically by coinjecting *zfp-1* dsRNA, indicating that RNAi against *zfp-1* has a negative effect on the efficiency of RNAi (Dudley et al., 2002). Many SynMuv genes on the other hand have been found to increase the efficiency of RNAi when mutated and in particular mutations in *lin-35* are often used to sensitise worms to RNAi. However not all RNAi sensitive *C. elegans* mutants are belonging to the class of SynMuv genes (Wang et al., 2005). While a mechanistic insight in how these two functions are coming about is missing there is increasing evidence that ZFP-1 is playing a role in regulation of transcription. Grishok et al. showed in 2005 that genes required for proper execution of the RNAi pathway, such as *rde-1* or *rrf-1* lead, when mutated, to desilencing of a repetitive transgene. This same effect has been observed for *zfp-1*

(Grishok et al., 2005). In a microarray study the same authors found that in *zfp-1* mutants as well as *lin-35* mutants a large number of genes is deregulated, in both cases leading to approximately 400 – 500 up-regulated genes and a similar number of significantly down-regulated genes (Grishok et al., 2008). In their first study the authors conclude that the silencing effect mediated by ZFP-1 is reducing transcription itself, rather than degrading mRNA such as in standard RNAi. In the second publication they detect an accumulation of putative target genes of endogenous siRNAs among genes up-regulated in *zfp-1, lin-35* and *rde-4* mutants. Taken together these reports show that ZFP-1 and LIN-35 have a major and broad influence on transcription.

Both genes *zfp-1* and *lin-35* have clear homologues in mammals. *lin-35* is the sole *C. elegans* Rb homologue and *zfp-1* is homologous to AF10, a gene that has received attention primarily because of its involvement in paediatric acute myeloid leukaemia (AML) (Chaplin et al., 1995), a rather severe type of leukaemia affecting children at an age between 2 and 10 years. In this type of leukaemia chromosomal translocations are often found to be the reason for the onset of the disease. These translocations happen between a gene called MLL (mixed lineage leukaemia) and one of more than 60 possible fusion partners of which AF10 is the second most frequent accounting for about 13% of all MLL rearranged paediatric AML cases. Depending on the MLL fusion partner patients have different outcomes. The MLL-AF10 fusion is characterized by rather poor prognosis with a 5 year overall survival rate of about 45% (Balgobind et al., 2011). The AF10 protein and its *C. elegans* homologue ZFP-1 contain a zinc finger at their N terminal end and an octapeptide motive (OM) and a leucin zipper (LZ) in their C-terminal portion. MLL-AF10 fusions are always in frame leading to a functional fusion protein retaining the OM and the LZ of AF10 and the N terminal portion of MLL. This OM-LZ region of AF10 has been found to be required for leukaemogenesis since it is necessary for binding of the MLL-AF10 fusion protein to hDOT1L, a histone methyltransferase. This interaction in turn leads to hypermethylation of lysine 79 on histone 3 in particular in the region of Hoxa9, resulting in over-expression of Hoxa9 and ultimately leukaemogenesis (Okada et al., 2005).

Also RB1, the gene coding for the Retinoblastoma protein pRb, has a long history in cancer research. It is a tumour suppressor gene and has ever since received a lot of

attention because a mutation in RB1 alone seems to be sufficient to induce a cancer (Friend et al., 1986). While the typical RB1 mutation induced retinoblastoma always appears during childhood carriers of a mutant RB1 allele have an increased risk to develop secondary cancers. For example in small cell lung cancer RB1 is mutated in about 90% of the cases (for a comprehensive review of pRb function in cancer and development refer to Chinnam and Goodrich, 2011). Indeed deregulation of the anti growth pathway in which pRb functions is found in virtually every type of cancer examined to date (Hanahan and Weinberg, 2000). The reasons for these divers consequences of a RB1 mutation could be explained by the fact that pRb is a transcriptional regulator influencing a whole range of processes during development. The diversity of functions of pRb are a result of the ability of pRb to interact with more than 150 different proteins and even act as an adaptor by interacting with more than one protein at a time (Morris and Dyson, 2001). Most data has been accumulated regarding the interaction of pRb and its family members p107 and p130 with E2F transcription factors. E2F family members can have either activating or repressive function on transcription of a target gene. Interaction of E2Fs and pRb usually has a negative effect on transcription, which can happen in at least three different ways. First, by binding to activator E2Fs pRb competes with other E2F binding partners that have a positive effect on transcription. Second, recruitment of pRb to a promoter via E2F proteins can counteract the activity of other transcription factors in the vicinity. Third, once located at a promoter pRb can negatively regulate transcription by recruiting chromatin remodelling factors to initiate the formation of closed chromatin that is unfavourable for transcription (reviewed by Frolov and Dyson, 2004).

Results

op481 carries a premature stop codon in *zfp-1*

FLP mapping of the candidate *op481* indicated that a gene on the right arm of chromosome III between the FLP markers snp_F22B7[1] and snp_ZK643[1] is affected. Of the 74 gene contained in this interval 49 have a clone in the Ahringer RNAi library (Kamath and Ahringer, 2003) and were chose for RNAi knock down. Only the clone targeting *zfp-1* gave an axon guidance phenotype in the *sdn-1(zh20); eri-1(mg366)* double mutant. The *eri-1(mg366)* mutation was used to render worms more susceptible to RNAi (Kennedy et al., 2004). Sequencing of *zfp-1* in *op481* revealed a premature stop codon in the third last exon of the gene (Fig. 1).

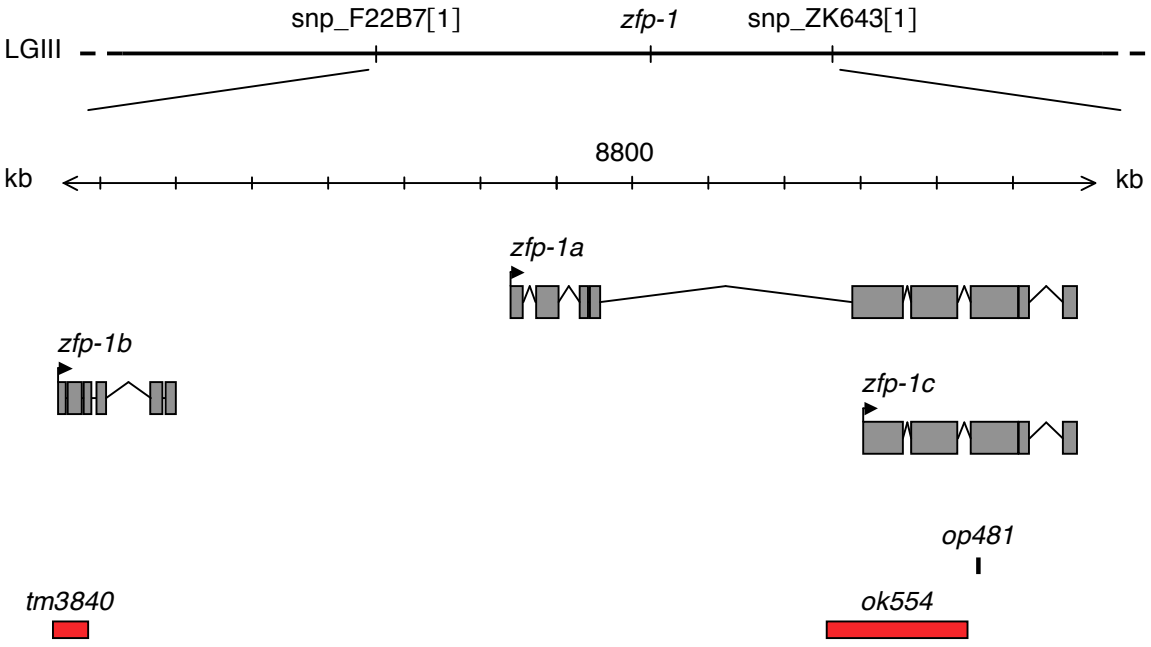

Figure 1: Genomic organization of the *zfp-1* locus. The two alleles *ok554* and *op481* affect the same two isoforms. While *ok554* is a deletion truncating the A isoform and deleting the ATG of the C isoform *op481* introduces a premature stop codon in the third last exon of the A and the C isoform. The *tm3840* deletion covers the putative ATG of the distant B isoform, which however most likely does not belong to the *zfp-1* locus.

According to wormbase gene predictions (www.wormbase.org) there are three different isoforms and two deletion alleles available. *tm3840* affects the distant ZFP-1B isoform, which may not be transcribed at all. *tm3840* has no effect on axon guidance (Fig. 2). *ok554* is a deletion in the ZFP-1A and ZFP-1C isoforms, which are also affected by the *op481* point mutation. *ok554* and *op481* have identical effects on axon guidance (Fig. 2). All domains conserved between ZFP-1 and AF10 are contained in the ZFP-1A isoform. We believe that ZFP-1B is either a wrong gene prediction or a different gene and are therefore focussing our studies on ZFP-1A and C. In an attempt to find which of the two remaining isoforms of *zfp-1* are involved in axon guidance Ronny Egli (a master student working on the project) tried to generate extrachromosomal arrays containing either a long (ZFP-1A) or a short (ZFP-1C) rescue construct. However the establishment of transgenic animals in a *zfp-1* mutant background turned out to be difficult and the single lines obtained for the two constructs both showed only a very weak rescue (data not shown). To gain more knowledge about which isoform is important for the screening phenotype a mutation affecting only the ZFP-1A isoform would be needed but is currently not available yet.

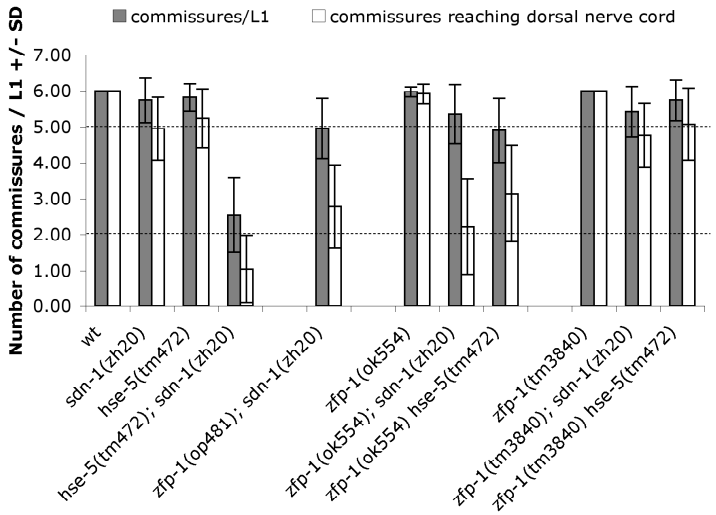

Figure 2: Effect of different *zfp-1* alleles. While *op481* and *ok554* behave identical *tm3840* has no influence on axon guidance in worms carrying either the *sdn-1(zh20)* or *hse-5(tm472)* deletions plus the *oxIs12* transgene.

A mutation in *lin-35* enhances the *sdn-1(zh20)* mutant

With the aim of producing an RNAi sensitive strain carrying the *sdn-1(zh20)* mutation and the *oxIs12* transgene we built the *lin-35(n745); sdn-1(zh20) oxIs12* double mutant

strain. The idea was to use this strain for RNAi of candidate genes even before we started the mutagenesis screen. However, to our great surprise these animals showed increased axon guidance defects without application of RNAi (Fig. 3) and this strain was therefore unusable for RNAi approaches. When we found that candidate *op481* was carrying a premature stop codon mutation in the gene *zfp-1* our attention was drawn back to the *lin-35(n745); sdn-1(zh20) oxIs12* strain because, as Cui and co-workers reported in 2006, *zfp-1* is a SynMuv suppressor gene and *lin-35* a SynMuv gene. While both genes when mutated lead to a similar and moderate increase in axon guidance defects in parallel to *sdn-1*, they do not enhance each other (Fig. 3).

oxIs12 influences the phenotype of *zfp-1* and *lin-35* mutants

In *C. elegans* transgenes are usually produced by labelling them with a coinjection marker. In the old days a marker that was often used was a rescuing fragment for the *lin-15A* and *lin-15B* genes, leading to an over-expression of these two genes from the

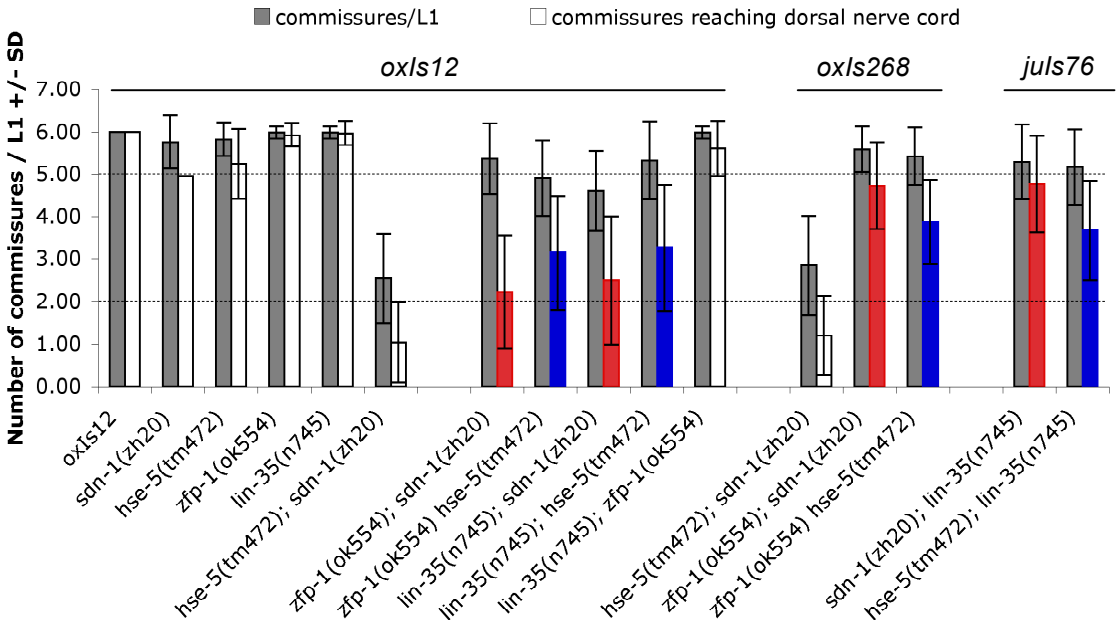

Figure 3: Defects of *zfp-1(ok554)* mutants compared to those of *lin-35(n745)* mutants with different transgenes to stain D-type motor neurons. While both *zfp-1* and *lin-35* mutations lead to a clear increase in axon guidance defects in the *sdn-1(zh20)* background if *oxIs12* is present, these defects almost entirely disappear if *oxIs268* or *juIs76* are used to stain the D-type motor axons (compare the red bars for the different genotypes). The effect is less dramatic for the *hse-5(tm472)* background (blue bars).

transgene. This procedure was used to create the *oxIs12* transgene. Since *lin-15A* and *lin-15B* are themselves SynMuv genes we decided to check the effect of the *zfp-1(ok554)* and the *lin-35(n745)* mutations on axon guidance by using two other transgenes called *oxIs268* and *juIs76* as alternatives to *oxIs12.* All three transgenes label the same neurons but *oxIs268* contains no *lin-15(+)* fragment. To our great surprise the defects of *zfp-1(ok554); sdn-1(zh20)* and *lin-35(n745); sdn-1(zh20)* double mutants were greatly reduced if any other transgene than *oxIs12* was used to label D-type motor neurons (Fig.3).

lin-15A and _lin-15B_ and other SynMuv genes do not influence guidance of D-type motor neurons

A first possible explanation for the transgene dependency of *zfp-1* and *lin-35* mutants was that over-expression of *lin-15A* and *lin-15B* from the transgene could be responsible for this finding. *lin-15B* mutations as well as mutations in some other SynMuv genes have been described to influence RNAi in a similar way as *lin-35* mutations (Wang et al., 2005). To test these possibilities we took two approaches:

(1): If *lin-15* over-expression is responsible for the transgene effect, it should be possible to reproduce the defects observed in *zfp-1(ok554); sdn-1(zh20) oxIs12* animals by reintroducing *lin-15* over-expression in *oxIs268; zfp-1(ok554); sdn-1(zh20)*. For this approach we chose to cross the *oyIs14* transgene, that carries a *lin-15(+)* fragment into *oxIs268; zfp-1(ok554); sdn-1(zh20)*. However *oxIs268; oyIs14; zfp-1(ok554); sdn-1(zh20)* animals do not show increased axon guidance defects (Fig. 4A). Additionally a third transgene labelling the D-type motor neurons, *juIs76*, which contains a *lin-15(+)* fragment did also not result in the same effect as *oxIs12* (Fig. 3).

(2): We chose to test mutations in *lin-8*, *lin-9*, and *lin-65* to test the involvement of other SynMuv genes (Fig. 4B). Additionally we knocked down all SynMuv genes as listed in Fay and Yochem, 2007 by RNAi (for a list of all genes knocked down by RNAi in this study see Materials and Methods). Also these approaches showed no *zfp-1* or *lin-35* like function of other SynMuv genes.

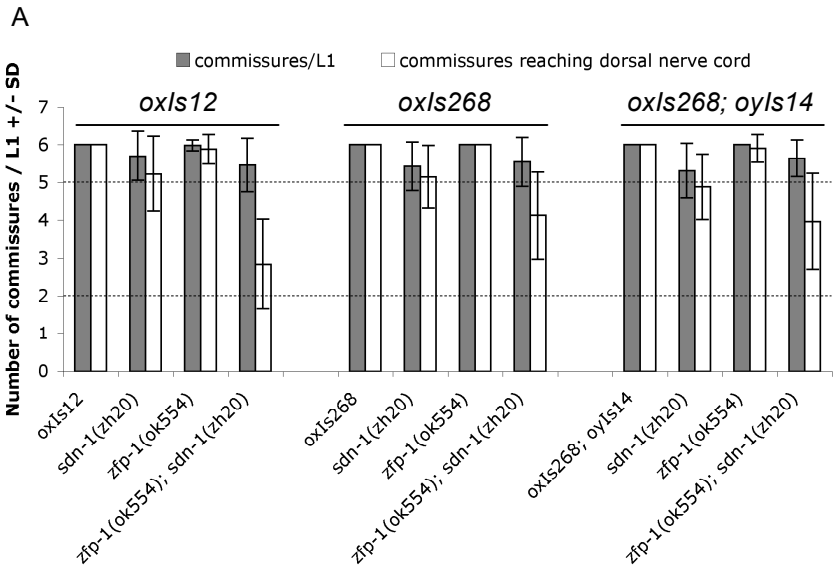

Figure 4A: Over-expression of *lin-15AB* is not the reason for the trans-gene effect of *zfp-1* mutants. Only if *oxIs12* is present the *zfp-1; sdn-1* double mutant has clear de-fects. If *oxIs268* is used to stain axons defects are weaker and bringing back *lin-15* over-expression with the *oyIs14* trans-gene leads to no change in phenotype.

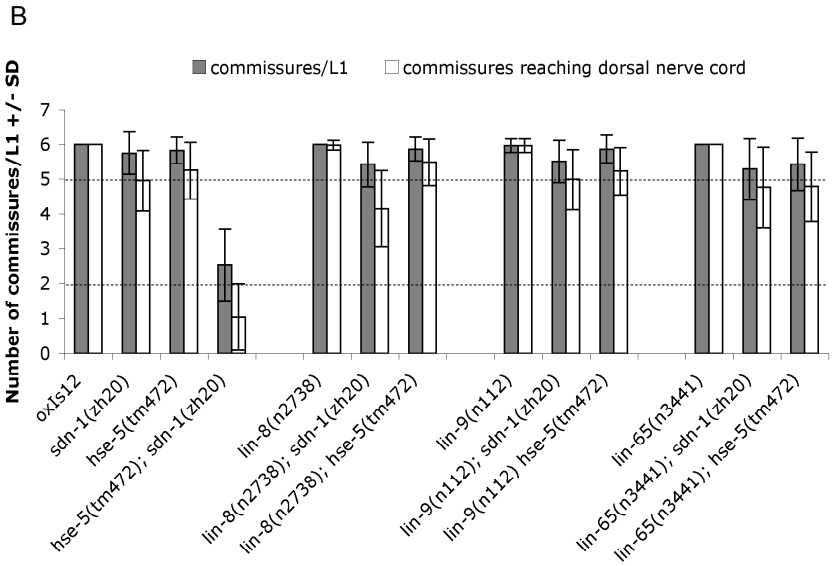

Figure 4B: SynMuv genes do not gene-rally have an effect on axon guidance. Mutations in *lin-8, lin-9* and *lin-65* do not lead to an increase in D-type motor axon guidance in the *sdn-1(zh20)* or *hse-5(tm472)* background.

Search for genes that are transcriptionally influenced by ZFP-1 and LIN-35

Since we considered it unlikely that ZFP-1 and LIN-35 have a direct influence on axon guidance but rather regulate transcription of an as yet unknown target gene, we hoped to gain further insight to the function of ZFP-1 and LIN-35 by finding this putative target gene. Grishok et al., 2008 have carried out a microarray study on mutations in both of these genes. In their list of genes with significantly altered transcription we found the

gene *VC5.2*, which wormbase (www.wormbase.org) predicts to be a basement membrane HSPG core protein of the Perlecan type, making it a high priority target for us. Furthermore Bahri et al., 2001 described the *Drosophila* homologue of *zfp-1* (*Dalf*) to be required for maintenance of *even-skipped* expression. The *C. elegans* homologue of *even-skipped* is *vab-7*. Both mutations in *VC5.2* (*ok1796* and *ok1797*) as well as the *vab-7(e1562)* mutation did not enhance *sdn-1(zh20)* or *hse-5(tm472)* (Fig. 5). In addition we knocked down by RNAi genes that were found to be commonly down regulated in *lin-35(n745)* and *zfp-1(ok554)* with no positive result.

Since it has been hypothesised that ZFP-1 and LIN-35 are acting in the endo-siRNA pathway (Grishok et al., 2008) we also tested whether RNAi against any of the known Argonaute genes of *C. elegans* (Yigit et al., 2006) would reproduce the phenotype of a *zfp-1* or *lin-35* mutation. However none of the RNAi clones (see Materials and Methods) resulted in guidance defects in D-type motor neurons in an *eri-1(mg366); sdn-1(zh20) oxIs12* strain (data not shown).

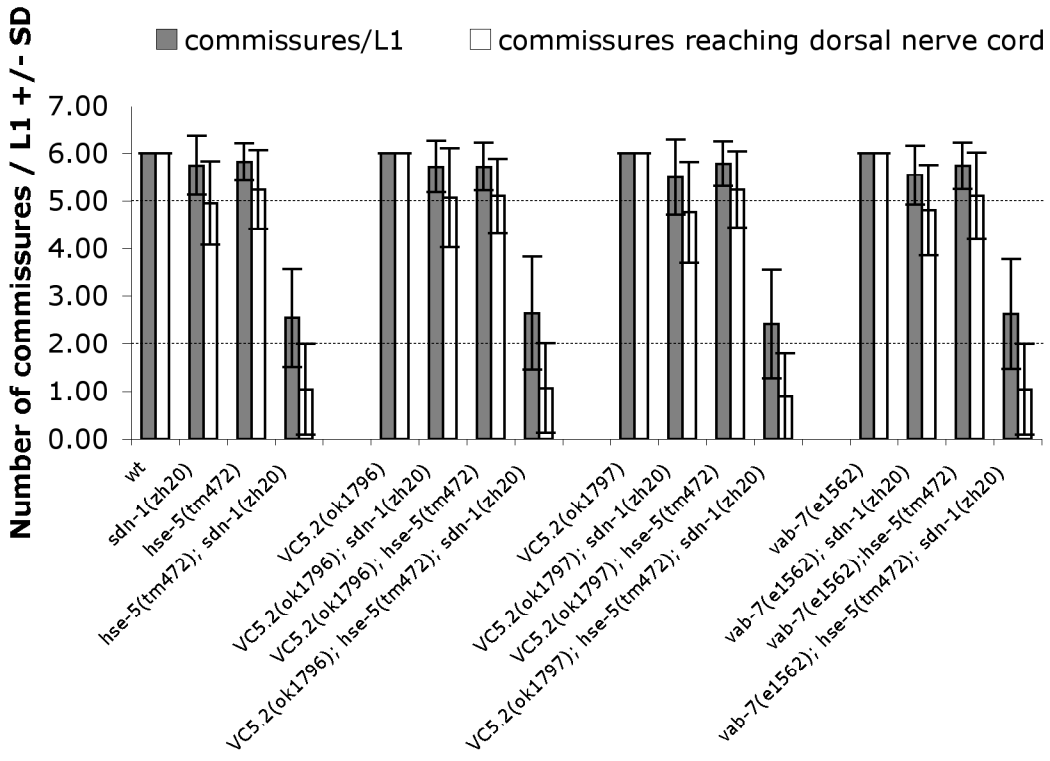

Figure 5: Search for a possible target gene of LIN-35 and ZFP-1. None of the two possible target genes *VC5.2* and *vab-7* showed a phenotype comparable to *zfp-1* or *lin-35* mutants.

Detection of the precise site of integration of *oxIs12*

The above-mentioned data led us to conclude that the integration site rather than the composition of *oxIs12* is the reason why *zfp-1(ok554); sdn-1(zh20) oxIs12* and *lin-35(n745); sdn-1(zh20) oxIs12* animals show axon guidance defects. Therefore we used the whole genome sequencing (WGS) data sets originally obtained to find mutations to identify the precise integration site of *oxIs12*. Knowing that *oxIs12* is in an interval of +/- 1cM around *sdn-1* we were able to find the integration site by manually going through the alignments (for a detailed description of the procedure see Materials and Methods of this chapter). *oxIs12* was found to be located between the genes *grd-1* and *R08B4.5* introducing a short deletion of 232bp including the last 25bp of the *grd-1* 3'UTR (Fig. 6A).

According to the original publication mentioning *oxIs12* (McIntire et al., 1997) it was first raised in an extrachromosomal array that was subsequently integrated. Two constructs were used: EK L15 (*lin-15(+)*) was used as coinjection marker and the *unc-47::gfp* construct that was constructed by digesting a 5.2kb *BamHI* fragment out of cosmid *T20G5* containing the whole *unc-47* open reading frame and inserting *gfp* followed by a 553bp part of the *unc-54* 3'UTR in a native *BspHI* site 470bp downstream of the *unc-47* ATG. In order to estimate the size of *oxIs12* from the WGS data set we compared the coverage at the *lin-15, unc-47,* and *unc-54* loci to the average coverage of the whole chromosomes X, III, and I respectively. We assumed that most sequencing reads from the two constructs *lin-15(+)* and *unc-47::gfp* would align at the place of the endogenous gene. While the average coverage on LGX is 76.23x there is a very steep increase in coverage across the *lin-15* locus resulting in an average coverage at this locus of 11'030x across a stretch of 10970bp (Fig. 6B). The picture looks similar for the *unc-47* locus with an average coverage of 70.04x for LGIII and an average of 11'800x at *unc-47* across 5180bp. For *unc-54* we found a region of 411bp in the *unc-54* 3'UTR with an average coverage of 9359x while the average for LGI is 71.29x. This means that there are about 144 copies of the *lin-15(+)* construct and roughly 168 copies of the *unc-47::gfp* construct. The fact that we only find 131 copies of the *unc-54* fragment of the *unc-47::gfp* construct reflects the highly variable coverage for all the three regions indicating that most copies of the two constructs are not complete. Additionally we estimate the

presence of about 150 copies of *gfp* sequence with a length of 867bp. The size of the backbones of the two plasmids is estimated to be roughly 3kb and in total we set the number of backbones present in the transgene to 312. Summing this up results in an estimated size of *oxIs12* of about 3.6Mb.

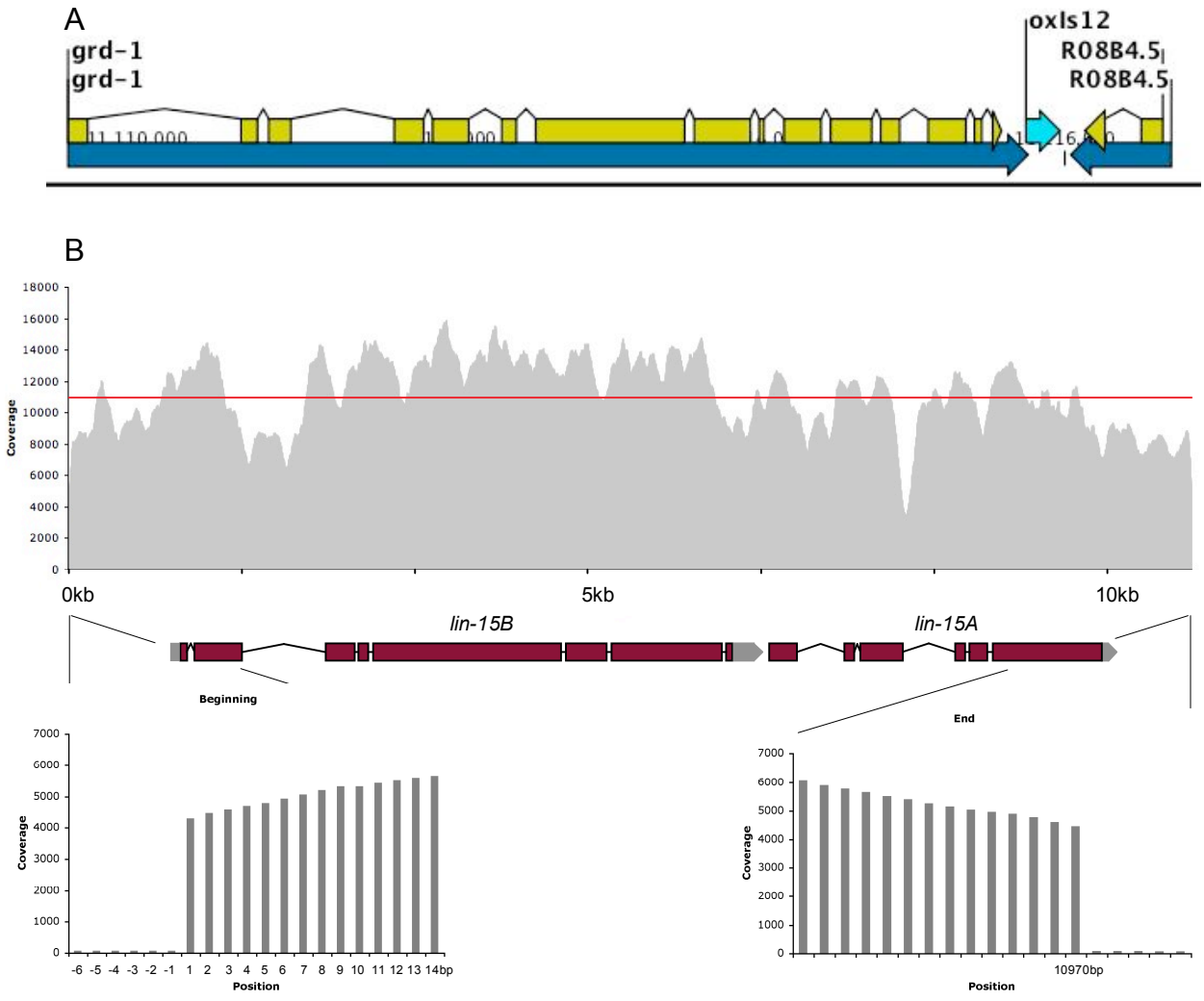

Figure 6: Site of integration and degree of repetitivity of *oxIs12*. A: *oxIs12* is inserted at the very end of the 3'UTR of *grd-1*. Yellow boxes represent exons, the blue thick arrow comprises introns, exons and the predicted UTRs, the turquoise arrow shows the size of the deletion introduced by *oxIs12*. B: coverage across the *lin-15AB* locus with the gene organization of *lin-15A* and *lin-15B*. At the beginning and the end coverage drops off steeply to about 50x at the first/last base pair contained in the transgene (see enlargements of the beginning and the end). The red line represents the average of about 11'000x coverage.

Could ZFP-1 and LIN-35 influence chromatin remodelling in the context of repetitive chromosomal regions?

As mentioned previously ZFP-1 and LIN-35 have been implicated in chromatin remodelling (Cui et al., 2006). This prompted us to inspect the close environment of *oxIs12* on LGX and indeed we found that the ATG of *hst-2* is located only 91kb away from the integration site. Since mutations in *hst-2* are known to enhance the defects of an *sdn-1(zh20)* mutant (Fig. 1, chapter II) we hypothesised that ZFP-1 and LIN-35 could in fact have a chromatin remodelling function, thereby influencing the silencing mechanisms acting on *oxIs12* in a way that leads to a repression of *hst-2* transcription in *zfp-1(ok554); oxIs12* and *lin-35(n745); oxIs12* animals. We envisioned two possible mechanisms:

(1): ZFP-1 and LIN-35 act directly in the pathway leading to silencing of the repetitive transgene. In *zfp-1(ok554); oxIs12* and *lin-35(n745); oxIs12* animals the transgene is over-repressed and this increased silencing is spreading up to the *hst-2* locus.

(2): ZFP-1 and LIN-35 are involved in the spreading of the silencing coming from the transgene, may be by influencing some sort of boundary mechanisms. In the mutants the boundary mechanisms is not as effective as in animals carrying only the *oxIs12* transgene, which allows the silencing to spread up to *hst-2.*

To test this hypothesis and to distinguish between these two possibilities we performed qRT PCR. Obtaining stable qRT PCR data turned out to be a problem. Internal standardisation to house keeping genes (*mpk-1, tbp-1, pgk-1*) seemed to be problematic because the expression of these house-keeping genes fluctuated dramatically between samples. Therefore we used an external standardisation method, briefly we chose to spike *Arabidopsis thaliana* RNA into worm RNA samples to then normalize to three *Arabidopsis* genes, chosen according to Czechowski et al., 2005 (for a precise description of the workflow see Materials and Methods). While this strategy led to more stable results than before, the quality of the data after 3 independent runs is still debatable. Basically the results indicate that transcription from the X chromosome is generally slightly reduced in *zfp-1(ok554); oxIs12* animals compared to animals with either only the *zfp-1(ok554)* mutation or the *oxIs12* transgene (Fig. 7A).

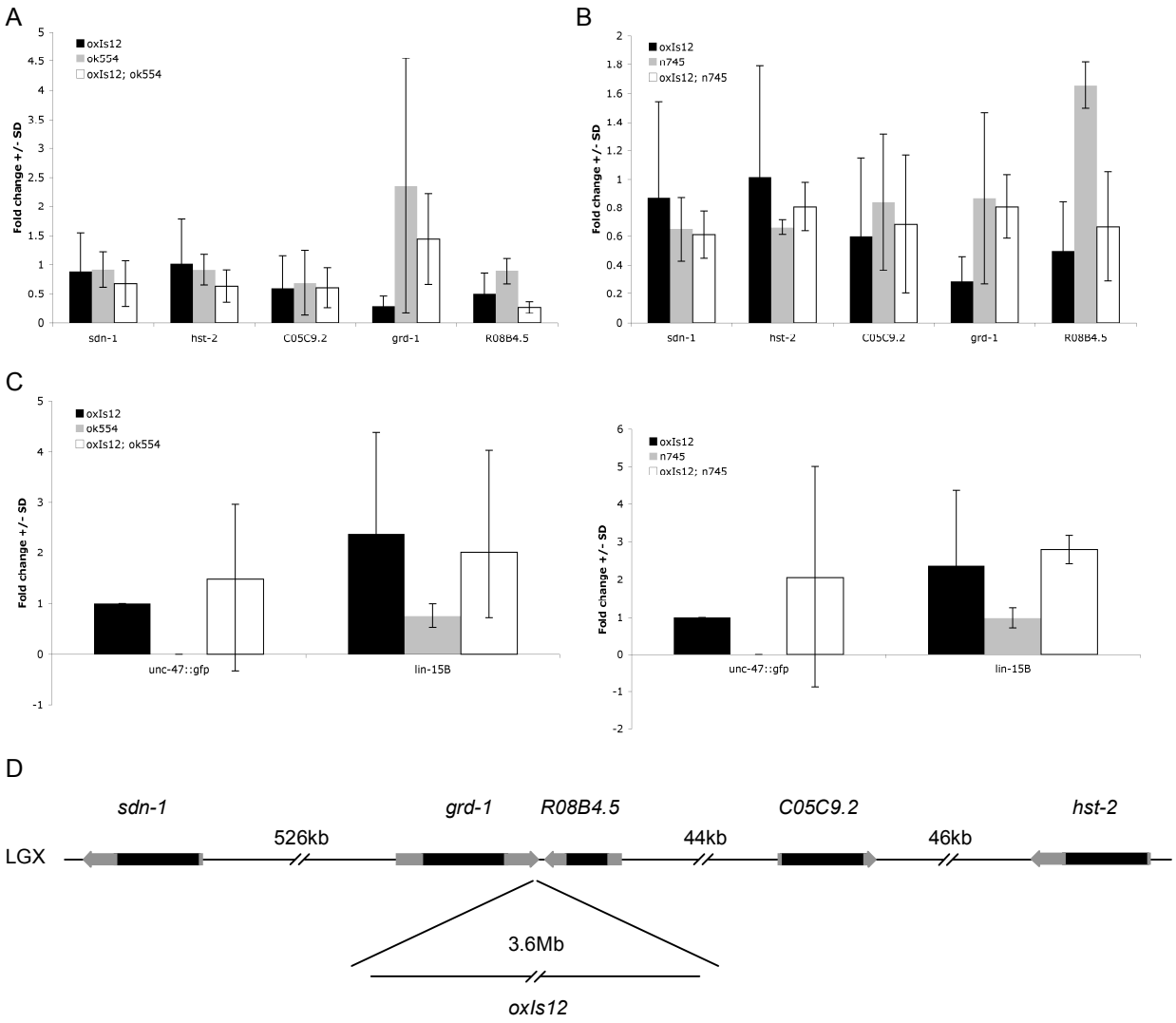

Figure 7: Assay of transcription by qRT PCR. If only the *oxIs12* transgene is present there is a clear reduction of transcriptional rates towards the transgene (black bars in A and B, for the organization of genes on the X chromosome and distance from the *oxIs12* transgene see 7D). A: The *zfp-1(ok554)* mutant (grey bars) leads to no significant changes except may be an over-expression of *grd-1*, however standard deviations are huge and this data should be taken with caution. In *zfp-1(ok554); oxIs12* animals transcription for all the genes rather seems to be reduced. B: In *lin-35(n745); oxIs12* animals transcription of the X chromosome seems equally reduced and the silencing trend towards the *oxIs12* transgene is not visible anymore. C: Transcription from the transgene seems not to be greatly changed if *zfp-1(ok554)* or *lin-35(n745)* are present. It is interesting to note that *oxIs12*, despite its high degree of repetitivity only leads to a two to three fold over-expression of *lin-15B*. D: Cartoon showing the organization of tested genes on the X chromosome plus distances between genes. (qRT PCR data +/- SD from three independent runs)

A similar tendency is visible for *lin-35(n745); oxIs12* animals (Fig. 7B). Testing transcription from the transgene reveals that *lin-15* and *unc-47::gfp* expression remains more or less unchanged (Fig. 7C).

In an attempt to shed further mechanistic light onto this process we performed RNAi against genes known or predicted to be Methyl-/Acetyltransferases, Demethylases or Deacetylases. However none of these RNAi clones resulted in a phenotype comparable to *zfp-1* RNAi (see Materials and Methods section for a complete list of RNAi clones).

Epistasis analysis

Since we hypothesised that ZFP-1 could influence transcription of another gene we sought to test whether one of the other candidates of the screen could be this target gene via epistasis. We decided to test *unc-53* and *unc-129/130*. Animals doubly mutant for *zfp-1* and either *unc-53* or *unc-129* did not show an increase in axon guidance defects. This would point towards an action in a common pathway. However in the light of the data presented earlier this epistasis analysis cannot be interpreted. There was a slight increase of defects in the *unc-53(ok2736); unc-129(ok1443)* compared to the *unc-129(ok1443)* single mutant pointing out that they have at least partially parallel function (Fig. 8).

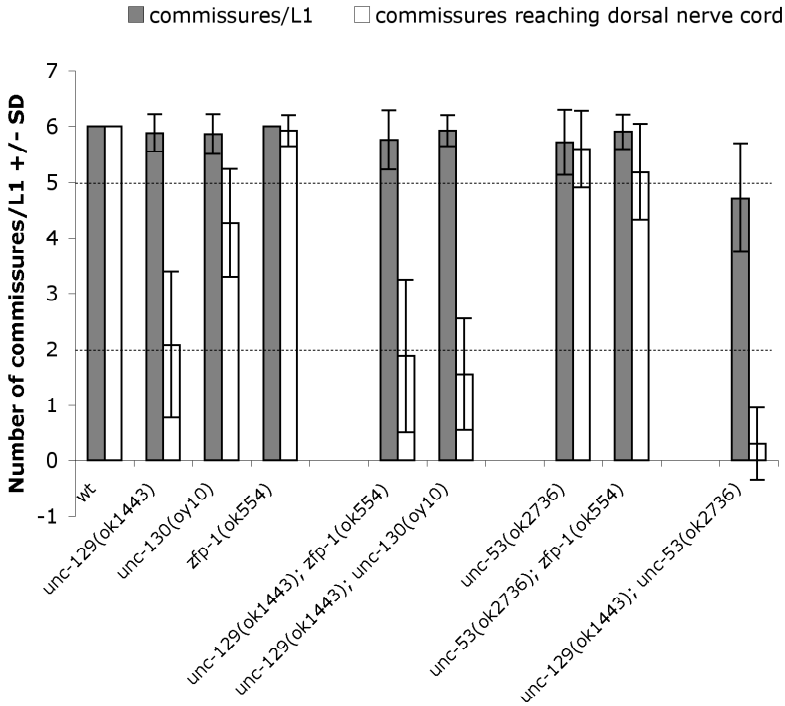

Figure 8: Epistasis analysis. The data would indicate that *zfp-1, unc-129* and *unc-53* act in a common pathway. However since the influence of *zfp-1* on D-type axon guidance is of indirect nature no clear interpretation can be made from this data. Mutations in *unc-53* and *unc-129* mildly enhance each other meaning that they have at least partially parallel function. (Data by Ronny Egli)

As a result of the transgene dependency of *zfp-1* and *lin-35* mutant phenotypes we assumed that also a possible target gene would show this effect. Since we obtained a total of 4 alleles of *unc-5* and this locus is within one of the 21U RNA clusters of *C. elegans* on LGIV (Ruby et al., 2006) we decided to test these 4 alleles to check the hypothesis that the transcription of *unc-5* is influenced by ZFP-1 via the endo-siRNA pathway. However none of the *unc-5* alleles recovered from the screen showed a change of defects depending on the transgene in the background (data not shown).

Discussion

The screen for genes influencing axon guidance in parallel to either *sdn-1* or *hse-5* revealed a number of genes that were previously known to play a role in axon guidance. For candidate *op481* we got very good, clear FLP mapping data and following this one RNAi clone from the FLP interval gave a clear phenotype, which is rather unusual for genes involved in axon guidance even if RNAi is performed in an RNAi sensitive background, in our case the *eri-1(mg366)* mutant. Mapping of *op481* was completed while five other candidates were undergoing arrayCGH for mutation detection. From the whole screen *zfp-1* was certainly the most surprising candidate, it has a very clear link to a human disease and we already knew that *lin-35* mutants have a similar phenotype. These were the reasons why we decided to focus on *zfp-1* and *lin-35*. Relatively soon it became clear that the effect seen in those two mutants was not a direct consequence of the mutation as such. Much rather we hypothesised that ZFP-1 and LIN-35 influence transcription of an axon guidance gene, most likely through the endo-siRNA pathway. Therefore we looked at genes that were found to be commonly up or down regulated in both mutants according to the microarray study carried out by Grishok et al., 2008, however without success.

Next we asked whether other SynMuv genes would show similar effects, which did not seem to be the case but only then we noticed that *oxIs12* is leading to an over-expression of *lin-15AB*. In order to avoid potential unwanted cross reactions resulting from (a) mutating a SynMuv suppressor (*zfp-1*) or a SynMuv gene (*lin-35*) and (b) over-expressing two SynMuv genes (*lin-15A* and *lin-15B*) we decided to test the relevant mutants with two other transgenes *oxIs268* and *juIs76.* The finding that *zfp-1(ok554); sdn-1(zh20)* and *lin-35(n745); sdn-1(zh20)* double mutants loose the defects if *oxIs12* was not present was extremely unexpected and we decided to try to find the reason for this. A first step was to determine the precise integration site of *oxIs12.* Since transgenes that have been produced like *oxIs12* are randomly integrated in the genome we needed whole genome sequencing (WGS) data plus a relatively precise idea of where *oxIs12* is located. We knew that *sdn-1* is very close to *oxIs12.* From recombination frequencies we estimated the two to be less than 0.5cM away form each other. To make sure we would

not miss the integration site we decided to screen manually through the alignment of WGS reads in an interval of +/- 1cM from *sdn-1* and were indeed able to find the site. With PCR reactions across the break points we were able to confirm the integration site. Whether the integration site as such plays a role in the transgene dependence of the *zfp-1* and *lin-35* mutant phenotypes is difficult to assess. *oxIs12* introduces a small deletion of 232bp cutting off the last 25bp of the 3'UTR of *grd-1,* one of the many hedgehog homologues of *C. elegans* (Bürglin, 1996). Both available alleles of *grd-1* can unfortunately not be used because they either have a linked lethal mutation (*ok680*) or contain a large duplication (*tm730*). However qRT PCR data indicate that in *oxIs12* animals *grd-1* expression is not greatly changed. Additionally the WGS data made it possible to gain an insight to the size of *oxIs12,* which we think is in the range of 3.6Mb. This size estimation may be a surprise but recently another group has found similar transgene sizes in *C. elegans* (Wang et al., 2010) indicating that these transgenes are repetitive regions on the corresponding chromosomes and therefore likely to be target of chromatin silencing mechanisms.

It is well known that repetitive regions on chromosomes such as telomeres are transcriptionally inhibited (Hsieh and Fire, 2000). Transcriptionally less active regions are marked by heterochromatic histone modifications and multi copy transgenes in *C. elegans* display all these features of silenced chromatin (Towbin et al., 2010). There is also accumulating evidence that the RNAi pathway could in fact play into formation of heterochromatin (Lippman and Martienssen, 2004). Therefore it seemed possible that the solution to the problem had to do with histone modifications. The X chromosome of *C. elegans,* which is where *oxIs12* can be found contains an amazing accumulation of HSPG related genes: *sdn-1, lon-2, hst-6,* and *hst-2* are all on X with *hst-2* being only 91kb away from *oxIs12*. Silencing mechanisms for repetitive regions need to be shut off at the end of the silenced chromatin domain. This function is fulfilled by so-called insulator proteins, that are conserved in most species, but in *C. elegans* (and a couple other nematodes) none of the otherwise well conserved insulator genes has been found and no other protein with insulator function is known (Heger et al., 2009). Therefore it seemed tempting to speculate that ZFP-1 and LIN-35 could have insulator function. However the qRT PCR data do not support this hypothesis in its entire form. It should be kept in mind that the

quality of qRT PCR data is still not the best despite various tries to improve the situation. Nevertheless I think that we can conclude that transcription in the vicinity of the transgene is changed in the *zfp-1* and *lin-35* mutants. There is even some evidence that transcription along the whole X chromosome is reduced. It remains to be tested whether reduced transcription is a genome wide feature in the two mutants.

RNAi approaches to knock down histone methylating and demethylating as well as acetylating and deacetylating enzymes as well as an approach to knock down all the Argonaute genes of *C. elegans* did not shed further light on a possible mechanism. Taken together all this data are rather inconclusive and leave a lot of room for interpretations. To follow the "spreading silencing" hypothesis I would recommend a microarray approach on LGX to overcome the normalization issues of qRT PCR. We are currently testing the possibility that there may be a background mutation close to *oxIs12* sensitising the system for axon guidance defects. We also have to take into account that there might not be a direct answer as to why *oxIs12* has an influence in axon guidance if *zfp-1* or *lin-35* are mutated. As previously mentioned both genes regulate transcription on a relatively broad level (Grishok et al., 2008). In addition LIN-15B has recently been described to be a "HOT region transcription factor" by the *C. elegans* modENCODE consortium (Gerstein et al., 2010) and is therefore also potentially influencing transcription of a lot of genes. The defects of *zfp-1(ok554); sdn-1(zh20) oxIs12* and *lin-35(n745); sdn-1(zh20) oxIs12* could simply be a result of the fact that we disturb the system with the *sdn-1* mutation already to a certain extent and then further destroy the system by adding the transgene *oxIs12* plus either the *zfp-1* or *lin-35* mutation, which interfere strongly with transcription. What we end up with in this case would be defects in axon guidance, which are purely a result of severely changed transcription of a large number of genes.

I believe that with the present data it is nearly impossible to make a safe statement. In order to gain more knowledge about a potential mechanism that could be underlying the whole situation I would recommend doing a rigorous mutagenesis screen, searching for genes that (a) increase D-type axon guidance defects in parallel to *sdn-1* and (b) have a phenotype that depends on *oxIs12*. This however would certainly be a risky approach!

Materials and Methods

For mutations and transgenes used please refer to the corresponding section of chapter II

Detection of integration site of *oxIs12*

The WGS data from all three sequenced strains containing *oxIs12* (originally sequenced for mutation detection) were pooled and assembled using the CLC Genomic Workbench (www.clcbio.com) to the *C. elegans* reference sequence using standard alignment settings given by CLC. This means that a sequence read is only aligned if no more than 30-35 bases were misaligned. The reads of our datasets were 76 bases long. This led to an average coverage across the whole genome of +/- 70x. Following this first assembly all aligned reads were discarded. The non-aligned reads were assembled to the *E. coli* reference sequence to get rid of contaminating reads from *op50* bacteria and aligned reads were discarded. The reads that remained non-aligned after this second assembly were once more assembled to the *C. elegans* reference, this time allowing for much more misaligned bases per read than in the first run. In order for a read to be aligned no more than 20 correctly aligned bases were required. The rational of this procedure was that upon the second assembly to the *C. elegans* reference the vast majority of the genome would remain uncovered but reads that were spanning the break points of the transgene and had more than 35 bases of transgene sequence would have remained unaligned after the first assembly and only the reduced assembly settings would allow them to be aligned. Manual inspection of an interval of +/- 1cM from *sdn-1*, which is were we expected the integration site from recombination frequencies, revealed two piles of reads with a sharp break point (Fig. 9). The so detected break points were subsequently confirmed by PCR with a primer located in the normal genomic close environment of the insertion site and random primers annealing within the transgene. On both sides of the transgene specific reaction could be designed to span the break points.

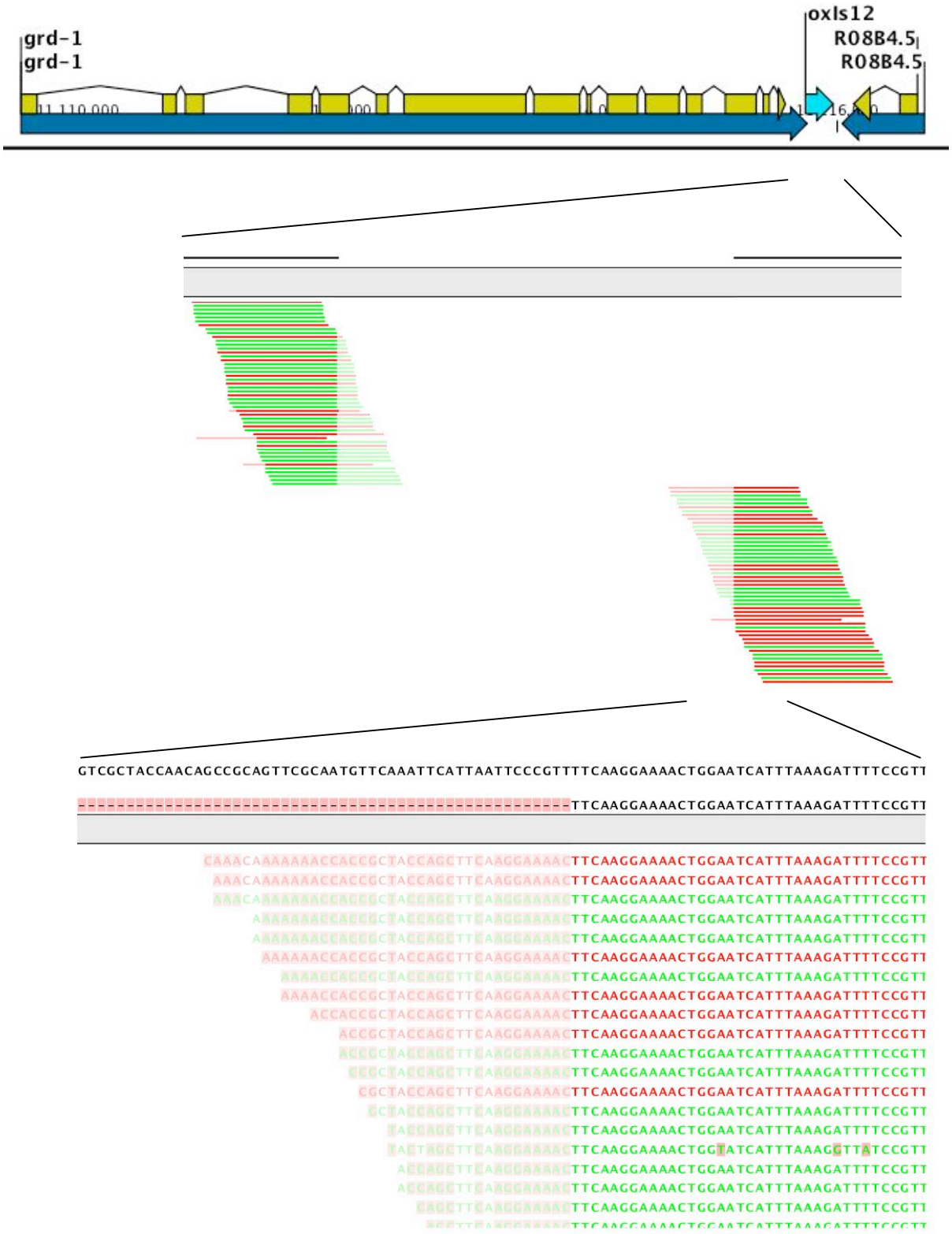

Figure 9: Break points of *oxIs12*. Shown are the reads of the first alignment to the *C. elegans* reference. Solid green or red lines or letters represent correctly aligned bases (regions of the read) while shaded green or red indicates misaligned areas. Blasting of the non-aligned parts of the reads reveals a vector backbone sequence.

qRT PCR

Sample preparation

Well fed gravid hermaphrodites were bleached in the evening and put on unseeded plates over-night. Embryos were allowed to hatch for 15 hours before L1 larvae were washed off the plates in M9 buffer. In six droplets of 5µl each the number of L1 animals was counted to estimate the number of animals per ml. +/- 3000 L1s were subsequently put on a seeded plate to feed for six hours before harvesting them in M9. Harvested L1s were washed in M9 three times to get rid of contaminating *op50* bacteria, frozen in liquid nitrogen and stored at -80°C until RNA extraction.

In parallel also *Arabidopsis thaliana* wild type samples were collected. Seeds were put on an agarose plate and given about ten days to germinate and create a tight lawn of seedlings. Twice seedlings from about 1cm^2 of the lawn were picked without agarose and snap frozen in liquid nitrogen together with RNase free glas beads. Samples were homogenized with a bead beater and subsequently treated the same way as worm samples.

RNA extraction

To lyse samples add 1ml Trizol Reagent (Invitrogen, cat. nr. 15596-026) and put the samples through 10 freeze-thaw cycles (freezing in liquid nitrogen, thawing in 30°C water) followed by incubation at room temperature (RT) for 15 min. Add 200µl chlorophorm, incubate at RT for 2-3 min and spin at 4°C for 15 min at 12'000g to separate phases. Transfer aqueous upper phase to a new tube. For RNA precipitation add 1/10 volume 3M sodium acetate, 2µl glycogen (Fermentas, cat. nr. R0551) and 1 volume isopropanol and store at -80°C for about 30 min before spinning at 12'000g for 15 min at 4°C. Remove supernatant and wash pellet in 200µl 70% cold ethanol, air dry pellet and dissolve in RNase free water. To remove contaminating DNA I performed a DNase digest using the Turbo DNA free kit from Ambion (cat. nr. AM1907) according to manufacturer's protocol and tested for remaining DNA contamination with a DNA specific PCR. After DNase digestion PCR did not detect any DNA.

cDNA synthesis and quantitative PCR

For cDNA synthesis the SuperScript III kit from Invitrogen (cat. nr. 11752-050) was used following the manufacturer's protocol. Prior to cDNA synthesis equal amounts of *C. elegans* and *A. thaliana* RNA were mixed and this mix used for reverse transcriptase (rt) reaction. Total DNase digested RNA should not be more than 5% of the volume of the rt reaction, because residual traces of the DNase reaction buffer can inhibit the rt reaction. I used 75ng of worm RNA and 75ng of *A. thaliana* RNA in a 20µl rt reaction. 10µl of the rt reaction were used for qPCR that was performed on an ABI prism 7900HT sequence detection system. Prior to qPCR I tested the cDNA library for presence of the *sdn-1* cDNA to make sure the rt reaction worked. For normalization the following three genes were chosen: AT1G13320, AT2G28390, AT3G01150.

List of all genes tested by RNAi

Table 1: Summary of all genes treated with RNAi.

gene name	function	Ahringer clone	comments
F56A6.1/sago-2	Argonaute[a]	1 D6	clone contains C18E3.7, will knock down both!
Y110A7A.18/ppw-2	Argonaute[a]	-	reclone
F55A12.1	Argonaute[a]	-	reclone
R06C7.1	Argonaute[a]	11 C11	
D2030.6/prg-1	Argonaute[a]	-	reclone
C04F12.1	Argonaute[a]	-	reclone
T23D8.7	Argonaute[a]	17 B1	
T07D3.7/alg-2	Argonaute[a]	33 C3	
Y49F6A.1	Argonaute[a]	-	reclone
ZK1248.7	Argonaute[a]	45 G3	
F58G1.1	Argonaute[a]	-	reclone
C14B1.7	Argonaute[a]	69 E2	
C16C10.3	Argonaute[a]	70 C6	
ZK757.3/tag-76	Argonaute[a]	83 C8	
M03D4.6	Argonaute[a]	100 E7	
C01G5.2/prg-2	Argonaute[a]	100 H6	
F20D12.1/csr-1	Argonaute[a]	104 C1	
T22B3.2	Argonaute[a]	-	reclone
T22H9.3	Argonaute[a]	125 D12	
R09A1.1/ergo-1	Argonaute[a]	127 C6	
K12B6.1/sago-1	Argonaute[a]	139 F7	
K08H10.7/rde-1	Argonaute[a]	148 H11	
ZK218.8	Argonaute[a]	166 H10	
R04A9.2/nrde-3	Argonaute[a]	176 A9	

F48F7.1/alg-1	Argonaute[a]	198 B8	
C18E3.7/ppw-1	Argonaute[a]	-	C18E3.7/ppw-1 is more or less identical to sago-2, specific primers are impossible to design!
C06A1.4	Argonaute[a]	-	C06A1.4 is a pseudogene very similar to F58G1.1!
K11G9.4/egl-46	[b]	140 F1	
K12F2.2/vab-8	[b]	153 H3	
F02G3.1/ncam-1	[b]	176 E9	
F22D3.6	[b]	48 C12	
C04F5.3/unc-46	[b]	137 C4	
VC5.2	[b]	141 E3	
Y37D8A.23/unc-25	[b]	87 H12	
B0454.1/lin-8	SynMuv A[c]	38 F9	
ZK678.1/lin-15a	SynMuv A[c]	-	
lin-38	SynMuv A[c]	-	
ZK673.3/lin-56	SynMuv A[c]	-	
K12C11.2/smo-1	SynMuv A[c]	1 H7	++ (very sick)
W02A11.4/uba-2	SynMuv A[c]	23 A8	++
T23G7.1/dpl-1	SynMuv B[c]	53 D7	
Y102A5C.18/efl-1	SynMuv B[c]	166 D11	
W07B3.2/gei-4	SynMuv B[c]	66 E7	
C53A5.3/hda-1	SynMuv B[c]	159 C6	
K01G5.2/hpl-2	SynMuv B[c]	85 A1	
F26F12.7/let-418	SynMuv B[c]	138 H8	
ZK637.7/lin-9	SynMuv B[c]	81 B4	
C03B8.4/lin-13	SynMuv B[c]	-	
ZK662.4/lin-15b	SynMuv B[c]	-	
C32F10.2/lin-35	SynMuv B[c]	7 G8	
F44B9.6/lin-36	SynMuv B[c]	79 A5	
ZK418.4/lin-37	SynMuv B[c]	77 A4	
ZK632.13/lin-52	SynMuv B[c]	83 B12	
K07A1.12/lin-53	SynMuv B[c]	16 B7	
JC8.6/lin-54	SynMuv B[c]	116 C5	+
R06C7.7/lin-61	SynMuv B[c]	11 D5	
Y71G12B.9/lin-65	SynMuv B[c]	29 G10	
M04B2.1/mep-1	SynMuv B[c]	112 F5	
R05D3.11/met-2	SynMuv B[c]	79 H12	
F26G5.9/tam-1	SynMuv B[c]	137 A4	
F53B3.1/tra-4	SynMuv B[c]	180 A9	+
F29B9.6/ubc-9	SynMuv B[c]	97 F3	+
E01A2.4	SynMuv B[c]	4 B10/11	
W01G7.3/rpb-11	SynMuv B[c]	63 A12	
Y111B2A.11/epc-1	SynMuv C[c]	87 E7	+
VC5.4/mys-1	SynMuv C[c]	141 E5	

Y111B2A.22/ssl-1	SynMuv C[c]	-	
C47D12.1/trr-1	SynMuv C[c]	58 G10	
C01C7.1/ark-1	RTK-Ras[c]	-	
T24C12.2/gap-1	RTK-Ras[c]	-	
M02A10.3/sli-1	RTK-Ras[c]	176 E12	
C34B7.4/mys-4	SynMuv Sup., chr. remod.[d]	13 D11	
M04B2.3/gfl-1	SynMuv Sup., chr. remod.[d]	112 F7	
Y37D8A.9/mrg-1	SynMuv Sup., chr. remod.[d]	87 G12	
Y105E8A.17/ekl-4	SynMuv Sup., chr. remod.[d]	-	
ZK1127.3	SynMuv Sup., chr. remod.[d]	48 E4	
C08B11.6	SynMuv Sup., chr. remod.[d]	50 G8	
C17E4.6	SynMuv Sup., chr. remod.[d]	15 F8	
CD4.7	SynMuv Sup., chr. remod.[d]	138 D5	
C14B1.4/tag-125	SynMuv Sup., chr. remod.[d]	69 D11	
ZK863.6/dpy-30	SynMuv Sup., chr. remod.[d]	153 G9	
C46A5.9/hcf-1	SynMuv Sup., chr. remod.[d]	103 G4	
Y2H9A.1/mes-4	SynMuv Sup., chr. remod.[d]	156 E7	
F37A4.8/isw-1	SynMuv Sup., chr. remod.[d]	76 C8	
C01G8.9/lss-4	SynMuv Sup., chr. remod.[d]	6 E9/10	
C34D4.14	SynMuv Sup., chr. remod.[d]	102 C2	
F30A10.10	SynMuv Sup., chr. remod.[d]	15 H5	
B0205.3/rpn-10	SynMuv Sup., chr. remod.[d]	18 G4	
ZK20.5/rpn-12	SynMuv Sup., chr. remod.[d]	58 G8	
R08C7.3/htz-1	SynMuv Sup., chr. remod.[d]	97 B11	
T02C12.3	SynMuv Sup., chr. remod.[d]	70 A11	
ZK856.9/tag-143	SynMuv Sup., chr. remod.[d]	149 D11	
F52B11.1	SynMuv Sup., chr. remod.[d]	117 G1	
Y53G8AR.2	SynMuv Sup., chr. remod.[d]	90 H6	
B0035.4/pfd-4	SynMuv Sup., chr. remod.[d]	112 B8	
F54F2.2/zfp-1	SynMuv Sup., chr. remod.[d]	80 H9	++++
F02E9.4/pqn-28	SynMuv Sup., chr. remod.[d]	13 F2	
C06E7.1	SynMuv Sup., chr. remod.[d]	100 A11	
C34E10.8	SynMuv Sup., chr. remod.[d]	73 A10	
F54D11.2	SynMuv Sup., chr. remod.[d]	136 A12	
K08F4.2	SynMuv Sup., chr. remod.[d]	109 D9	
M03C11.3	SynMuv Sup., chr. remod.[d]	84 D2	
T07E3.3	SynMuv Sup., chr. remod.[d]	76 F1	
ZK593.4/rbr-2	lysine demethylase[e]	-	reclone
Y40B1B.6/spr-5	lysine demethylase[e]	24 D1	
C29F7.6	lysine demethylase[e]	197 C11	
F23D12.5	lysine demethylase[e]	199 A3	
D2021.1/utx-1	lysine demethylase[e]	189 E5	+
F18E9.5/tag-279	lysine demethylase[e]	189 F1	
F29B9.2	lysine demethylase[e]	97 E12	
Y48B6A.11/jmjd-2	lysine demethylase[e]	-	reclone

Y40B1B.6/spr-5	LSD1 homologue[f]	24 D1	
T08D10.2/lsd-1	LSD1 homologue[f]	194 H9	
C26E6.9/set-2	H3K4 methyl transferase[g]	72 D5	
T12D8.1/set-16	H3K4 methyl transferase[g]	89 B6	
Y17G7B.2/ash-2	H3K4 methyl transferase[g]	-	nd
F52B11.1	H3K4 methyl transferase[g]	117 G1	
F21H12.1/rbbp-5	H3K4 methyl transferase[g]	46 C8	
C33H5.6/swd-2.1	H3K4 methyl transferase[g]	103 G9	
C33H5.7/swd-2.2	H3K4 methyl transferase[g]	103 G10	+
C14B1.4/wdr-5.1	H3K4 methyl transferase[g]	69 D11	
ZK863.6/dpy-30	H3K4 methyl transferase[g]	153 G9	
Y39G10AR.18	hDOT1 homologue[h]	27 C9	
ZC53.6	hDOT1 homologue[h]	178 F12	
D1053.2	hDOT1 homologue[h]	194 E5	
F54F7.7	hDOT1 homologue[h]	194 G2	
F55G7.2	hDOT1 homologue[h]	-	reclone
W06D11.4	hDOT1 homologue[h]	195 E3	
C53A5.3/hda-1	Rpd3 homologue[i]	159 C6	
R06C1.1/hda-3	Rpd3 homologue[i]	-	nd
C08B11.2/hda-2	Rpd3 homologue[i]	50 G4	
F41H10.6/hdac-6	Rpd3 homologue[i]	99 C12	
C10E2.3/hda-4	Rpd3 homologue[i]	202 A11	
Y51H1A.5/hda-6	Rpd3 homologue[i]	62 G3	
C35A5.9/hdac-11	Rpd3 homologue[i]	-	nd
F43G6.11	Rpd3 homologue[i]	59 B2	
R08C7.3/htz-1	Htz1 homologue[i]	97 B11	
C50F4.13/his-35	Htz1 homologue[i]	-	nd
T23D8.6/his-68	Htz1 homologue[i]	17 A12	
ZK1251.1/htas-1	Htz1 homologue[i]	108 A12	
K03D10.3/mys-2	Sas2 homologue[i]	-	nd
VC5.4/mys-1	Sas2 homologue[i]	141 E5	+
C34B7.4/mys-4	Sas2 homologue[i]	13 D11	
R07B5.9/lsy-12	Sas2 homologue[i]	148 F2	

Gene name: given are sequence name/main name according to www.wormbase.org. **Function:** indicates why gene has been chosen for knock down; superscript is giving the reference or a more precise description. **Ahringer clone:** clone nr of the clone corresponding to the gene. Clones were confirmed to contain the right sequence by sequencing; - means that the gene was either not contained in the library or the clone contained a wrong sequence. **Comments:** reclone indicates that the RNAi clone was cloned newly; phenotype indications: D-type axon guidance defects in: + = 25%; ++ = 50%; +++ = 75%; ++++ = 100% of the animals; nd = not determined. [a]: Yigit et al., 2006; [b]: down regulated in *zfp-1(ok554)* and *lin-35(n745)* (Grishok et al., 2008); [c]: Fay and Yochem, 2007; [d]: Cui et al., 2006; [e]: lysin demethylases, wormbase search; [f]: LSD1 protein blast; [g]: Simonet et al., 2007; [h]: hDOT1 blast, gene; [i]: Verzijlbergen et al., 2009.

References

Bahri SM, Chia W, Yang X. (2001). The *Drosophila* homolog of human AF10/AF17 leukemia fusion genes (Dalf) encodes a zinc finger/leucine zipper nuclear protein required in the nervous system for maintaining EVE expression and normal growth. *Mech Dev*. **100**(2): 291-301.

Balgobind BV, Zwaan CM, Pieters R, Van den Heuvel-Eibrink MM. (2011). The heterogeneity of pediatric MLL-rearranged acute myeloid leukemia. *Leukemia*. **25**(8): 1239-48.

Bürglin TR. (1996). Warthog and groundhog, novel families related to hedgehog. *Curr Biol*. **6**(9): 1047-50.

Chaplin T, Ayton P, Bernard OA, Saha V, Della Valle V, Hillion J, Gregorini A, Lillington D, Berger R, Young BD. (1995). A novel class of zinc finger/leucine zipper genes identified from the molecular cloning of the t(10;11) translocation in acute leukemia. *Blood*. **85**(6): 1435-41.

Chinnam M, Goodrich DW. (2011). RB1, development, and cancer. *Curr Top Dev Biol.* 94: 129-69.

Cui M, Kim EB, Han M. (2006). Diverse chromatin remodeling genes antagonize the Rb-involved SynMuv pathways in *C. elegans*. *PLoS Genet*. **2**(5): e74.

Czechowski T, Stitt M, Altmann T, Udvardi MK, Scheible WR. (2005). Genome-wide identification and testing of superior reference genes for transcript normalization in *Arabidopsis*. *Plant Physiol*. **139**(1): 5-17.

Dudley NR, Labbé JC, Goldstein B. (2002). Using RNA interference to identify genes required for RNA interference. *Proc Natl Acad Sci U S A*. **99**(7): 4191-6.

Fay DS, Yochem J. (2007). The SynMuv genes of *Caenorhabditis elegans* in vulval development and beyond. *Dev Biol.* **306**(1): 1-9.

Ferguson EL, Horvitz HR. (1989). The multivulva phenotype of certain *Caenorhabditis elegans* mutants results from defects in two functionally redundant pathways. *Genetics*. **123**(1): 109-21.

Friend SH, Bernards R, Rogelj S, Weinberg RA, Rapaport JM, Albert DM, Dryja TP. (1986). A human DNA segment with properties of the gene that predisposes to retinoblastoma and osteosarcoma. *Nature.* **323**(6089): 643-6.

Frolov MV, Dyson NJ. (2004). Molecular mechanisms of E2F-dependent activation and pRB-mediated repression. *J Cell Sci.* **117**(Pt 11): 2173-81.

Gerstein MB, Lu ZJ, Van Nostrand EL, Cheng C, Arshinoff BI, Liu T, Yip KY, Robilotto R, Rechtsteiner A, Ikegami K, Alves P, Chateigner A, Perry M, Morris M, Auerbach RK, Feng X, Leng J, Vielle A, Niu W, Rhrissorrakrai K, Agarwal A, Alexander RP, Barber G, Brdlik CM, Brennan J, Brouillet JJ, Carr A, Cheung MS, Clawson H, Contrino S, Dannenberg LO, Dernburg AF, Desai A, Dick L, Dosé AC, Du J, Egelhofer T, Ercan S, Euskirchen G, Ewing B, Feingold EA, Gassmann R, Good PJ, Green P, Gullier F, Gutwein M, Guyer MS, Habegger L, Han T, Henikoff JG, Henz SR, Hinrichs A, Holster H, Hyman T, Iniguez AL, Janette J, Jensen M, Kato M, Kent WJ, Kephart E, Khivansara V, Khurana E, Kim JK, Kolasinska-Zwierz P, Lai EC, Latorre I, Leahey A, Lewis S, Lloyd P, Lochovsky L, Lowdon RF, Lubling Y, Lyne R, MacCoss M, Mackowiak SD, Mangone M, McKay S, Mecenas D, Merrihew G, Miller DM 3rd, Muroyama A, Murray JI, Ooi SL, Pham H, Phippen T, Preston EA, Rajewsky N, Rätsch G, Rosenbaum H, Rozowsky J, Rutherford K, Ruzanov P, Sarov M, Sasidharan R, Sboner A, Scheid P, Segal E, Shin H, Shou C, Slack FJ, Slightam C, Smith R, Spencer WC, Stinson EO, Taing S, Takasaki T, Vafeados D, Voronina K, Wang G, Washington NL, Whittle CM, Wu B, Yan KK, Zeller G, Zha Z, Zhong M, Zhou X; modENCODE Consortium, Ahringer J, Strome

S, Gunsalus KC, Micklem G, Liu XS, Reinke V, Kim SK, Hillier LW, Henikoff S, Piano F, Snyder M, Stein L, Lieb JD, Waterston RH. (2010). Integrative analysis of the *Caenorhabditis elegans* genome by the modENCODE project. *Science.* **330**(6012): 1775-87.

Grishok A, Sinskey JL, Sharp PA. (2005). Transcriptional silencing of a transgene by RNAi in the soma of *C. elegans. Genes Dev.* **19**(6): 683-96.

Grishok A, Hoersch S, Sharp PA. (2008). RNA interference and retinoblastoma-related genes are required for repression of endogenous siRNA targets in *Caenorhabditis elegans*. *Proc Natl Acad Sci U S A*. **105**(51): 20386-91.

Hanahan D, Weinberg RA. (2000). The hallmarks of cancer. *Cell.* **100**(1): 57-70.

Heger P, Marin B, Schierenberg E. (2009). Loss of the insulator protein CTCF during nematode evolution. *BMC Mol Biol.* 10:84.

Hsieh J, Fire A. (2000). Recognition and silencing of repeated DNA. *Annu Rev Genet.* 34: 187-204.

Kamath RS, Ahringer J. (2003). Genome-wide RNAi screening in *Caenorhabditis elegans*. *Methods*. **30**(4): 313-21.

Kennedy S, Wang D, Ruvkun G. (2004). A conserved siRNA-degrading RNase negatively regulates RNA interference in *C. elegans. Nature.* **427**(6975): 645-9.

Lehner B, Calixto A, Crombie C, Tischler J, Fortunato A, Chalfie M, Fraser AG. (2006). Loss of LIN-35, the *Caenorhabditis elegans* ortholog of the tumor suppressor p105Rb, results in enhanced RNA interference. *Genome Biol.* **7**(1): R4.

Lippman Z, Martienssen R. (2004). The role of RNA interference in heterochromatic silencing. *Nature*. **431**(7006): 364-70.

McIntire SL, Reimer RJ, Schuske K, Edwards RH, Jorgensen EM. (1997). Identification and characterization of the vesicular GABA transporter. *Nature.* **389**(6653): 870-6.

Morris EJ, Dyson NJ. (2001). Retinoblastoma protein partners. *Adv Cancer Res.* **82**: 1-54.

Okada Y, Feng Q, Lin Y, Jiang Q, Li Y, Coffield VM, Su L, Xu G, Zhang Y. (2005). hDOT1L links histone methylation to leukemogenesis. *Cell*. **121**(2): 167-78.

Ruby JG, Jan C, Player C, Axtell MJ, Lee W, Nusbaum C, Ge H, Bartel DP. (2006). Large-scale sequencing reveals 21U-RNAs and additional microRNAs and endogenous siRNAs in *C. elegans. Cell*. **127**(6): 1193-207.

Simonet T, Dulermo R, Schott S, Palladino F. (2007). Antagonistic functions of SET-2/SET1 and HPL/HP1 proteins in *C. elegans* development. *Dev Biol.* **312**(1): 367-83.

Towbin BD, Meister P, Pike BL, Gasser SM. (2010). Repetitive transgenes in *C. elegans* accumulate heterochromatic marks and are sequestered at the nuclear envelope in a copy-number- and lamin-dependent manner. *Cold Spring Harb Symp Quant Biol.* 75: 555-65.

Verzijlbergen KF, Faber AW, Stulemeijer IJ, van Leeuwen F. (2009). Multiple histone modifications in euchromatin promote heterochromatin formation by redundant mechanisms in *Saccharomyces cerevisiae*. *BMC Mol Biol.* **10**:76.

Wang D, Kennedy S, Conte D Jr, Kim JK, Gabel HW, Kamath RS, Mello CC, Ruvkun G. (2005). Somatic misexpression of germline P granules and enhanced RNA interference in retinoblastoma pathway mutants. *Nature.* **436**(7050): 593-7.

Wang J, Chen PJ, Wang GJ, Keller L. (2010). Chromosome size differences may affect meiosis and genome size. *Science*. **329**(5989): 293.

Yigit E, Batista PJ, Bei Y, Pang KM, Chen CC, Tolia NH, Joshua-Tor L, Mitani S, Simard MJ, Mello CC. (2006). Analysis of the *C. elegans* Argonaute family reveals that distinct Argonautes act sequentially during RNAi. *Cell*. **127**(4): 747-57.

CHAPTER IV

ccz-1 mediates the digestion of apoptotic corpses in *C. elegans.*

Nieto C, Almendinger J, Gysi S, Gómez-Orte E, Kaech A, Hengartner MO, Schnabel R, Moreno S, Cabello J. *J Cell Sci.* (2010). 123(Pt 12): 2001-7.

Preface

This publication places the gene *ccz-1* in the pathway for phagosome maturation during apoptotic cell corps engulfment in *C. elegans*. In a screen for maternal-effect lethal mutations on chromosome V the three alleles *t2010, t2129,* and *t2170* were found to affect the same gene and *t2129* chosen for FLP and SNP mapping. I was involved in generation of transgenic animals via micro-injection for the cosmid rescue following genetic mapping and the *rab-7* over-expression study.

ccz-1 mediates the digestion of apoptotic corpses in *C. elegans*

Cristina Nieto[1], Johann Almendinger[2], Stephan Gysi[2], Eva Gómez-Orte[3], Andres Kaech[4], Michael O. Hengartner[2], Ralf Schnabel[5], Sergio Moreno[1,*] and Juan Cabello[1,3,*]

[1]Instituto de Biología Molecular y Celular del Cáncer, CSIC/Universidad de Salamanca, 37007 Salamanca, Spain
[2]Institute of Molecular Life Sciences, and [4]Center for Microscopy and Image Analysis, University of Zurich, 8057 Zurich, Switzerland
[3]Center for Biomedical Research of La Rioja (CIBIR), C/Piqueras 98, 26006 Logroño, Spain
[5]Institute of Genetics, TU Braunschweig, 38106 Braunschweig, Germany
*Authors for correspondence (smo@usal.es; juan.cabello@riojasalud.es)

Accepted 29 March 2010
Journal of Cell Science 123, 2001-2007

doi:10.1242/jcs.062331

Summary

During development, the processes of cell division, differentiation and apoptosis must be precisely coordinated in order to maintain tissue homeostasis. The nematode *C. elegans* is a powerful model system in which to study cell death and its control. *C. elegans* apoptotic cells condense and form refractile corpses under differential interference contrast (DIC) microscopy. Activation of the GTPase CED-10 (Rac) in a neighbouring cell mediates the recognition and engulfment of the cell corpse. After inclusion of the engulfed corpse in a phagosome, different proteins are sequentially recruited onto this organelle to promote its acidification and fusion with lysosomes, leading to the enzymatic degradation of the cell corpse. We show that CCZ-1, a protein conserved from yeasts to humans, mediates the digestion of these apoptotic corpses. CCZ-1 seems to act in lysosome biogenesis and phagosome maturation by recruiting the GTPase RAB-7 over the phagosome.

Key words: Apoptosis, *C. elegans*, Phagosome maturation, *ccz-1*, Digestion pathway

Introduction

The development of *Caenorhabditis elegans* offers an invaluable opportunity to understand and characterize events taking place at the level of single cells. In early embryos, cells have a defined and precise contact map that ensures the correct fate specification via cell-cell inductive signals (Hutter and Schnabel, 1995). During developmental progression, cell death occurs in specific cells of its invariant lineage (Sulston et al., 1983) and in the germ line of the adult in response to DNA damage, genotoxic stress or bacterial infection (Gumienny et al., 1999; Gartner et al., 2000; Aballay and Ausubel, 2001). Apoptotic corpses in embryos are engulfed and digested by neighbouring cells. The *C. elegans* hermaphrodite gonad is composed of two U-shaped syncytia (Hubbard and Greenstein, 2000). Apoptotic germ cells cellularize away from the syncytium and generate refractile cell corpses under differential interference contrast (DIC) optics. Such corpses are engulfed and digested by the sheath cells, which encase the germ line (Gummienny et al., 1999).

Pathways that regulate corpse recognition and engulfment have been extensively characterized (for a review, see Kinchen and Hengartner, 2005), but few genes that are involved in the maturation of the apoptotic-corpse-containing phagosome have been identified. These genes have been ordered in a linear pathway that includes, among others, the HOPS complex and the GTPases RAB-5 and RAB-7 (Kinchen et al., 2008) (and see below). These GTPases act as 'molecular switches' that, in the inactive form, are bound to GDP and are located in the cytoplasm in complexes with RAB GDP-dissociation inhibitors (RabGDI) (Ullrich et al., 1994; Seabra and Wasmeier, 2004). Following activation of this pathway – in this case after engulfment of an apoptotic corpse – RabGDI releases the Rab GTPase. Free GDP-bound Rab GTPases can then bind to the membranous organelle and then recruit its own guanine nucleotide-exchange factor (GEF), resulting in the exchange of GDP for GTP and hence activation of the Rab protein (Ullrich et al., 1994).

These proteins are recruited sequentially onto the phagosome. Each protein needs the more upstream component to be charged, and is required for the next downstream protein to bind to the phagosome. The maturation process allows other vesicles, such as lysosomes, to bind and fuse to the phagosome, first acidifying and then enzymatically digesting the apoptotic corpse (Kinchen et al., 2008; Yu et al., 2008). This pathway is well conserved during evolution from worms to humans and its deregulation has been linked to human diseases such as Hermansky-Pudlak syndrome, an autosomal recessive disease that results from abnormalities in the intracellular transport of vesicles such as melanosomes, causing skin and hair hypopigmentation and reduced visual acuity. *HSP4*, one of the human genes associated with this disorder, is in fact the human homologue of *ccz-1* (Hoffman-Sommer et al., 2005). Failures in the digestion of apoptotic corpses also lead to chronic polyarthritis caused by DNA that escapes from degradation in macrophages. The accumulation of this DNA in joints induces arthritis (Kawane et al., 2006).

In the present report we describe CCZ-1 as a new element in the pathway that mediates the degradation of apoptotic corpses. CCZ-1 seems to act both at the level of the exchange of the GTPase RAB-5 with the GTPase RAB-7 by recruiting RAB-7 onto the phagosome and also during lysosome biogenesis.

Results and Discussion

In a screening for maternal-effect lethal mutations on chromosome V of *C. elegans*, we found that three alleles (named *t2070*, *t2129* and *t2170*) of the same gene caused a striking set of defects. The first phenotype observed, in oocytes and embryos laid by mothers

Journal of Cell Science

homozygous for any of these mutations, was an accumulation of large vesicle-like structures (Fig. 1A,B). These vesicles were more abundant in the cortex of the anterior cell (named AB) at the two-cell-stage embryo and its descendants than in the posterior cell (P1). The second phenotype was that the mitotic spindle of the blastomeres EMS and ABar did not rotate, unlike the wild type (Fig. 1C,D; supplementary material Table S1), producing an abnormal pattern of cell-cell contacts. As a consequence of this, the normal left-right asymmetry of these embryos was disrupted, as determined by the position of apoptosis in the cell lineage, and the embryos died owing to an abnormal morphogenesis. Embryos in which the spindle rotated properly acquired a normal cell fate and underwent normal morphogenesis, but arrested at the two- to three-fold stage of morphogenesis. The accumulation of vesicles was still present in the cells of those late-arrested embryos. To better understand the nature of these vesicles, we expressed a fusion of yolk protein to GFP (VIT-2–GFP) (Poteryaev et al., 2007) in the *t2129* mutant. The yolk appeared properly endocytosed in the *t2129* oocytes but accumulated in the large and peripheral granules (supplementary material Fig. S1). Although we cannot exclude other defects, the inability to metabolize the yolk reserve during development might explain the arrest of the mutant embryos. The lethality of these mutants reached 99.5% of the embryos. The remaining escapers arrested as L1 larvae.

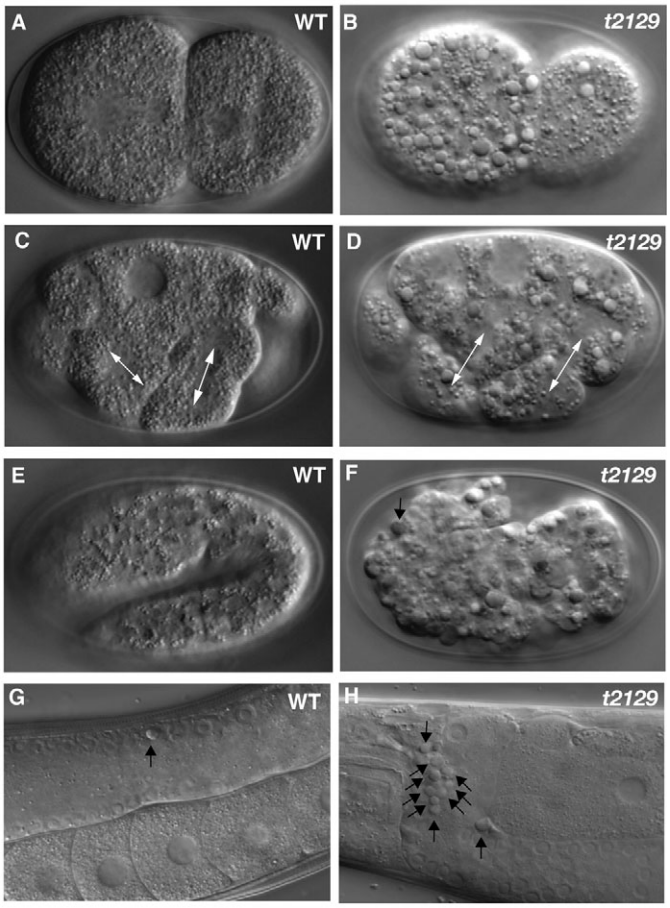

Fig. 1. Microscopic analysis of *ccz-1* mutants. Left column shows wild-type (WT) *C. elegans* at different stages: (**A**) two-cell stage, (**C**) 12-cell stage and (**E**) two-fold stage. Right column shows *ccz-1(t2129)* mutant embryos at the same stages as the corresponding left-hand WT panels. (**B**) *ccz-1(t2129)* homozygous embryos accumulate vesicles that can be observed with DIC microscopy. (**D**) The mitotic spindle of the blastomeres EMS and ABar does not rotate, unlike the WT. Double-headed arrows indicate orientation of the mitotic spindle. (**F**) *ccz-1(t2129)* mutant embryos at late stages still show an accumulation of vesicles as well as persistent undigested corpses. The black arrow shows an apoptotic corpse. See supplementary material Movie 1 for the explanation of how the embryonic corpses are detected. (**G**) In the WT hermaphrodite gonad, one or two corpses can be observed by DIC microscopy at 36 hours post-L4/adult molt. (**H**) However, in the homozygous *ccz-1(t2129)* hermaphrodites, a high accumulation of apoptotic cells is shown. Black arrows point to apoptotic corpses.

In addition, four-dimensional (4D) microscope analysis both of maternal and zygotic-defective *t2129*, *t2070* or *t2170* embryos revealed an accumulation of apoptotic corpses due to a defect in the clearance of corpses from apoptotic cells. A total of 25 focal planes of the embryos were recorded for 10 hours. As a result, 4D movies (three dimensions of the embryo + time) were obtained for each genotype. The SIMI Biocell software (SIMI GmbH, Germany) allowed each cell of the embryo to be traced in time and space, as well as tracing the mitosis and terminal differentiation of each cell. The cells placed in the lineage tree at positions in which the wild-type or the new ectopic fate corresponded to apoptosis were followed by 4D microscopy. These cells exhibited all the properties of a typical *C. elegans* apoptotic cell (asymmetric division, condensation, erythrocyte-like stage and refractile lentil stage), but remained as undigested persistent corpses (Fig. 1E,F; see also supplementary material Movie 1). To further confirm their identity as apoptotic cells, we generated a double mutant, *t2129*; *ced-3* (caspase) (allele *n717*). The absence of the only caspase-encoding gene in the *C. elegans* genome inactivated programmed cell death and no apoptosis took place in those embryos (supplementary material Table S1 and Movie 2). These results indicated that they really were apoptotic cells.

In *C. elegans*, the genetic pathways involved in apoptosis have been shown to play a role both in somatic cell death during development and germline apoptosis in adulthood (Kinchen and Hengartner, 2005). We then analyzed the gonad of the maternally rescued adult *t2070*, *t2129* and *t2170* mutant worms for persistent corpses. In the three mutants, we found a significant accumulation of persistent corpses, the number of which increased with time (Fig. 1H; supplementary material Fig. S2A) until they reached 22.9±6.34 (mean ± s.d.) corpses per gonadal arm 48 hours after the last molt, whereas a wild-type worm contained 1.75±2.22 corpses in the same conditions.

To better understand the state of these persistent corpses, we stained the worms with Acridine Orange (AO), a vital dye that selectively stains engulfed apoptotic cells within acidic organelles (Kinchen et al., 2005). Persistent corpses in the gonads of *t2070*, *t2129* and *t2170* mutant worms were AO positive, indicating that their accumulation is not due to a defect in the engulfment process, as has been described in *ced-1*, *ced-6*, *ced-5*, *ced-2*, *ced-12* or *ced-10* mutants (Kinchen and Hengartner, 2005). The AO staining suggested that, in these mutants, the corpses were efficiently engulfed and that they accumulated within phagosomes as undigested corpses (Fig. 2A). To further confirm this result, we performed transmission electron microscopy of the germline-persistent corpses in two *ccz-1(t2129)* mutant worms. As shown in Fig. 2B, five out of five analyzed corpses seemed to be totally engulfed within the sheath cells, indicating that the *t2129*, and by extension the *t2070* and *t2170*, mutations abolished digestion of apoptotic corpses, whereas earlier processes, such as dying itself or engulfment, remained unaffected. In addition, contrary to many

engulfment-defective mutants (Reddien and Horvitz, 2000), migration of the distal tip cells (DTCs) of the gonads from *t2070*, *t2129* and *t2170* maternally rescued homozygous worms was normal and the gonads developed the typical U-shaped structure of the wild type.

We identified the three mutations by using three-factor mapping, followed by single nucleotide polymorphism (SNP) mapping. These mutations define three alleles of the gene F58G11.6, hereafter referred to as *ccz-1* owing to its homology to the *Saccharomyces cerevisiae CCZ1* gene. The *t2070* mutation abolished splicing of the first intron, producing an abnormal mRNA (supplementary material Fig. S2B and Fig. S3A). *t2129* and *t2170* mutations result in premature STOP codons (supplementary material Fig. S2B and Fig. S3A,B). *t2070* and *t2129* both have a similar phenotype that is likely to be null. A knockout in *ccz-1* has recently become available (*ok2182*) from the *C. elegans* Gene Knockout Consortium. However, this deletion has an alternative splicing that restores a truncated but otherwise in-frame protein that retains some activity, as indicated by the viability of the homozygous mutant strain (supplementary material Fig. S3C,D). *ok2182* is therefore a hypomorph allele. RNA interference (RNAi)-mediated knockdown of *ccz-1* strikingly caused a similar weak phenotype, suggesting that either CCZ-1 is a very stable protein or that the double-stranded RNA (dsRNA) treatment was not very effective for this gene.

To further test whether these mutations were responsible for the phenotype, we performed a complementation experiment using plasmids containing a translation fusion of *ccz-1* to YFP under the control of the *ced-1* promoter, which drives the expression of the transgene in the engulfing cells, and another under the control of the endogenous *ccz-1* promoter. The embryonic lethality was rescued and the transgenic homozygous mutant worms cleared apoptotic corpses properly (supplementary material Fig. S4). These results indicate that loss of *ccz-1* function is responsible for the observed phenotypes in *C. elegans*: lethality, accumulation of vesicles, problems in spindle orientation and defects in the digestion of apoptotic corpses.

ccz-1 encodes a protein of 528 amino acids that is highly conserved from yeasts to mammals. The yeast protein has been characterized as being involved in a pathway for the fusion of vesicles to vacuoles or phagosomes (Sato et al., 2000; Wang et al., 2003). At the molecular level, the N-terminal part of CCZ-1 is predicted to have a ChiPS domain that might interact with GTPases (Kinch and Grishin, 2006). This N-terminal part is also structurally similar to SAND-1 and members of the TRAPPII complex, which is a tethering complex at the Golgi (Soding et al., 2005).

The yeast homologues of SAND-1 and CCZ-1 interact with each other, forming a complex that seems to link the HOPS complex to Ypt7p (the yeast orthologue of *C. elegans* GTPase RAB-7). Ccz1p-Sand1p, Ypt7p and the HOPS complex are sequentially recruited. Each protein mediates the loading of the following on the phagosome. Finally, recruitment of the HOPS complex enables interaction with surface proteins from other vesicles, allowing the fusion of their membranes to the phagosome

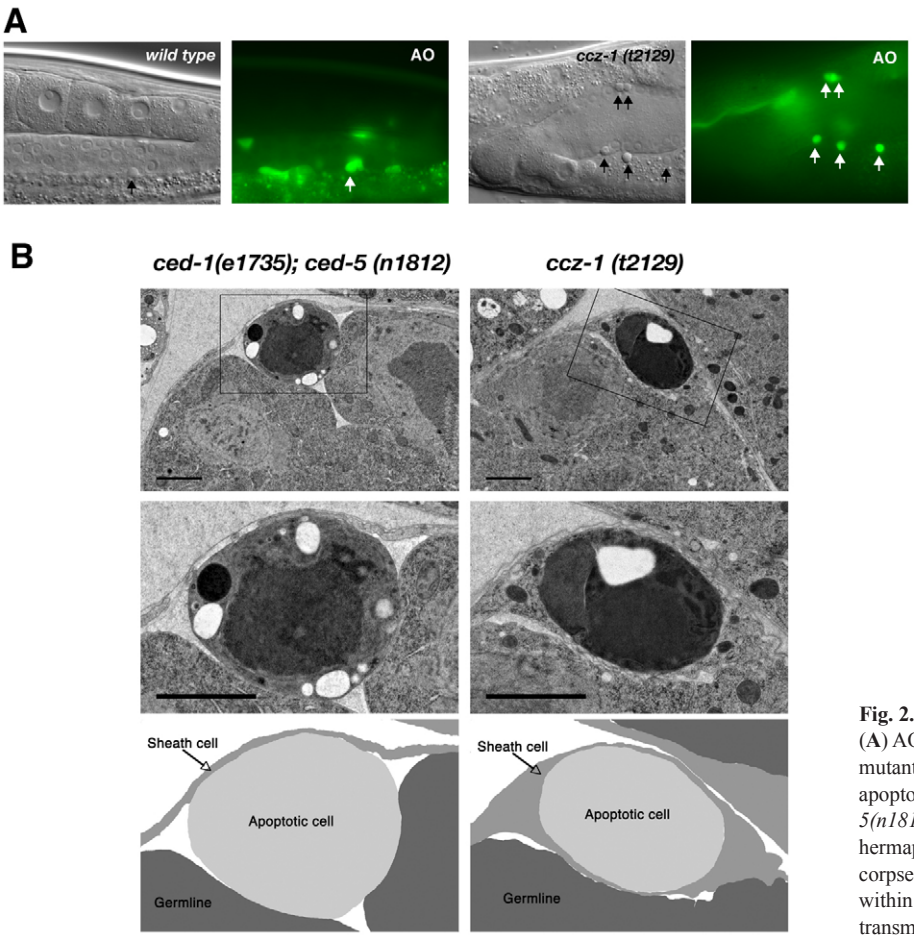

Fig. 2. Apoptotic cells are internalized in *ccz-1* mutants. (**A**) AO staining of wild type (left panels) and the *ccz-1* mutant apoptotic corpses (right panels). Arrows point to apoptotic corpses. (**B**) Double-mutant *ced-1(e1735); ced-5(n1812)* corpses are not engulfed by the sheath cells of the hermaphrodite adult gonad (left column), whereas cell corpses in the *ccz-1* mutant (right column) are internalized within the sheath cells (100%, *n*=5), as shown by transmission electron microscopy. Scale bars: 2 µm.

(Kucharczyk et al., 2001; Kinch and Grishin, 2006, Sato et al., 2000; Wang et al., 2003).

Similarly to yeast proteins, *C. elegans* SAND-1 and CCZ-1 can form a complex, as shown by their interaction in two-hybrid assays (Poteryaev et al., 2007). In addition, mutant worms defective in the GTPase *rab-7* or in proteins of the HOPS complex have recently been described as members of a pathway involved in the digestion of apoptotic cells whose inactivation leads to an accumulation of undigested corpses within phagosomes (Kinchen et al., 2008; Yu et al., 2008), similar to the defect we describe here for *ccz-1* mutants.

Because SAND-1 and CCZ-1 form a protein complex, we analyzed whether *sand-1* had a similar function to *ccz-1* in the digestion of apoptotic cells. Inactivation of *sand-1* indeed revealed the same three phenotypes that we detected in the *ccz-1* mutants: spindle orientation defects, embryonic corpses and germline corpses (supplementary material Table S1).

To further address the function of CCZ-1, we generated animals expressing fluorescent CCZ-1 protein. In the wild type, CCZ-1-tagged yellow fluorescent protein (CCZ-1–YFP) localized around refractile apoptotic corpses (Fig. 3Ba,Ba′). This localization was

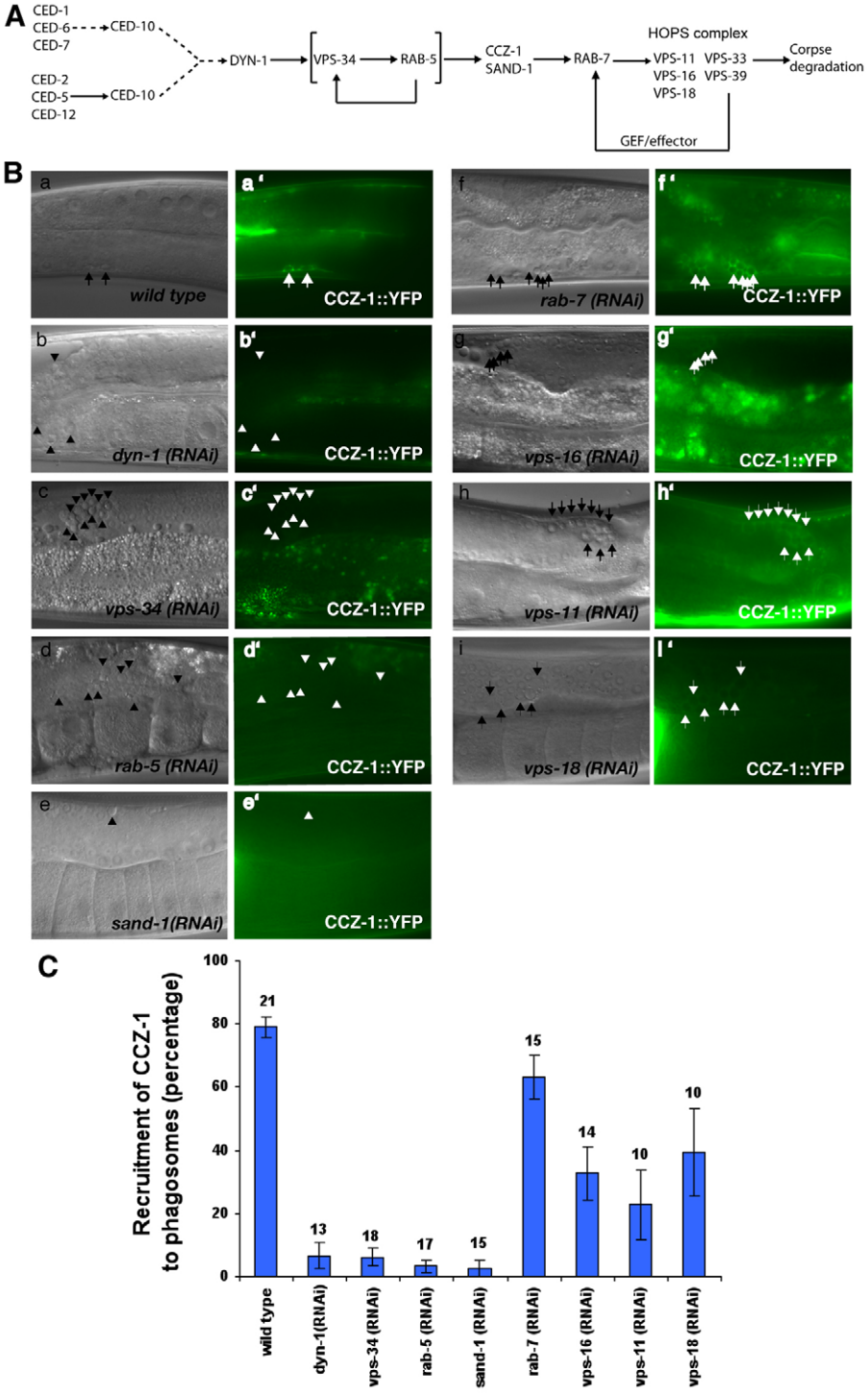

Fig. 3. Role for CCZ-1 in the phagosome-maturation pathway during the engulfment of apoptotic cells. (**A**) Genetic pathway: CCZ-1 acts downstream of RAB-5 GTPase and upstream of RAB-7 GTPase in the pathway for phagosome maturation. (**B**) CCZ-1 localization in the wild type and different mutants defective in the phagosome-maturation pathway. In the wild type (a,a′) CCZ-1–YFP forms halos around phagosomes containing engulfed apoptotic cells in the *C. elegans* gonad. In *dyn-1(RNAi)* (b,b′), *vps-34(RNAi)* (c,c′) and *rab-5(RNAi)* (d,d′) worms, these CCZ-1–YFP halos disappear, indicating that CCZ-1 acts downstream in the pathway. In *sand-1(RNAi)* mutants (e,e′), the correct localization of CCZ-1 is also blocked. In *rab-7(RNAi)* mutants (f-f′), the CCZ-1–YFP halos are visible, indicating that CCZ-1 acts upstream of RAB-7. In *vps-16(RNAi)* (g,g′), *vps-18(RNAi)* (i,i′) and in *vps-11(RNAi)* (h,h′) mutants, the CCZ-1–YFP halos are visible. Arrows indicate corpses positive for YFP halos; arrowheads indicate corpses negative for YFP halos. (**C**) Quantified data showing the recruitment of CCZ-1–YFP around the germline corpses. Apoptotic corpses were counted under DIC optics and scored for YFP-positive halos under ultraviolet light. The result was expressed in percentage. Numbers over the columns refer to the number of analyzed worms in each case. Columns indicate means ± s.e.m.

the same as that of RAB-5 and RAB-7 (Fig. 4) (Kinchen et al., 2008). In addition, the inactivation of *rab-7* by RNAi in a *ccz-1(t2129)* mutant worm produced an accumulation of apoptotic corpses in the gonad, similar to that produced by inactivation of *rab-7* alone (supplementary material Table S1). The defect caused by the inactivation of both genes was therefore not additive. These results (same localization of CCZ-1 and proteins of the 'corpse-digestion pathway', same phenotype and no additive effect in the double mutant) suggest that CCZ-1 and RAB-7 act on a single linear pathway involved in the digestion of apoptotic corpses within phagosomes.

To further determine whether CCZ-1 acts in the apoptotic-corpse-digestion pathway, and at which level, we tested the effect of its inactivation on the localization of the proteins in this pathway. We used transgenic worms expressing a YFP–2×FYVE construct, which has been shown to specifically bind phosphatidylinositol 3-phosphate [PtdIns(3)*P*], which is generated by VPS-34 on endosomes (Roggo et al., 2002) and recruited to phagosomes containing apoptotic corpses (Kinchen et al., 2008). The phagosomal recruitment of YFP–2×FYVE was not affected in the *ccz-1(t2129)* mutants, indicating that CCZ-1 acts downstream of VPS-34 (Fig. 4Aa-Ab′,B). Similarly, the YFP-tagged GTPase RAB-5 formed clear halos around the internalized corpses in the *ccz-1(t2129)* mutants (Fig. 4Ac-Ad′). However, we found a significant increase in the number of RAB-5–YFP-positive corpses in a *ccz-1(t2129)* background compared with a wild-type background (Fig. 4B). This increase suggests that CCZ-1 acts downstream of RAB-5 and that it could be involved in a mechanism aimed at removing RAB-5 from phagosomes during phagosome maturation.

By contrast, the recruitment of RAB-7–YFP around the apoptotic-corpse-containing phagosomes was dramatically reduced in a *ccz-1(t2129)* mutant as compared with the wild type (Fig. 4Ae-Af′,B), indicating that CCZ-1 acts upstream of the GTPase RAB-7.

Our results suggest a model in which CCZ-1 and SAND-1 would participate in the exchange of the GTPase RAB-5 for RAB-7 during the maturation of phagosomes. Therefore, CCZ-1 would act downstream of the GTPase RAB-5 and upstream of the GTPase RAB-7, and would be required for efficient removal of RAB-5 from the surface of the phagosome and RAB-7 recruitment during digestion of apoptotic corpses (Fig. 3A). Indeed, inactivation of any of these genes leads to the accumulation of undigested corpses. If this is the case, the absence of elements of the pathway upstream of RAB-7 would abolish the recruitment of CCZ-1 onto phagosomes, whereas inactivation of RAB-7 or elements of the HOPS complex would lead to a normal recruitment of CCZ-1 onto apoptotic-corpse-containing phagosomes. To further test whether this was the case, we used transgenic worms expressing CCZ-1–YFP under the control of the *ced-1* promoter. These animals were

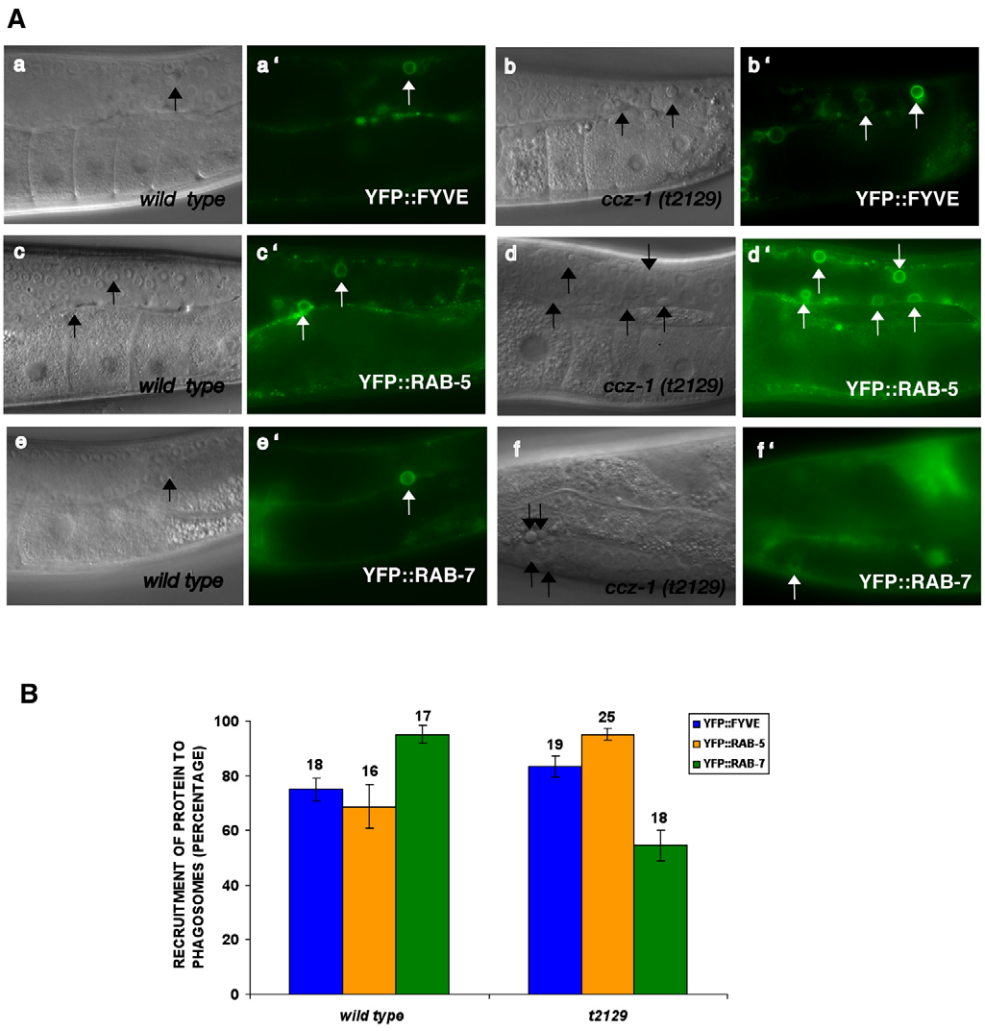

Fig. 4. Protein localization of phagosome-maturation components in *ccz-1* mutants. (**A**) In the wild type (a,a′), the YFP–2×FYVE construct is derived from EEA-1 and is bound to membranes containing PtdIns(3)*P* produced by VPS-34. This localization is similar in *ccz-1(t2129)* worms (b,b′). RAB-5–YFP is recruited normally in *ccz-1(t2129)* (d,d′) as compared with the wild-type worms. The recruitment of RAB-7–YFP is dramatically decreased in *ccz-1(t2129)* mutants (f,f′) compared with the wild type (e,e′). Arrows indicate corpses positive for YFP halos. (**B**) Quantified data showing the recruitment of YFP-FYVE, YFP–RAB-5 and YFP–RAB-7 around the germline corpses in a wild-type and in a *ccz-1(t2129)* background. Apoptotic corpses were counted under DIC optics and scored for YFP-positive halos under ultraviolet light. The result was expressed in percentage. Numbers over the columns refer to the number of analyzed worms in each case. Columns indicate means ± s.e.m.

fed with bacterial clones expressing dsRNA of different genes involved in the digestion pathway. Indeed, inactivation by RNAi of *dyn-1*, *vps-34* or *rab-5*, all of which function upstream of *rab-7*, completely abolished the recruitment of CCZ-1–YFP around the corpses (Fig. 3Bb-Bd′,C), indicating that the presence of these elements is necessary to load CCZ-1 onto the phagosome. However, inactivation of *rab-7* by RNAi allowed the recruitment of CCZ-1–YFP onto the apoptotic-corpse-containing phagosomes (Fig. 3Bf,Bf′,C). Furthermore, RNAi of members of the HOPS complex led to a recruitment of CCZ-1–YFP around the apoptotic-corpse-containing phagosomes, although this recruitment was partially impaired (Fig. 3Bg-Bi′,C). This result strongly indicates that CCZ-1 acts downstream of RAB-5 but upstream of RAB-7 in the digestion pathway. *rab-5* and *rab-7* were efficiently knocked down by RNAi, as indicated by the strong degree of accumulation of persistent undigested corpses in the gonad (supplementary material Table S1). The result is also consistent with previous reports that showed that the HOPS complex acts genetically downstream of RAB-7 (Kinchen et al., 2008; Yu et al., 2008), but in addition suggests that it partially contributes to the recruitment or stabilization of CCZ-1 on the phagosomes. The HOPS complex could stabilize the binding of CCZ-1 or alternatively could act in one of the several branches for CCZ-1 recruitment onto the phagosome.

The above results are based on the analysis of the location of the proteins on the maturing phagosomes. We next performed a functional assay. It has been described that a gain-of-function phenotype of the GTPase CED-10 (Rac) can be generated by overexpression of the *ced-10* gene. This GTPase overexpression does bypass the functional requirement for genes upstream in the cell-corpse phagocytosis pathway (Reddien and Horvitz, 2000; Cabello et al., 2010). We likewise analyzed the effect of overexpressing the GTPase RAB-7 by expressing its gene under the control of the *ced-1* promoter (which drives the expression of the transgene to the engulfing cells) in a *ccz-1(t2129)* mutant background and indeed found a partial but significant reduction in the number of germline-persistent corpses (supplementary material Table S1). This result support the finding that *rab-7* acts genetically downstream of *ccz-1*.

It has been shown that *vps-18* (a member of the HOPS complex) is involved in endosome and lysosome biogenesis, both of which are processes affecting the digestion of apoptotic corpses (Xiao et al., 2009). Our results suggest that, similar to *vps-18* and *rab-7*, but different to *sand-1* (Poteryaev et al., 2007), *ccz-1* mediates phagosome maturation and lysosome formation. The accumulation of the yolk proteins fused to GFP (VIT-2–GFP) in large and peripheral granules in *ccz-1(t2129)* mutant oocytes and embryos indicates that the early steps of receptor-mediated endocytosis were normal. Thus, the disruption of *ccz-1* in *C. elegans* leads to late defects in the endocytic pathway after normal internalization of membranes and solutes. The pathway involved in lysosome biogenesis seems to be also affected in *ccz-1(t2129)* mutant worms, as indicated by the following two observations. First, the autofluorescent gut granules were abnormal in *ccz-1(t2129)* embryos where the maternal and the zygotic product of the gene was disrupted and, second, AO staining of the intestine to mark the acidic compartments revealed that the lysosomes were mostly absent in the *ccz-1(t2129)* mutants (supplementary material Fig. S5).

Our results support a model in which *C. elegans* CCZ-1, the homologue of *S. cerevisiae* Ccz1p, plays a role in lysosome biogenesis and phagosome maturation during digestion of apoptotic corpses, a hitherto unknown feature of this protein. Both functions are closely associated and the strong blockage of the degradation of phagosomal corpses, in the absence of CCZ-1, could be ultimately caused by the absence of functional lysosomes. CCZ-1 acts genetically downstream of the GTPase RAB-5 and upstream of the GTPase RAB-7, mediating the exchange of these GTPases during phagosome maturation. CCZ-1 requires RAB-5 to be recruited onto the phagosomes and is required for proper RAB-7 localization on the phagosomes (Fig. 3A). CCZ-1 also mediates vesicle transport in *C. elegans*, as shown by the other defects observed in the mutants. In the absence of CCZ-1, the endosomes do not fuse to the few lysosomes present in the cell and the yolk is not metabolized. Embryos then die ‘by starvation’. In addition, similar to Wnt-pathway mutants, *ccz-1* mutant embryos show defects in spindle orientation (Rocheleau et al., 1997; Thorpe et al., 1997). These defects seem to be independent of lysosome biogenesis because they are also observed in *sand-1* mutants. Wnt signalling induces the asymmetric localization of proteins such as Frizzled or β-catenin in receptor cells. This polarity, underlying spindle orientation and fate diversification (Goldstein, 2000; Park et al., 2004; Nakamura et al., 2005), depends on localized endocytosis, transport and recycling mediated by the retromer complex (Coudreuse and Korswagen, 2007; Hardin and King, 2008; Seaman, 2005). Such a process could become compromised in the absence of CCZ-1. Indeed, *dyn-1* mutants (the most upstream element in the corpse digestion pathway) contain arrested phagosomes without recycling of the phagocytic receptor CED-1 back to the plasma membrane (Kinchen et al., 2008).

These findings define novel requirements for CCZ-1, a widely conserved protein that mediates key processes in the normal development of an organism, such as yolk metabolism, cell-cell signalling or digestion of the apoptotic corpses. Studying cell-corpse degradation is important not only for understanding a general biological process in animal development but also because efficient clearance of apoptotic cells protects humans from several diseases.

Materials and Methods

Strains and genetics

Animals were grown at 25°C as described (Brenner, 1974). The following mutations were used: LG II, *rab-7(ok511)*; LG IV, *sand-1(ok1963)*; LG V, *ccz-1(t2129)*, *ccz-1(t2070)*, *ccz-1(t2170)*, *ccz-1(ok2182)*, *dpy-11(e224)*. Other genes used in this work were inactivated using RNAi. Genetic mapping of mutations was carried out as described (Davis and Hammarlund, 2006).

RNAi

dsRNA-mediated gene interference was performed by feeding (Fraser et al., 2000). Synchronized L1 larvae were spotted onto feeding plates and incubated at 15°C until the gonads of adults and embryos of the next generation could be scored.

Light microscopy

Apoptotic corpses were detected by their refractile shape under a DIC light microscope and scored as described (Schnabel et al., 1997; Reddien and Horvitz, 2000). Fluorescent microscopy of transgenic worms was performed using a Zeiss Axioplan 2 microscope equipped with DIC optics and standard epifluorescence. Staining of worms with AO (Molecular Probes) was performed as described previously (Kinchen et al., 2005).

For the 4D microscope analysis of embryos, 25 focal planes of the embryos were recorded over 10 hours. As a result, 4D movies (3D of the embryo + time) were obtained for each genotype. The SIMI Biocell software (SIMI GmbH, Germany) allowed tracing each and every cell of the embryo in time and space, as well as tracing of the mitosis and the terminal differentiation of each cell.

Electron microscopy

C. elegans grown on *Escherichia coli* plates were high-pressure frozen with an EM Pact2 device (Leica Microsystems, Vienna, Austria) as described by the manufacturer. The frozen specimens were freeze-substituted in anhydrous acetone containing 2% OsO_4 in a Leica EM AFS2 freeze-substitution unit (Leica Microsystems). Specimens

were successively kept at –90°C, –60°C, and –30°C for 8 hours each, finally reaching room temperature. OsO_4 was removed by washing the specimens with anhydrous acetone twice. Subsequently, the specimens were gradually embedded in Epon/Araldite (Sigma-Aldrich, Buchs, Switzerland) prior to polymerization at 60°C for 48 hours. Thin sections were stained with aqueous uranyl acetate 2% and Reynolds lead citrate and imaged with a Phillips CM 100 transmission electron microscope (FEI, Eindhoven, Netherlands) using a Gatan Orius CCD camera and digital micrograph acquisition software (Gatan GmbH, Munich, Germany).

This work was supported by the Junta de Castilla y León (grants CSI03A08 and Grupo de Excelencia GR265), the Spanish Ministry of Science and Innovation (grants BFU2008-01808 and Consolider CSD2007-00015), the 'Fundación Rioja Salud', the 'Fundación Memoria D. Samuel Solorzano Barruso', the Swiss National Science Foundation and the Ernst Hadorn Foundation. C.N. and J.C. were each supported by the I3P programme of the Spanish National Research Council (CSIC). We thank Gery Barmettler, Therese Bruggmann and Ursula Lüthi for help with the electron microscopy, Lukas Neukomm for giving plasmids, the *C. elegans* Gene Knockout Consortium and CGC for providing strains, and Nicholas Skinner for corrections to the manuscript.

Supplementary material available online at
http://jcs.biologists.org/cgi/content/full/123/12/2001/DC1

References

Aballay, A. and Ausubel, F. M. (2001). Programed cell death mediated by ced-3 and ced-4 protects Caenorhabditis elegans from Salmonella typhimurium-mediated killing. *Proc. Natl. Acad. Sci. USA* **98**, 2735-2739.

Brenner, S. (1974). The genetics of *Caenorhabditis elegans*. *Genetics* **77**, 71-94.

Cabello, J., Neukomm, L. J., Günesdogan, U., Burkart, K., Charette, S. J., Lochnit, G., Hengartner, M. O. and Schnabel, R. (2010). The Wnt pathway controls cell death engulfment, spindle orientation, and migration through CED-10/Rac. *PLoS Biol.* **8**, e1000297.

Coudreuse, D. and Korswagen, H. C. (2007). The making of Wnt: new insights into Wnt maturation, sorting and secretion. *Development* **134**, 3-12.

Davis, M. W. and Hammarlund, M. (2006). Single-nucleotide polymorphism mapping. *Methods Mol Biol*. **351**, 75-92.

Fraser, A. G., Kamath, R. S., Zipperlen, P., Martinez-Campos, M., Sohrmann, M. and Ahringer, J. (2000). Functional genomic analysis of *C. elegans* chromosome I by systematic RNA interference. *Nature* **408**, 325-330.

Gartner, A., Milstein, S., Ahmed, S., Hodgkin, J. and Hengartner, M. O. (2000). A conserved checkpoint pathway mediates DNA damage mediated apoptosis and cell cycle arrest in C.elegans. *Mol. Cell* **5**, 435-443.

Goldstein, B. (2000). When cells tell their neighbors which direction to divide. *Dev. Dyn.* **218**, 23-29.

Gumienny, T. L., Lambie, E., Hartwieg, E., Horvitz, H. R. and Hengartner, M. O. (1999). Genetic control of programmed cell death in the Caenorhabditis elegans hermaphrodite germline. *Development* **126**, 1011-1022.

Hardin, J. and King, R. S. (2008). The long and the short of Wnt signaling in C. elegans. *Curr. Opin. Genet. Dev*. **18**, 362-367.

Hoffman-Sommer, M., Grynberg, M., Kucharczyk, R. and Rytka, J. (2005). The CHiPS Domain-ancient traces for the Hermansky-Pudlak syndrome. *Traffic* **6**, 534-538.

Hubbard, E. J. and Greenstein, D. (2000). The Caenorhabditis elegans gonad: a test tube for cell and developmental biology. *Dev. Dyn.* **218**, 2-22.

Hutter, H. and Schnabel, R. (1995). Establishment of left-right asymmetry in the Caenorhabditis elegans embryo: a multistep process involving a series of inductive events. *Development* **121**, 3417-3424.

Kawane, K., Ohtani, M., Miwa, K., Kizawa, T., Kanbara, Y., Yoshioka, Y., Yoshikawa, H. and Nagata, S. (2006). Chronic polyarthritis caused by mammalian DNA that escapes from degradation in macrophages. *Nature* **443**, 998-1002.

Kinch, L. N. and Grishin, N. V. (2006). Longin-like folds identified in CHiPS and DUF254 proteins: vesicle trafficking complexes conserved in eukaryotic evolution. *Protein Sci*. **15**, 2669-2674.

Kinchen, J. M. and Hengartner, M. O. (2005). Tales of cannibalism, suicide, and murder: programmed cell death in C. elegans. *Curr. Top. Dev. Biol*. **65**, 1-45.

Kinchen, J. M., Cabello, J., Klingele, D., Wong, K., Feichtinger, R., Schnabel, H., Schnabel, R. and Hengartner, M. O. (2005). Two pathways converge at CED-10 to mediate actin rearrangement and corpse removal in C. elegans. *Nature* **434**, 93-99.

Kinchen, J. M., Doukoumetzidis, K., Almendinger, J., Stergiou, L., Tosello-Trampont, A., Sifri, C. D., Hengartner, M. O. and Ravichandran, K. S. (2008). A pathway for phagosome maturation during engulfment of apoptotic cells. *Nat. Cell Biol*. **10**, 556-566.

Kucharczyk, R., Kierzek, A. M., Slonimski, P. P. and Rytka, J. (2001). The Ccz1 protein interacts with Ypt7 GTPase during fusion of multiple transport intermediates with the vacuole in S. cerevisiae. *J. Cell Sci.* **114**, 3137-3145.

Nakamura, K., Kim, S., Ishidate, T., Bei, Y., Pang, K., Shirayama, M., Trzepacz, C., Brownell, D. R. and Mello, C. C. (2005). Wnt signaling drives WRM-1/beta-catenin asymmetries in early C. elegans embryos. *Genes Dev*. **19**, 1749-1754.

Park, F. D., Tenlen, J. R. and Priess, J. R. (2004). C. elegans MOM-5/frizzled functions in MOM-2/Wnt-independent cell polarity and is localized asymmetrically prior to cell division. *Curr. Biol*. **14**, 2252-2258.

Poteryaev, D., Fares, H., Bowerman, B. and Spang, A. (2007). Caenorhabditis elegans SAND-1 is essential for RAB-7 function in endosomal traffic. *EMBO J*. **26**, 301-312.

Reddien, P. W. and Horvitz, H. R. (2000). CED-2/CrkII and CED-10/Rac control phagocytosis and cell migration in Caenorhabditis elegans. *Nat. Cell Biol*. **2**, 131-136.

Rocheleau, C. E., Downs, W. D., Lin, R., Wittmann, C., Bei, Y., Cha, Y. H., Ali, M., Priess, J. R. and Mello, C. C. (1997). Wnt signaling and an APC-related gene specify endoderm in early C. elegans embryos. *Cell* **90**, 707-716.

Roggo, L., Bernard, V., Kovacs, A. L., Rose, A. M., Savoy, F., Zetka, M., Wymann, M. P. and Müller, F. (2002). Membrane transport in Caenorhabditis elegans: an essential role for VPS34 at the nuclear membrane. *EMBO J.* **21**, 1673-1683.

Sato, T. K., Rehling, P., Peterson, M. R. and Emr, S. D. (2000). Class C Vps protein complex regulates vacuolar SNARE pairing and is required for vesicle docking/fusion. *Mol Cell*. **6**, 661-671.

Schnabel, R., Hutter, H., Moerman, D. and Schnabel, H. (1997). Assessing normal embryogenesis in *Caenorhabditis elegans* using a 4D microscope: variability of development and regional specification. *Dev. Biol*. **184**, 234-265.

Seabra, M. C. and Wasmeier, C. (2004). Controlling the location and activation of Rab GTPases. *Curr. Opin. Cell Biol*. **16**, 451-457.

Seaman, M. N. (2005). Recycle your receptors with retromer. *Trends Cell Biol.* **15**, 68-75.

Soding, J., Biegert, A. and Lupas, A. N. (2005). The Hhpred interactive server for protein homology detection and structure prediction. *Nucleic Acids Res.* **33**, 244-248.

Sulston, J. E., Schierenberg, E., White, J. G. and Thomson, J. N. (1983). The embryonic cell lineage of the nematode Caenorhabditis elegans. *Dev. Biol*. **100**, 64-119.

Thorpe, C. J., Schlesinger, A., Carter, J. C. and Bowerman, B. (1997). Wnt signaling polarizes an early C. elegans blastomere to distinguish endoderm from mesoderm. *Cell*. **90**, 695-705.

Ullrich, O., Horiuchi, H., Bucci, C. and Zerial, M. (1994). Membrane association of Rab5 mediated by GDP-dissociation inhibitor and accompanied by GDP/GTP exchange. *Nature* **368**, 157-160.

Wang, C. W., Stromhaug, P. E., Kauffman, E. J., Weisman, L. S. and Klionsky, D. J. (2003). Yeast homotypic vacuole fusion requires the Ccz1-Mon1 complex during the tethering/docking stage. *J. Cell Biol*. **163**, 973-985.

Xiao, H., Chen, D., Fang, Z., Xu, J., Sun, X., Song, S., Liu, J. and Yang, C. (2009). Lysosome biogenesis mediated by vps-18 affects apoptotic cell degradation in Caenorhabditis elegans. *Mol. Biol. Cell* **20**, 21-32.

Yu, X., Lu, N. and Zhou, Z. (2008). Phagocytic receptor CED-1 initiates a signaling pathway for degrading engulfed apoptotic cells. *PLoS Biol*. **6**, 581-600.